# Estimating Co-Seismic Subsidence in the Hutt Valley associated with Rupture of the Wellington Fault

D.B. Townsend
R.J. Van Dissen
W.S.A Saunders
J.G. Begg
D.A. Rhoades
T.A. Little

**GNS Science Report 2015/02**
**May 2015**

GNS SCIENCE
TE PŪ AO

**BIBLIOGRAPHIC REFERENCE**

Townsend, D.B.; Begg, J.G.; Van Dissen, R.J.; Rhoades, D.A.; Saunders, W.S.A.; Little, T.A. 2015. Estimating Co-Seismic Subsidence in the Hutt Valley associated with Rupture of the Wellington Fault, *GNS Science Report* 2015/02. 73 p.

D.B. Townsend, GNS Science, PO Box 30368, Lower Hutt 5040, New Zealand
J.G. Begg, GNS Science, PO Box 30368, Lower Hutt 5040, New Zealand
R.J. Van Dissen, GNS Science, PO Box 30368, Lower Hutt 5040, New Zealand
D.A. Rhoades, GNS Science, PO Box 30368, Lower Hutt 5040, New Zealand
W.S.A Saunders, GNS Science, PO Box 30368, Lower Hutt 5040, New Zealand
T.A. Little, School of Geography, Environment & Earth Sciences, Victoria University of Wellington, PO Box 600, Wellington 6040, New Zealand.

© Institute of Geological and Nuclear Sciences Limited, 2015
www.gns.cri.nz

ISSN 1177-2425 (Print)
ISSN 2350-3424 (Online)
ISBN 978-0-478-19905-5 (Print)
ISBN 978-0-478-19921-5 (Online)

## CONTENTS

## FIGURES

## TABLES

## APPENDICES



## APPENDIX TABLES

# ABSTRACT

This report is focused on the lower Hutt Valley, situated on the coastal fringe at the northern edge of Wellington Harbour. It is part of a sedimentary basin that includes geologically young, relatively soft sediment fill, deposited at the mouth of the valley; the active Wellington Fault borders the basin to the northwest.

The area was uplifted by about 1.5 m historically, during the 1855 Wairarapa earthquake that was associated with rupture of the Wairarapa Fault. However, the long-term vertical deformation (i.e., that which is responsible for basin formation) is subsidence. Therefore, there must be another driver of vertical deformation in this part of the Wellington Peninsula; the Wellington Fault is the most likely candidate.

In this report we use a database of subsurface drillhole information to calculate subsidence rates (over the last few hundred thousand years) for the lower Hutt Valley. This rate incorporates corrections for past variations in sea level, and also a correction for post-depositional sediment consolidation. The calculated subsidence rates include a component of uplift contributed by slip on the Wairarapa Fault. We remove this uplift component by reassessing and incorporating uplift rates calculated for beach ridges at Turakirae Head, on the southeastern Wellington coastline, also inferred to have been raised tectonically by slip on the Wairarapa Fault. We use the relative proportions of uplift experienced in the Hutt Valley and at Turakirae Head during the 1855 Wairarapa earthquake (assuming that this was about an average sized event on the Wairarapa Fault) to scale and remove the Wairarapa Fault contribution to vertical deformation rate from the Hutt Valley record. We also include other estimates of the mean uplift per event at Turakirae Head to 1) test the variability of uplift/slip and 2) to include other published information regarding recurrence intervals for the Wairarapa Fault. We then infer that the remaining subsidence rate in the Hutt Valley is entirely due to slip on the Wellington Fault. We use recently revised information for slip rate and single event displacement of the Wellington Fault to calculate the mean subsidence per event required to lower the strata in the drillholes to their current elevations below the floor of the Hutt Valley. All calculations are made by using a logic tree structure, whereby we weight the different input variables and propagate their uncertainties.

The subsidence calculated for an “average” sized Wellington Fault event is ~1.9 m in the western part of the valley near Petone, ranging to ~1.7 m near Ewen Bridge and ~1.4 m near Seaview. These subsidence values have been contoured, converted into a grid and subtracted from a LiDAR-derived digital elevation model (DEM); the resulting modelled elevation reveals that large areas of Alicetown-Petone, Moera-Seaview would subside below sea level, and could be inundated. We also supply “minimum” and “maximum” credible subsidence values by making some assumptions about the likely variability of future events. None of our calculated values incorporate any subsidence relating to the effects of liquefaction and/or lateral spreading.

Implications of the calculated Hutt Valley subsidence for planning and social impacts are discussed, and a range of possible mitigation and management options are suggested. These include a review of the Hutt City Plan, developing a managed retreat of critical facilities, limiting future development in the worst affected areas, developing a pre-event recovery plan, reassessing emergency management procedures, and engaging the public in a program of education and awareness to disseminate relevant information.

## KEYWORDS

Co-seismic subsidence, lower Hutt Valley, Petone, Wellington Fault, Wairarapa Fault, drillhole database, paleoshoreline, marine terrace, Turakirae Head, uplift, beach ridge, 1855 Wairarapa earthquake, logic tree, LiDAR, terrain model, sea level change.

# 1.0 INTRODUCTION

The area of the lower Hutt Valley between Avalon and Petone is one of low relief, situated on an alluvial plain near the coastal fringe at the northern edge of Wellington Harbour (Figure 1). It is part of a sedimentary basin that includes geologically young, and relatively soft, sediment deposited at the mouth of the valley. The active Wellington Fault borders the basin to the northwest. Although this fault has not ruptured historically, it has a pronounced scarp along the western side of the valley and also borders the Wellington Harbour for ~9 km farther to the south.

The first European settlers to Wellington landed at Petone and described the Hutt Valley as a windswept beach, backed by low vegetation, with swamp and dense bush behind the scrub. The first few decades of settlement were marked by earthquakes and floods, with severe earthquakes in 1848 and a particularly severe one in 1855 (e.g., Stevens, 1974). Added to that, the Hutt River flooded most of the valley floor on several occasions between settlement and 1880. While the 1855 Wairarapa earthquake uplifted the valley floor, generally improving drainage, undoubtedly the river had a new sediment burden borne of landslide and earthquake debris prior to coming to a new post-earthquake equilibrium. Following these difficult early years in Petone, many settlers moved to Wellington to establish a new settlement there.

The $M_W$ 8.2–8.3 1855 Wairarapa earthquake (on the Wairarapa Fault) caused 1.2–1.5 m of uplift in the Hutt Valley (e.g., Grapes & Downes, 1997). However, cumulative long term (over 100s of thousands of years) vertical deformation in the valley has long been known to involve subsidence (e.g., Begg & Mazengarb, 1996); therefore, there must be another source of vertical deformation that overwhelms the regional uplift produced by slip on the Wairarapa Fault. The most likely candidate for this subsidence is the Wellington Fault. Seismic surveys of Wellington Harbour reveal a stratigraphy that has been tilted westward towards the fault, implying that the harbour is a half-graben (Wood & Davy, 1992). Furthermore, the sediments in the harbour are increasingly deformed in proximity to the fault, implying that the Wellington Fault is a key driver of basin subsidence.

Begg et al. (2002) estimated several parameters describing vertical deformation associated with rupture of the Wellington Fault in the Hutt Valley between Avalon and Petone (Figure 1). They assessed sea level and drillhole data, local and regional uplift rates and recurrence intervals for the Wellington Fault to calculate the amount of subsidence that could be expected for a future Wellington Fault surface rupture event. Earthquake activity of the Wairarapa Fault was also incorporated. Since the time of the Begg et al. (2002) report, paleoseismic investigation work on the Wellington and Wairarapa faults, partly motivated by the “It’s Our Fault” project (Van Dissen et al., 2010; http://www.gns.cri.nz/Home/IOF/It-s-Our-Fault), has led to revised estimates of the slip rate and recurrence interval for these faults (Langridge et al., 2009, 2011; Little et al., 2009, 2010; Carne et al., 2011; Rhoades et al., 2011; Ninis et al., 2013; Van Dissen et al., 2013).

The damage caused by the 2010-2011 Christchurch earthquakes is a timely reminder that many of our towns and cities are developed in areas that could sustain permanent ground deformation during seismic events. Importantly for low-lying urban areas such as Lower Hutt, the effects of the 22 February, 2011 Mw 6.3 Christchurch earthquake have underscored the potential for severe co-seismic ground damage to adversely affect infrastructure and urban

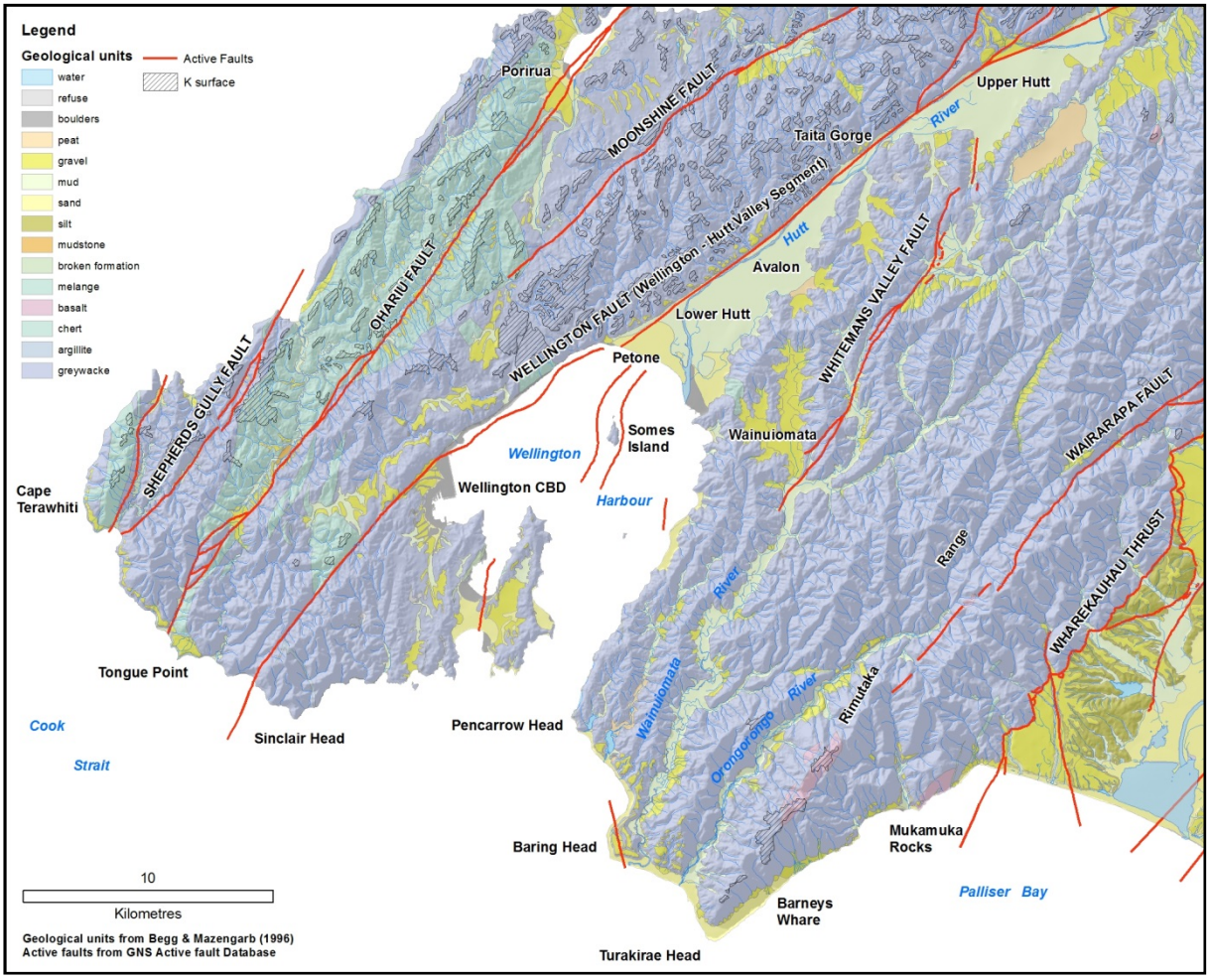


**Figure 1** The southwest Wellington region with prominent geographic features and places mentioned in the text. The digital geology base layer is from Begg & Mazengarb (1996) and active faults (shown in red) are from the GNS Active Fault Database (http://data.gns.cri.nz/af/). The segment of Wellington Fault northeast of Petone is from Beetham et al. (2012).

lifelines. Areas that experience permanent ground deformation (i.e., subsidence, drainage alteration, e.g., Cochran et al., 2014) suffer greater levels of loss (e.g., NZSEE, 2010, 2011; EQ Spectra, 2014).

Ongoing effects (i.e., three years later) from the Christchurch earthquake sequence include repeated suburb-scale flooding due to subsidence and damage to drainage networks, necessitating costly remedial work that is only now underway. One of the recommendations of the Canterbury Earthquakes Royal Commission was for local and regional authorities throughout New Zealand to work to recognise areas of high potential hazard and to mitigate those problems (Canterbury earthquakes Royal Commission, 2012).

The Wellington and Wairarapa faults have long been known to pose significant seismic hazards to the region (e.g., Stirling et al., 2002), and the Hutt Valley has the further potential for experiencing metre-scale co-seismic subsidence events that could render large parts of the valley (e.g., from Alicetown to Petone; Moera to Seaview) below sea level. This would also severely compromise drainage networks and stop-banks, and lead to a longer term increased flooding risk. For these reasons, it is opportune to reassess the co-seismic subsidence expected in the lower Hutt Valley that would result from a Wellington Fault rupture.

This report re-evaluates the co-seismic tectonic subsidence hazard in the lower Hutt Valley posed by a future Wellington Fault surface rupture. We use the approach outlined by Begg et al. (2002), but with incorporation of updated data for the Wellington and Wairarapa faults, and—for the first time—with careful quantification of associated uncertainties. We employ a logic tree structure (Kulkarni et al., 1984) to allow for different scenarios with different weightings of the input variables to produce a final mean subsidence (per event) value for the Hutt Valley. By assessing the potential variability in magnitude of a future Wellington Fault earthquake, we also present minimum and maximum credible values for the co-seismic subsidence in the valley. We use newly acquired (2013) Light Detection and Ranging (LiDAR) digital terrain data in association with the mean co-seismic subsidence calculated for a future Wellington Fault rupture to identify the areas that would be affected by such subsidence (equivalent in effect to a change in sea level). Throughout this report, the terms "subsidence" and "uplift" are taken to mean negative and positive vertical tectonic deformation, respectively. Note also that the subsidence estimates take no account of liquefaction-induced subsidence or lateral spreading, which is restricted to areas where surficial materials (<20 m in depth) are susceptible.

The implications for the planning zonation and social impacts for the Lower Hutt City area are discussed, and some options for managing and mitigating the hazard are suggested.

This page is intentionally left blank.

## 2.0 REGIONAL GEOLOGY AND GEOMORPHOLOGY

The Wellington area lies within the boundary zone between the Pacific and Australia tectonic plates, which runs through central New Zealand. The plate boundary zone in the North Island, also known as the Hikurangi margin, is characterised by subduction of the Pacific plate beneath the Australia plate (e.g., Wallace et al., 2009, 2012). A large part of the subduction zone interface is locked, especially beneath the Wellington region, and has potential to cause very large earthquakes of about Magnitude 8–9 (Reyners, 1998; Wallace et al., 2009; Stirling et al., 2012).

The rocks forming the land area are late Palaeozoic to Mesozoic aged Torlesse (composite) terrane, composed predominantly of sandstone and argillite, with other minor lithologies including conglomerate, basalt and chert (Begg & Mazengarb, 1996). These weakly metamorphosed rocks are commonly referred to as “greywacke”. Small remnants of Neogene strata, which must have once been more extensive, are preserved in some areas. Late Pleistocene and Holocene sediments are widespread throughout the region (Figure 1).

The Wellington Peninsula is a tectonically active area. The greywacke rocks of the peninsula have been folded and faulted into a series of discrete fault blocks, which extend north and east to the Tararua and Rimutaka ranges. Many of the faults, such as the Wellington, Shepherds Gully, Ohariu, Evans Bay, Baring Head and Whitemans Valley faults, remain active today and are potential sources of large earthquakes.

Some insight into the region-wide tectonic vertical deformation of the Wellington Peninsula can be gained from the elevation of the “K Surface” (Cotton, 1957; Stevens, 1974; Begg et al., 2002; Figure 1). This erosional surface formed between 4 and 1.5 million years ago as an erosion surface of low relief, but is now preserved at variable elevations around Wellington as relatively flat-topped remnants capping the greywacke hills and beneath the subsiding basins as the top of “basement”, now buried by Quaternary sediment (e.g., in Wellington Harbour and beneath the Hutt Valley). The deformation pattern of the K Surface is different on either side of the Wellington Fault: to the northwest it is elevated and gently warped, whereas to the southeast there is substantially more vertical differentiation to form some of the major geomorphological features of the peninsula, including Wellington Harbour-Lower Hutt Valley, and Upper Hutt and Kaitoke Basins. Some of this differentiation may be, in part, a consequence of erosion prior to the latest tectonic episode, in which case the (now eroded) K Surface would have lain somewhere above the basement-Quaternary cover contact. Nevertheless, development of these low-lying features is closely associated with the Wellington Fault, perhaps due to subtle changes in strike (and/or dip) of the fault in relation to the plate motion vector within the plate boundary zone, resulting in a greater or lesser component of dip-slip being resolved on the fault. Currently, we do not know whether the northwest side of the fault is uplifted (relative to sea level) during surface rupturing events.

Last Interglacial marine terraces, approximately 125 ka[1] old, are sporadically preserved along the fringes of the Wellington coastline (Ota et al., 1981; Begg & Mazengarb, 1996), affording another marker of vertical deformation. Even younger marine deposits, preserved at Turakirae Head as beach ridges, are an important tool for estimating uplift rates for the last ~7000 years and also the uplift associated with the 1855 Wairarapa earthquake (Hull & McSaveney, 1996; Grapes & Downes, 1997).

## 2.1 STRATIGRAPHY OF THE LOWER HUTT VALLEY

The Quaternary stratigraphy of the Hutt Valley has been established by surface, drillhole and seismic data (e.g., Wood & Davy, 1992; Begg & Mazengarb, 1996). The valley lies above part of a sedimentary basin that stretches from Taita Gorge in the northeast and includes Wellington Harbour in the south (Figure 1). The main source of sediment in the basin is currently the Hutt River. The oldest sediments are in the west, beneath Petone, and are inferred by correlation with glacial-interglacial cycles, or oxygen isotope (OI) stages, to be greater than about 400 ka old (Figure 2). The pattern of sediment accumulation has been similar for the last few hundred thousand years, suggesting that the overall basin structure has not altered much over this time. Sea level fluctuations throughout the Quaternary have meant that the position of the shoreline, now near Petone, has moved up and down the valley (and out past the harbour heads during cold climatic, or glacial periods), causing a complex interfingering of marine and terrestrial sediments at the edges of the basin. The maximum landward extent of Holocene (<12 ka) marine strata beneath the valley floor is at Mills Street, close to Melling Bridge (Begg & Mazengarb, 1996), about 4 km inland from the coast.

The basin is bounded to the northwest by the active Wellington Fault (Figure 1 and Figure 2). Over many thousands of years, vertical displacement (down on the southeast side) on the fault has produced a half-graben with sediments tilted towards the northwest (e.g., Wood & Davy, 1992). Quantifying this displacement and subsidence is the main subject of this report.

[1] One ka or “kilo annum” represents one thousand years.

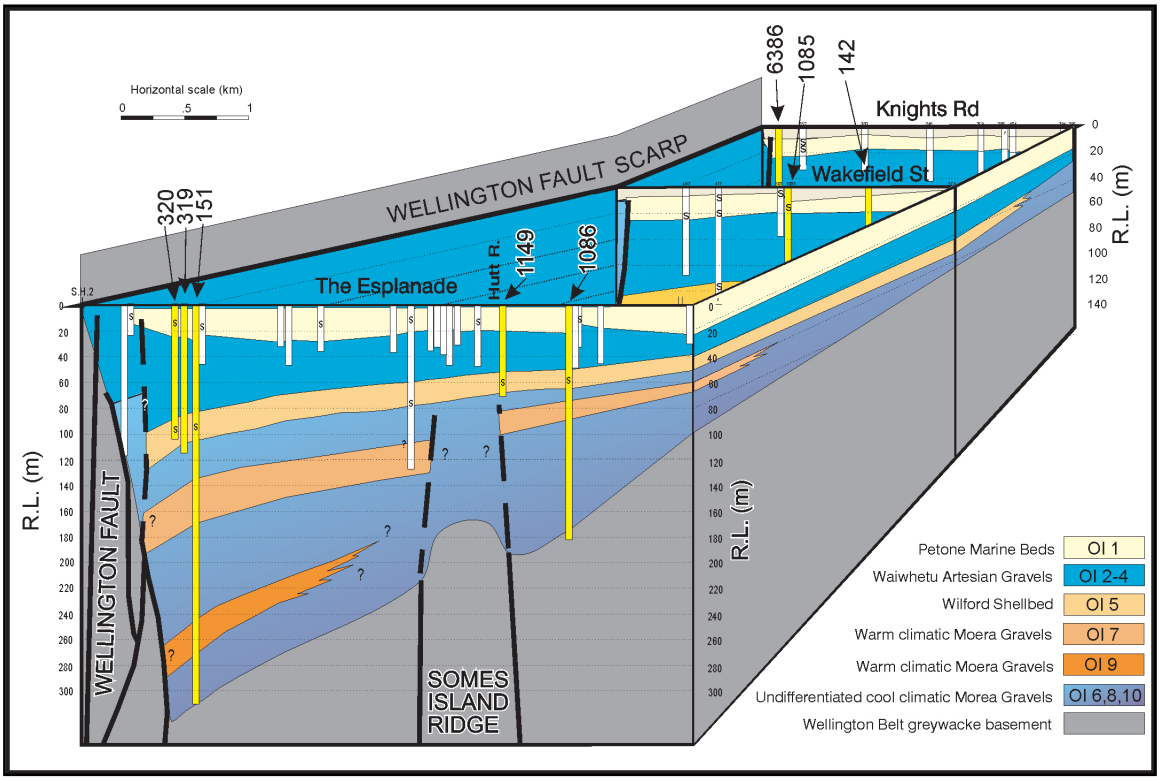


**Figure 2** Fence diagram illustrating the three dimensional relationships between stratigraphic units, the Wellington Fault and the basement rocks of the Lower Hutt Valley. Drillholes are shown as yellow (used in this report – see Figure 3) and white columns. Oxygen isotope (OI) stage correlations are marked on the legend, and the letter "s" on drillholes represents the presence of shells. The vertical exaggeration is about 10x. After Begg et al. (2002).

This page is intentionally left blank.

## 3.0 REASSESSMENT OF HUTT VALLEY SUBSIDENCE RATE(S) USING THE DRILLHOLE DATABASE

In this report we attempt to quantify all parameters involved in calculations of vertical deformation in the Hutt Valley, and their associated uncertainties. To achieve this, we use a database of drillhole information amassed by Greater Wellington Regional Council (GWRC) and its predecessors. Subsidence rates (and final subsidence per event; see below) for the Hutt Valley quoted in this report are calculated at the point locations of selected drillholes in the database (e.g., Begg et al., 2002; Figure 3). Only the drillholes with the most complete stratigraphic records are used.

As there has been no significant new stratigraphic (e.g., deep drillhole) sub-surface investigation in this area since 2002, we adopt the stratigraphy and unit correlations of Begg et al. (2002) for our calculations of subsidence rates for the Hutt Valley (Figure 2; Appendix 1). However, we reassess the rates accounting for past changes in sea level and also for sediment consolidation.

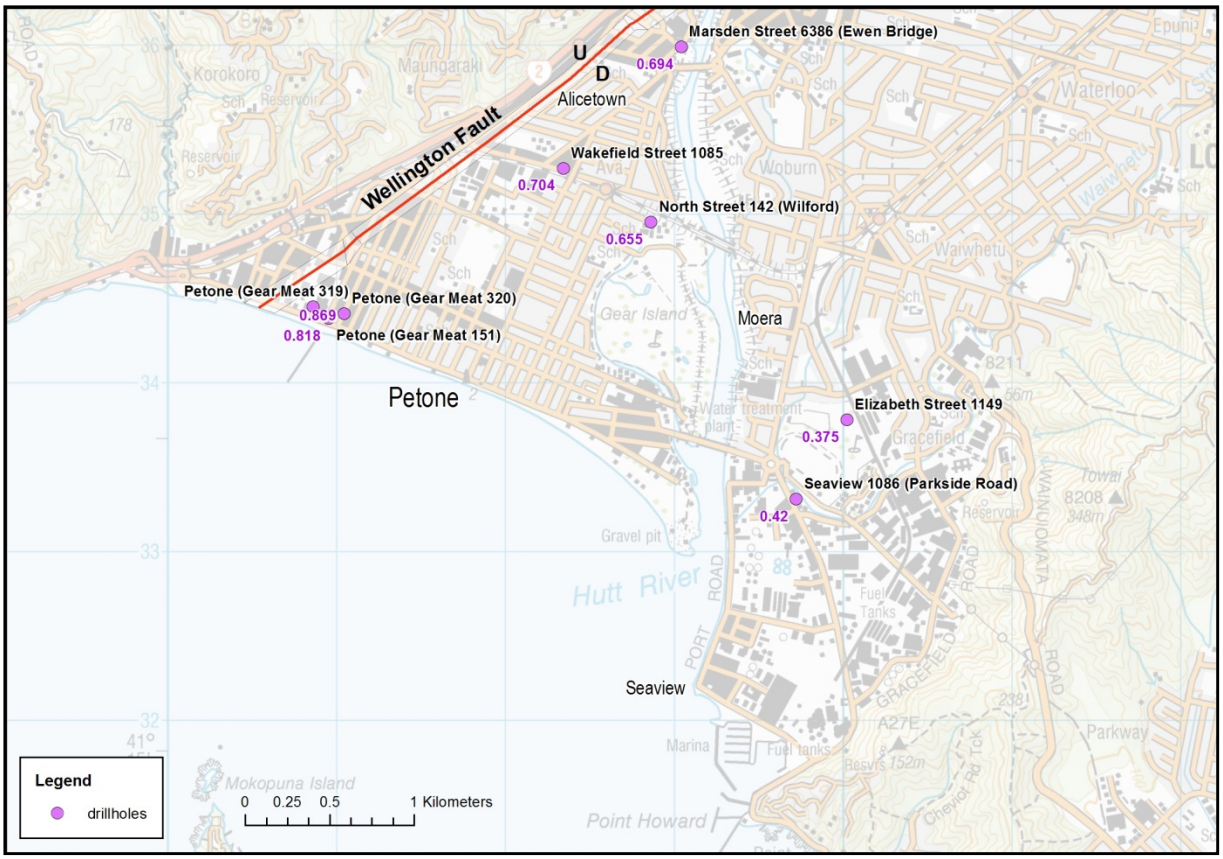


**Figure 3** Drillholes used in this report, showing names and locations, with final calculated mean subsidence rate (purple labels, in mm/yr). Drillhole numbers refer to Figure 2. See Appendices 1 and 2 for a summary of drillhole locations, their stratigraphy and derivation of subsidence rates.

## 3.1 CORRECTION FOR CHANGES IN RELATIVE SEA LEVEL

Eustatic (or global) sea levels have fluctuated through time. These changes in sea level are strongly correlated with temperature cycles responsible for ice ages, as greater or lesser volumes of water are frozen and locked up on land in the Earth's polar regions. Warmer periods (such as now) produce higher sea levels and colder, glacial periods produce lower eustatic sea levels.

These climatic cycles also correlate with changes in oxygen isotope (OI) ratios in deep marine microfossil shells, which are a useful tool for correlating global climatic events. Figure 4 shows recently published estimates of past eustatic international sea levels for the last 450 ka. Both the sea level and OI curves typically have a saw-tooth shape, with a sharp rise and a step-wise fall. The eustatic sea level during the last interglacial stage (~125 ka ago) was about the same as modern sea levels, whereas during the peak of the last ice age (~18 ka ago) it was about 120 m lower. These changing sea levels will affect the elevation at which the transitions between marine and terrestrial strata (i.e., paleoshorelines; see below) are formed; thus they are included in our calculations of subsidence rates, below.

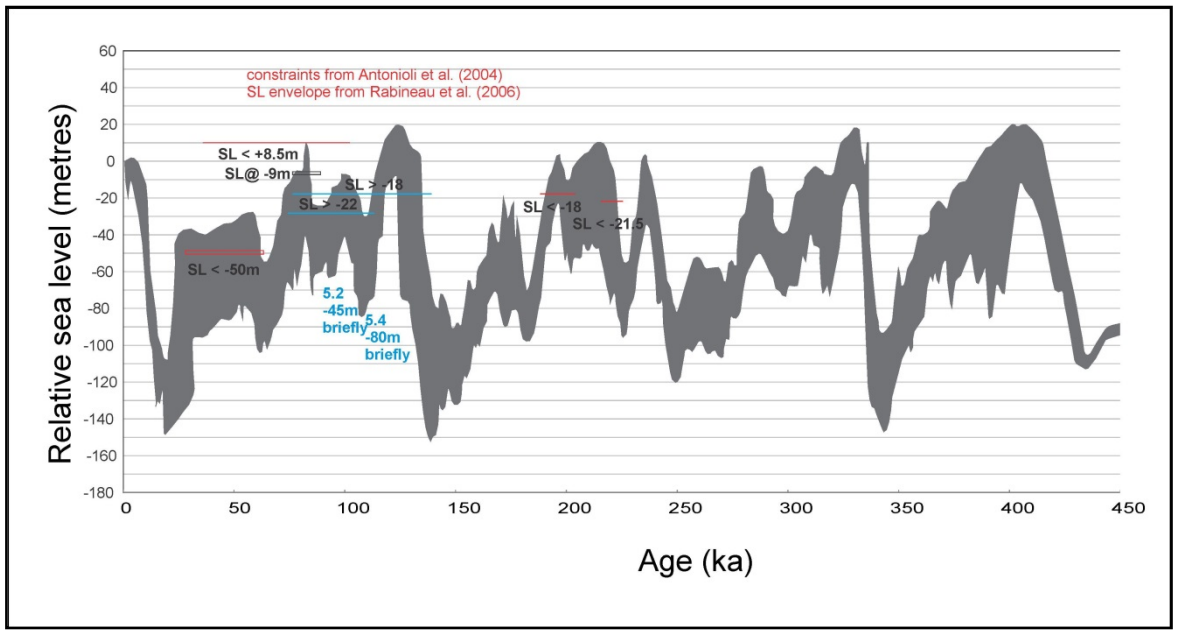


**Figure 4** Past sea levels (range of values) relative to present day for the last ~450 ka. Data from Rabineau et al. (2006), Antonioli et al. (2004) and Siddall et al. (2005).

Begg et al. (2002) used surface, drillhole and seismic data to assess the sediments beneath the lower Hutt Valley in the area between Avalon and Petone (e.g., Figure 2). They identified and correlated sub-surface deposits, including several paleoshorelines, which represent the past position of sea level at the drillhole locations. Paleoshorelines are recognised in drillholes by boundaries between materials deposited in marine environments and those deposited in terrestrial environments. By comparing the elevations of the paleoshorelines with published sea level curves (Gibb, 1986) and oxygen isotope (Imbrie et al., 1984; Bassinot et al., 1994; Martinson et al., 1987; Pillans et al., 1998) data, they inferred that if any paleoshoreline is lower than its time-correlative sea level, then that depressed landform must record subsidence. From the data available at the time, they inferred that all relevant paleoshorelines formed at a relative sea level of 0 m, and therefore did not require any eustatic sea level correction.

However, some recent studies of past sea levels in the Mediterranean Sea (Antonioli et al., 2004; Rabineau et al., 2006) and elsewhere (e.g., Siddall et al., 2005) have suggested that, for some of these paleoshorelines, the assumption that the relative sea level (RSL; i.e., relative to present day) was at zero was not valid. Table 1 shows a summary of recently published estimates of global sea levels for the relevant time periods of sediments in the Hutt Valley drillholes. It can be seen that some of these RSL values are significantly lower than the assumed zero value used by Begg et al. (2002) and we incorporate these differences into our subsidence rate calculations for drillhole data by subtracting the RSL range from the depth of the paleoshorelines.

**Table 1** Paleoshoreline data and corresponding relative sea level values for the last c. 450 ka. Columns 1 and 2 are paleoshoreline age and stratigraphy from Begg et al. (2002); column 3 shows correlation with global oxygen isotope (OI) stages, and age of corresponding peaks or troughs in OI record in column 4. Adopted mean sea levels used in our calculations of subsidence rates (and their uncertainty ranges) for the paleoshorelines are from the published sources listed in column 8. We use multiple sources, which best cover the range of relative sea levels over a particular time interval. Values in grey are data additional to the paleoshorelines used in this study. References are 1: Gibb (1986; as calibrated in Cochran et al., 2006); 2: Rabineau et al. (2006); 3: Antonioli et al. (2004); 4: Lisiecki & Raymo (2005); 5: Siddall et al. (2005). Data marked * are from Begg et al. (2002).

| Age (ka)* | Paleoshorelines* | Correlation with OI stage | OI age (ka) | Adopted mean sea level (m) | Min sea level (m) | Max sea level (m) | Ref. |
|---|---|---|---|---|---|---|---|
| 9 | Base of Petone Marine | E. Holocene | 9 | -18 | -20 | -16 | 1 |
| | | OI 2 | 19 | -102 | -108 | -96 | 2 |
| | | OI 3 | 45 | -22 | -27 | -17 | 3 |
| 78 | Top of Wilford | d18O falling? | 78 | -15 | -20 | -10 | 4 |
| 83 | Base of OI 5a | OI 5a | 80 | -16 | -21 | -11 | 3 |
| | | OI 5b (briefly) | 86.5 | -45 | -50 | -40 | 3 |
| 106 | Base of OI 5c | OI 5c | 100 | -16 | -21 | -11 | 3 |
| | | OI 5d (briefly) | 108 | -80 | -85 | -75 | 3 |
| 114 | Top of OI 5e | d18O falling? | 114 | -5 | -10 | 0 | 4 |
| 128 | Base of Wilford | OI 5e | 122 | 3 | 2 | 4 | 5 |
| | | OI 6 | 136 | -97 | -104 | -90 | 2 |
| 190 | Top of OI 7 | OI 7a | 190 | -18 | -23 | -13 | 3 |
| | | OI 7a | 197 | -10 | -15 | -5 | 5 |
| | | OI 7c | 214 | -21 | -26 | -16 | 3 |
| 222 | Base of OI 7 | OI 7c | 216 | -10 | -15 | -5 | 5 |
| | | OI 7e | 232.5 | -10 | -15 | -5 | 5 |
| | | OI 8 | 249 | -86 | -94 | -78 | 2 |
| | | OI 9c | 321 | 2.5 | -3 | 8 | 5 |
| | | OI 10 | 340 | -150 | -159 | -141 | 2 |
| | | OI 11 | 404 | 4 | -3 | 11 | 5 |
| | | OI 12 | 436 | -149 | -159 | -139 | 2 |

Inherent difficulties in dating and thus estimating sea level elevation significantly compromise uplift rate values for the ~9 ka "Base of Petone Marine beds" paleoshoreline. This early Holocene value is the most often recorded feature that could help in estimating vertical deformation. Gibb (1986) published a sea level curve for the New Zealand area, built from data obtained from parts of the country then deemed as tectonically stable (including many dates from the Christchurch area), which indicates that the relative sea level for 9 ka was about 16 to 20 m below present (allowing for calibration of stated radiocarbon years by GNS Rafter Laboratory 2006; see Cochran et al., 2006). This time is within a period of rapidly rising sea level from the end of the last glaciation into the early Holocene before sea level stabilisation at the modern level at about 7 ka (Figure 4). Thus, if we allow for this -16 to -20 m value in the calculations of vertical deformation from the drillhole data, it requires early Holocene uplift to accommodate the current elevation of the ~9 ka paleoshoreline at some locations (Appendix 2). Clearly there has been consistent late Pleistocene net subsidence in the lower Hutt Valley, based on geomorphological and stratigraphic reasoning as outlined by Begg et al. (2002), and net uplift during this period (over the past few thousand years) is not plausible.

The 9 ka paleoshoreline represents fewer earthquakes averaged over a shorter time and therefore the young tectonic signal using this datum incorporates much more noise and may not be representative of the long-term signal. There is also the issue raised above regarding age and relative sea level at the time. For these reasons we do not use the 9 ka datum for calculating our subsidence rates.

## 3.2 CONSOLIDATION CORRECTION OF SEDIMENT THICKNESSES

Consolidation of sediment is an important factor because it induces surface (and near-surface) subsidence which must be accounted for when calculating tectonic subsidence rates. Begg et al. (2002) applied a "compactibility factor" to the thicknesses of stratigraphic units identified in the drillholes to account for post-depositional consolidation of the sediments (Table 2). This factor was applied to various lithologies in a 30 m band beneath each of the identified paleoshorelines. The 30 m cut-off was chosen because any sediment deeper than that would have already been loaded and consolidated (and shaken) by the time that the subsequent shoreline sediments were deposited (e.g., Read et al., 1991).

Begg et al. (2002) used values of between 5% and 70% depending on lithology, but with no uncertainty range. We apply a similar consolidation factor to the unit thicknesses, but allow for uncertainties. Given the dearth of published geotechnical data for young sediments, we use a range of values to allow for its uncertainty by applying uncertainty "margins of error" of +/- 10% and +/- 25% to the original "compactibility factor" of Begg et al. (2002) (Table 2). We apply this margin of error to the lithological units in each of the eight drillholes used to calculate the total subsidence in the lower Hutt Valley and weight the +/- 10% and the +/- 25% values at 70% and 30%, respectively, in the logic tree (Appendix 3).

Other factors already incorporated in the Begg et al. (2002) data include an uncertainty in the recognition of the material boundary (or paleoshoreline horizon) and its depth down-hole as recorded in the logs. A value of +/- 1.5 m was assigned to each horizon, which we promulgate through our calculations.

**Table 2** Factors for deconsolidation of drillhole sediments applied to stratigraphic thicknesses (of each lithology in the "materials" column) in the 30 m band beneath each identified paleoshoreline. We now apply uncertainties of +/- 10% and +/- 25% to the original factors used by Begg et al. (2002).

| Materials | Original factor | Original +/- 10% | | Original +/- 25% | |
|---|---|---|---|---|---|
| Mud, silt, clay, sandy clay | 5% | 4.5% | 5.5% | 3.75% | 6.25% |
| Peaty clay and wood | 10% | 9% | 11% | 7.5% | 12.5% |
| Sandy silt, clay with organics | 15% | 13.5% | 16.5% | 11.25% | 18.75% |
| Sandy silt, peat | 70% | 63% | 77% | 52.5% | 87.5% |

## 3.3 SUMMARY OF HUTT VALLEY SUBSIDENCE RATE DATA

Mean subsidence rates calculated for each drillhole are shown on Figure 3. These rates have been calculated using the adopted mean sea level values and respective OI ages listed Table 1, combined with the deconsolidated depths of paleoshorelines identified in the drillholes (Appendix 1). A summary of the rates with each of the new uncertainty ranges is given in Appendix 2. For the western Gear Meat drillholes, this analysis indicates that the total subsidence rate is on the order of 0.7 to 0.9 mm/yr. Further up the valley, the Wakefield St drillhole has a total subsidence rate of ~0.6–0.8 mm/yr. The drillhole farthest up the valley at Ewen Bridge (Marsden St) indicates a subsidence rate of about 0.6–0.7 mm/yr, approximately the same as the North St drillhole which is further down and close to the centre of the valley. In the eastern side of the valley, two nearby drillholes (Seaview/Parkside Rd and Elizabeth St) indicate the lowest subsidence rates of about 0.3–0.5 mm/yr. All of these values include a component of uplift contributed by slip on the Wairarapa Fault, which will be accommodated in the steps below as part of our estimation of co-seismic subsidence associated with Wellington Fault rupture.

This page is intentionally left blank.

# 4.0 METHODOLOGY AND EQUATIONS FOR CALCULATING THE SINGLE EVENT DISPLACEMENT (SUBSIDENCE) RESULTING FROM RUPTURE OF THE WELLINGTON FAULT IN THE HUTT VALLEY

The focus of this report is determining single-event co-seismic subsidence in the Hutt Valley resulting from rupture of the Wellington Fault. In this section we present the equations that we use for this assessment and we summarise the various input parameters. These parameters are discussed in more detail in separate sections, below.

## 4.1 EQUATIONS

Long-term vertical deformation in the Hutt Valley is a combination of subsidence attributable to movement on the Wellington Fault, the uplift resulting from rupture of the Wairarapa Fault and vertical deformation that may, or may not, result from other factors. The relationship between these variables is given in equation (1) and each variable is discussed further in separate sections, below. Most of the variables have a range of uncertainties, which we propagate through the equations. We weight these uncertainties by using a logic tree structure (Appendix 3; Kulkarni et al., 1984) to give mean values of subsidence per event at the location of drillhole data. The total subsidence rate in the Hutt Valley can be described as:

$$\mathbf{Subs_{HV}} = \mathbf{Subs_{WrF}} + \mathbf{Subs_{WgF}} + \mathbf{Other} \quad \textbf{(1)}$$

Where $Subs_{HV}$ is the subsidence rate recorded in the Hutt Valley drillholes (Section 3, above),

$Subs_{WrF}$ is the negative subsidence (i.e., uplift) rate attributable to movement on the Wairarapa Fault (Section 5, below),

$Subs_{WgF}$ is the subsidence rate attributable to movement on the Wellington Fault (Section 6), and

Other is a factor of other influences on vertical deformation (e.g., subduction interface-related earthquakes) that may impact on the Hutt Valley (Section 7).

To remove the component of subsidence (uplift) in the Hutt Valley contributed by slip on the Wairarapa Fault ($\mathbf{Subs_{WrF}}$), we scale the known amount of uplift from geological records at Turakirae Head to the known amount of co-seismic uplift in the Hutt Valley that occurred during the 1855 Wairarapa earthquake using equation (2).

We use the 1855 uplift (i.e., for the most recent event) at Turakirae Head as one estimate of the single event vertical displacement (SEVD). As a comparison, we also use an average SEVD calculated from the elevation difference between the older beach ridges at Turakirae Head. This yields a similar value to the 1855 uplift and gives us more confidence that the 1855 event is approximately characteristic which, by inference, gives us confidence that the 1855 uplift value measured in the Hutt Valley is also representative of Wairarapa Fault vertical deformation there. We also acknowledge possible uncertainty in the number of Wairarapa Fault events (which affects the SEVD estimate at Turakirae Head) by allowing for possible earthquake events on the Wairarapa Fault as noted in paleoseismic trench investigations (e.g., Little et al., 2009; Van Dissen et al., 2013).

$$\mathbf{Subs_{WrF}} = \mathbf{Subs_{Turak}} * \left(\frac{\mathbf{SEVD_{1855HV}}}{\mathbf{SEVD}}\right) \quad \textbf{(2)}$$

Where $Subs_{Turak}$ is the Holocene subsidence (uplift) rate at Turakirae Head (Section 5.1),

SEVD is an estimate of the single event vertical displacement (uplift per event) for the Wairarapa Fault at Turakirae Head (Section 5.2), and

$SEVD_{1855HV}$ is the amount of subsidence (uplift) surveyed in the Hutt Valley during the 1855 Wairarapa earthquake (Section 5.2.5).

Once we have scaled and subtracted the past subsidence (uplift) rate attributable to the Wairarapa Fault in the Hutt Valley from the Hutt Valley subsidence rate (as deduced for the Hutt Valley drillhole record – see Section 3), the remaining subsidence rate is inferred to be caused by displacement on the Wellington Fault. We can use the recurrence interval (RI) of the Wellington Fault to calculate the co-seismic subsidence (***X***, in metres, per event) required to lower the stratigraphic horizons identified in drillhole data to their current elevations below sea level (at any one drillhole location) by using equation (3):

$$\mathbf{Subs_{WgF}} = \frac{\boldsymbol{X}\ \mathbf{(m\ per\ event)}}{\mathbf{RI}} \quad \textbf{(3)}$$

Where RI, the Recurrence Interval of the Wellington Fault, is taken from published data specific to that fault (Section 6.1).

## 5.0 CONTRIBUTION OF VERTICAL DEFORMATION IN THE HUTT VALLEY FROM THE WAIRARAPA FAULT

The tectonic influence of the Wairarapa Fault is manifest over a broad part of the south-western North Island, including the Hutt Valley. It was noted that during the 1855 Wairarapa earthquake, the lower Hutt Valley/Petone area was uplifted on the order of 1.2–1.5 m (Grapes & Downes, 1997, and references therein) (Figure 5). However, as outlined in the previous sections, the long-term net vertical deformation in the lower Hutt Valley has been subsidence (e.g., Begg & Mazengarb, 1996; Begg et al. 2002). To determine the amount of long-term tectonic subsidence in the Hutt Valley that has been contributed by slip on the Wellington Fault, it is necessary to identify and remove the component of uplift caused by the Wairarapa Fault. To achieve this we use the world-renowned, tectonically raised Holocene beach ridges preserved at Turakirae Head, on the south-eastern Wellington coast, which have also been uplifted by movement on the Wairarapa Fault. For a summary of the formation and tectonic significance of the preserved beaches, see McSaveney et al. (2006) and Little et al. (2009), and references therein.

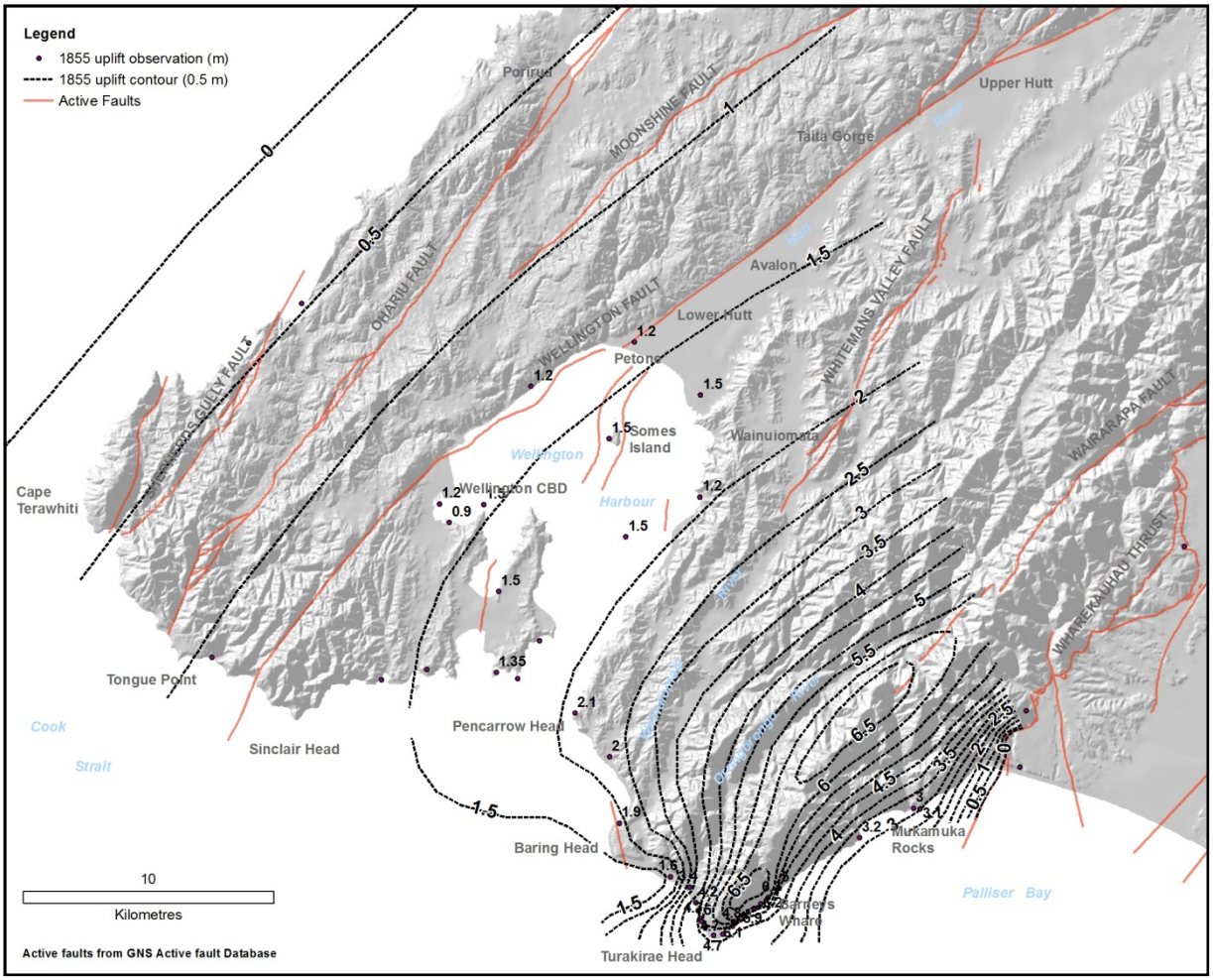


**Figure 5** Uplift (in metres) accompanying the 1855 Wairarapa earthquake, based on historical reports and topographic survey data (after Wellman, 1967; Grapes & Downes, 1997; and Hull & McSaveney, 1996).

## 5.1 CALCULATION OF UPLIFT RATES AT TURAKIRAE HEAD

Calculation of robust uplift rates is pivotal to this study. Using a remote sensing approach, we compare the survey locations of Hull & McSaveney (1996) with LiDAR digital elevation data (2013 acquisition, supplied by Hutt City Council) to reassess the relative heights of preserved beach ridges at Turakirae Head (see Appendix 4 for original and LiDAR survey data). We present no new data on the ages of the beach ridges and instead draw upon the dates published by Van Dissen et al. (2013), which are a compilation of various other sources listed in Table 3. The natural surface variability of the beach ridges is approximately +/- 0.3 m (Hull & McSaveney, 1996), which we incorporate as our elevation uncertainty value. Calculation of uplift rates is based on the following assumptions:

*ASSUMPTION 1*: The wave climate has not changed significantly during the Holocene. Therefore, the height above sea level of the modern, active beach ridge at any profile location is the same as that which previously existed for the now-elevated and inactive beach ridges that lie inland from the modern beach ridge.

*ASSUMPTION 2*: Ages of the beach ridges initially established by Hull & McSaveney (1996) and refined by Little et al. (2009) and Van Dissen et al. (2013) by correlation with region-wide tectonic events (Table 3) are correct.

We use the nomenclature of Hull & McSaveney (1996; after Moore, 1987), who importantly recognised that the lowest continuous beach ridge (BR1) preserved along the coast is in fact the modern storm beach and not the one raised in the 1855 Wairarapa earthquake, which is defined as BR2 (Figure 6; see also Grapes & Downes 1997). We also allow for the possibility of Wairarapa Fault earthquake events that are missing from the record at Turakirae Head, not preserved as discrete beach ridges, and insert two extra events (BR2A, BR3A) based on the ages of region-wide tectonic events as recorded in trench data for the Wairarapa Fault (Little et al., 2009; Van Dissen et al., 2013) (Table 3; Figure 6).

**Table 3** Adopted ages (calibrated) of beach ridges and their source, as outlined in Van Dissen et al. (2013). Dates are calculated relative to 1950 (years BP) but quoted in text relative to 2010 to give a more modern time reference and to acknowledge the time since the 1855 Wairarapa earthquake. The ages of BR2A and BR3A are based on paleoseismic trench data from the Wairarapa Fault (Little et al., 2009).

| | 1950 age datum | | | 2010 age datum | | | Adopted age source |
|---|---|---|---|---|---|---|---|
| | Mean age | Age min | Age max | Mean age | Age min | Age max | |
| BR1 | 0 | 0 | 0 | 0 | 0 | 0 | Modern |
| BR2 | 95 | 95 | 95 | 155 | 155 | 155 | Historic/AD 1855 |
| BR2A | 860 | 800 | 920 | 920 | 860 | 980 | Little et al. 2009 |
| BR3 | 2205 | 2110 | 2300 | 2265 | 2170 | 2360 | Little et al. (2009)/Cochran et al. (2007) |
| BR3A | 3495 | 3300 | 3690 | 3555 | 3360 | 3750 | Little et al. (2009)/Cochran et al. (2007) |
| BR4 | 5025 | 4840 | 5210 | 5085 | 4900 | 5270 | Little et al. (2009) |
| BR5 | 6765 | 6610 | 6920 | 6825 | 6670 | 6980 | McSaveney et al. (2006) |

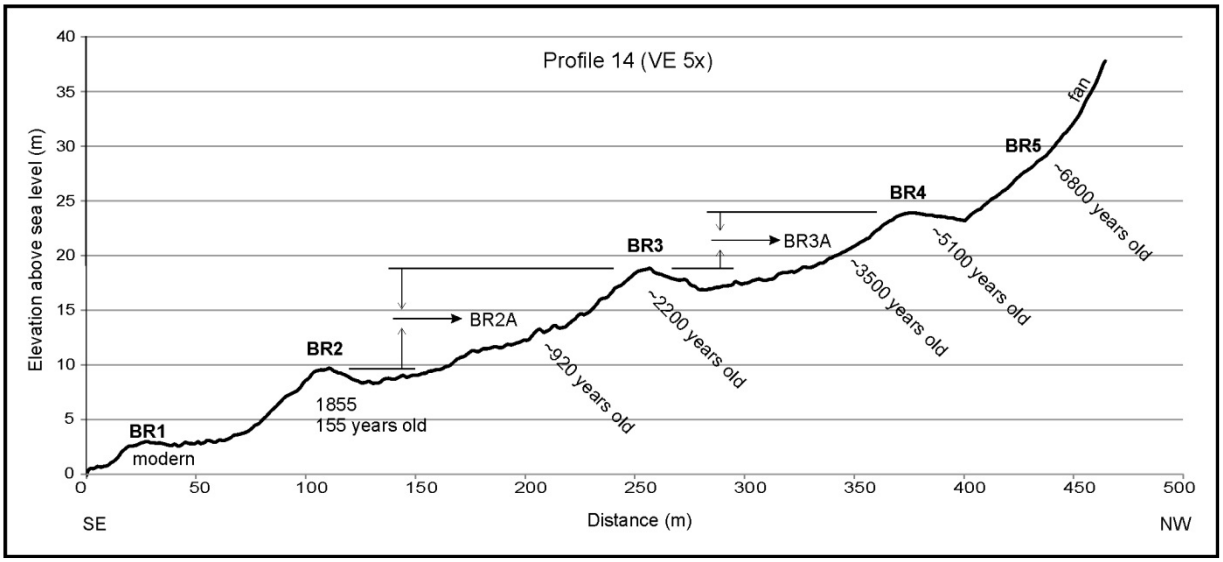


**Figure 6** Representative topographic profile of the uplifted coastal plain at Turakirae Head using LiDAR elevation data (Profile 14 of Hull & McSaveney, 1996). Beach ridge 1 is currently forming along the coastline at variable elevations (c. 2-4 m) above present mean sea level. Vertical exaggeration is 5x.

As a cross check on the currently published beach ridge elevations, we re-evaluated the survey data of Hull & McSaveney (1996) and compared them with the 2013 LiDAR data supplied by Hutt City Council (Figure 7). Correlative elevations of Hull & McSaveney (1996) survey points were obtained using a bi-linear interpolation of the LiDAR dataset in ArcMap® (using the Rastervalue function). The LiDAR data have a mean elevation that is 0.17 m lower than the correlative Hull & McSaveney (1996) survey data. This offset, which appears to be consistent ($R^2$=0.9995), is about half of the natural variability of the beach ridge topography (estimated by Hull & McSaveney to be +/- 0.3 m). Because the difference is consistent throughout the data, the calculations of *uplift rates*, which depend on elevation differences between beach ridges, will not differ significantly (i.e., the base datum is slightly lower, but differences *between* beach levels are affected equally); however, where available we use the LiDAR data to extract new values for elevations of the raised beaches (especially for BR2) so that we can compare them directly with LiDAR-derived elevations in the Hutt Valley.

We note that on Profiles 16 and 21–24 of Hull & McSaveney (1996) there is a significant difference in elevation of BR1 (as much as 2.2 m lower on the LiDAR data than measured by those authors; red squares on Figure 7). We interpret this difference to be real, and to be a consequence of recent shore-face erosion of the modern storm beach (including the original surveyed location) that has occurred in the time between the surveys. Thus we cannot rely on the LiDAR data for these survey points to represent the elevation of BR1 (and therefore the 1855 uplift calculation for BR2). By comparison with early 1900s photographs, Hull & McSaveney (1996) concluded that in the decades prior to their report there was some minor accretion of the modern storm beach, but that it had "substantially formed by 1911".

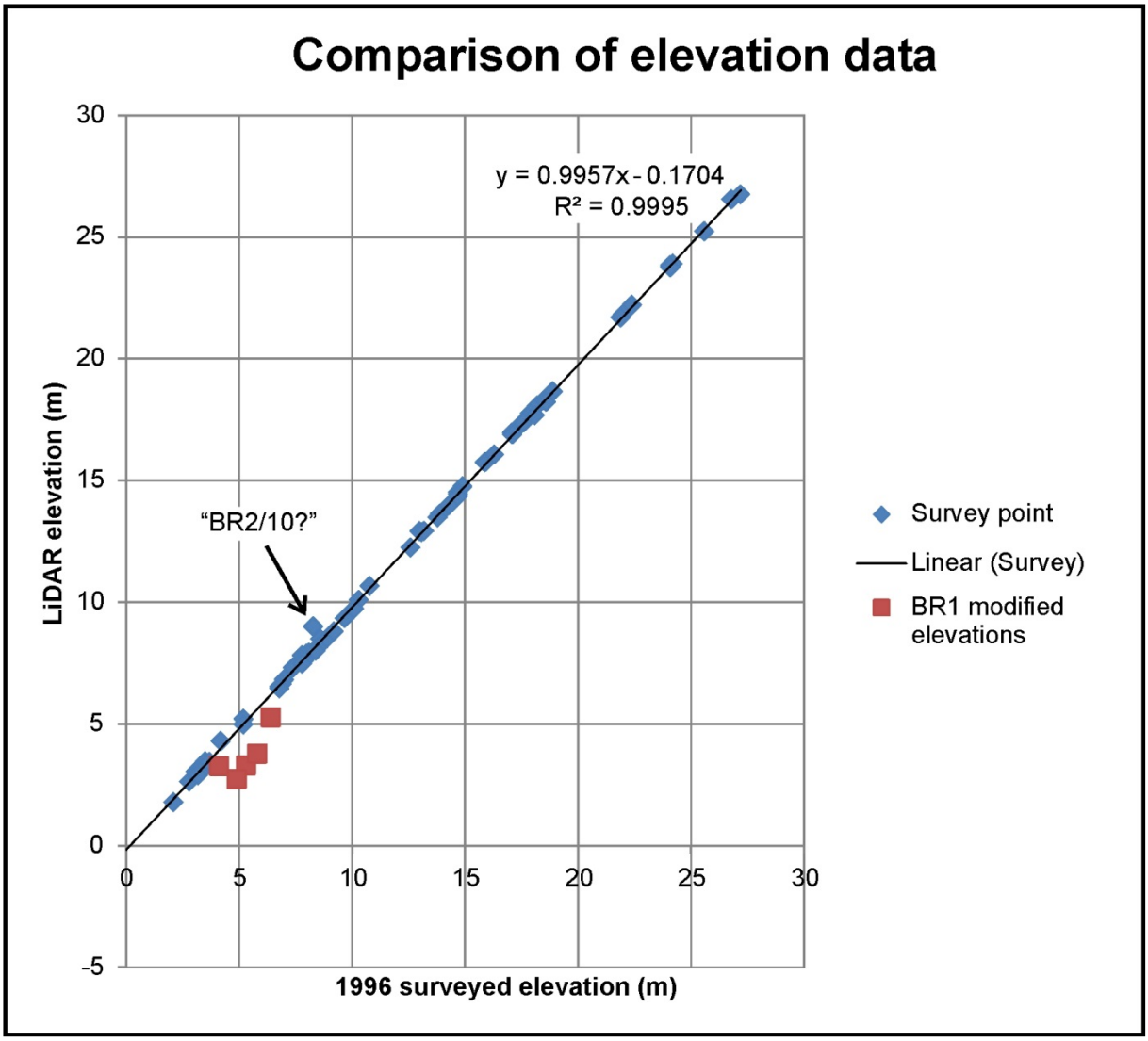


**Figure 7** Comparison of LiDAR elevation data (Hutt City Council) with surveyed elevations from Hull & McSaveney (1996) show that the two datasets are in good agreement with each other. We use the elevations derived from a bilinear interpolation of the LiDAR for our Wairarapa Fault uplift rate and single event displacement calculations at Turakirae Head.

Thus, we are confident that the upper extent of the modern storm beach had developed by 1996, and therefore the elevations measured relative to BR1 reflect tectonic uplift. Where LiDAR data are not available, or where we infer inter-survey modification of the modern beach ridge (e.g., through storm processes), we use Hull & McSaveney's (1996) surveyed elevation data. Another apparent outlier survey point is "BR2/10?" which, in the LiDAR data is 0.7 m above the 1996 surveyed elevation. This location is within a dispersed field of large (~5 m) boulders, and therefore the digital interpolation of the LiDAR data may be averaging this uneven topography (note also the "?" on the original notation of Hull & McSaveney (1996); see Appendix 4).

### 5.1.1 Correction for relative sea levels

Because the eustatic sea level was rising rapidly from the end of the Last Glacial stage (~18 ka) into the early Holocene (~7 ka), it is a potentially important factor to account for when determining the original elevation of formation for each of the Holocene beach ridges at Turakirae Head. We know that the modern beach ridge forms at varying elevations above present sea level due to factors such as the fetch of open-ocean, sea bottom contour and

aspect relative to prevailing major storms (Hull & McSaveney, 1996; McSaveney et al., 2006; Little et al., 2009). This height difference can be accounted for by assuming that, for any one profile, the ridges have formed at the same elevation relative to the contemporary sea level (*Assumption 1*, above).

We address variations in eustatic sea level by using sea level curves constructed from data relevant to stable New Zealand for the Holocene Epoch, and infer from them values of relative sea level (RSL) at the time of formation of each beach ridge (Table 3 and Table 4). These values are subtracted from the beach ridge elevations (older than BR2) to give their heights of formation relative to modern sea level. We use two different curves to account for uncertainty in published Holocene sea levels for the New Zealand region (e.g., Figure 8). We favour the (calibrated) curve of Gibb (1986) as it is constructed using data from areas within New Zealand considered tectonically stable; this curve implies stability at approximately the modern sea level, with minor fluctuations of less than 1 m, since about 7 ka ago (90% weighting in logic tree). We also include recently published Holocene sea level data from Clement et al. (2012) and Hayward et al. (2012), which suggest that there have been periods since 7 ka when sea levels have been up to 2 m higher than present (10% weighting in logic tree). We reject the model-derived RSL values of -4.27 m and -1.32 m for BR5 and BR4, respectively, used by McSaveney et al. (2006), in favour of empirically derived local sea level data.

Over the last century, mean sea level has risen by about 200 mm, averaging 2 mm/year (Parliamentary Commissioner for the Environment, 2014). The current projection for global sea level rise by the Intergovernmental Panel on Climate Change is about 300 mm by 2050, averaging about 40 mm/year (IPCC, 2013). This human-induced sea level rise is not accounted for in our calculations (by far the majority of the time interval involved in our calculations had no human-induced sea level rise) and the impact of human-induced sea level rise will compound (add) to the tectonic subsidence values that we present.

**Table 4** Corrections for relative sea level (RSL) at the time of beach ridge formation at Turakirae Head using two different correction curves. See text for explanation. In our subsequent calculations, we give 90% weight to the Gibb values, and 10% to the Hayward values. The ages of BR2A and BR3A are based on paleoseismic trench data from the Wairarapa Fault (Little et al., 2009; Van Dissen et al., 2013).

| | **Gibb (1986) sea level values (m)** | | **Hayward et al. (2012) sea level values (m)** | |
|---|---|---|---|---|
| | **RSL (m)** | **Uncertainty +/-** | **RSL (m)** | **Uncertainty Err+/-** |
| BR1 | 0 | - | 0 | - |
| BR2 | 0 | - | 0 | - |
| BR2A | 0 | 0.5 | -0.25 | 0.25 |
| BR3 | 0 | 0.5 | 1 | 0.5 |
| BR3A | 0.25 | 0.75 | 1.25 | 0.75 |
| BR4 | -0.25 | 0.75 | 1.25 | 0.75 |
| BR5 | 0.5 | 1 | 0.75 | 0.5 |

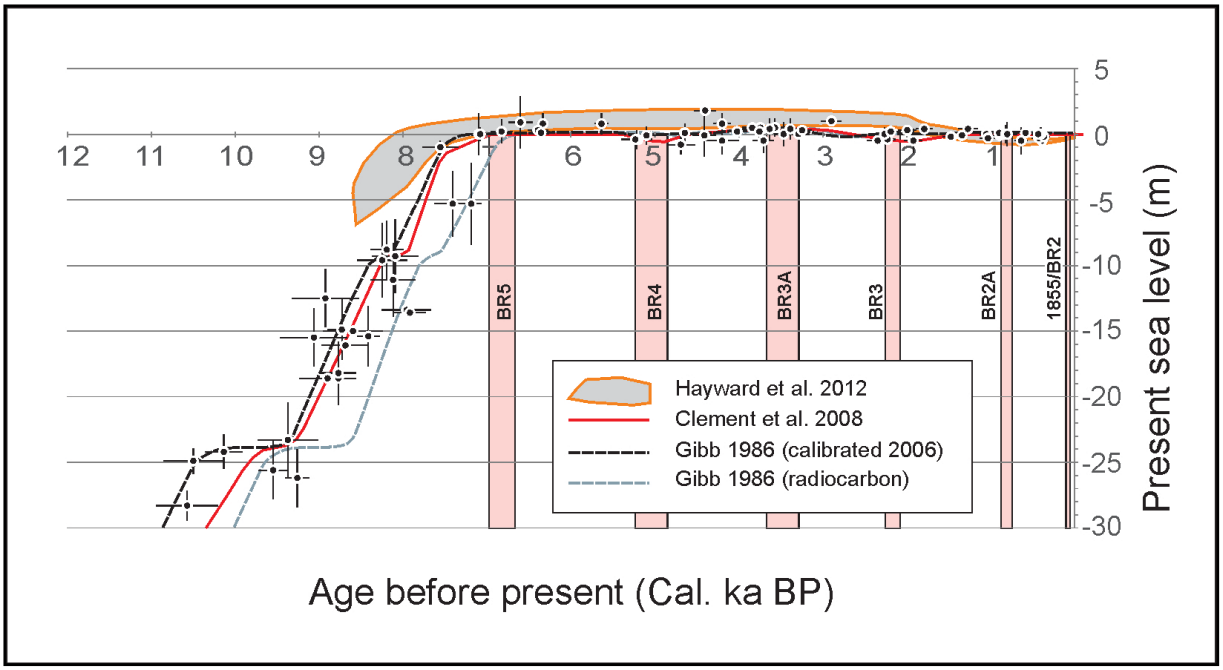


**Figure 8** Beach ridges at Turakirae Head in relation to Holocene sea levels. Data points (with age and elevation uncertainty range) are modified from Gibb (1986). Pink bands represent the timing of beach ridge uplift and abandonment. The ages of BR2A and BR3A are based on paleoseismic trench data from the Wairarapa Fault (Little et al., 2009; Van Dissen et al., 2013; see below).

### 5.1.2 Holocene uplift rates ($Subs_{Turak}$)

We derive Holocene uplift rates for the tectonically raised beaches at Turakirae Head for each profile where BR4 or BR5 is identified (Table 5, Figure 9). The rates for each profile are then scaled, using equations 2a-2c below, to each of the drillholes and then averaged. We compare the Holocene rate with one calculated from higher, Late Pleistocene (OI 5) marine terraces preserved nearby (Ota et al., 1981; Begg & Mazengarb, 1996).

All our uplift calculations use elevations of beach ridges relative to BR1 (the modern beach) along each profile. This is because BR1 is the current (pre-uplift) equivalent height of formation of the older ridges, and it has not undergone any Wairarapa Fault tectonic uplift events. In our opinion, the best long-term Holocene uplift rates are derived from the oldest beach ridges because they have undergone more uplift events and therefore smooth out some of the inherent uplift variability. In our choice of rate calculation, we use BR5 or BR4 where available, and rates for the younger beach ridges are not used (Table 5). The results using the Hayward et al. (2012) relative sea level corrections (based mostly on data from Clement et al., 2012) produce lower rates because sea level is inferred to have been up to 2 m higher compared with the Gibb (1986) sea level curve for the Holocene (see above).

The magnitude of uplift rates at Turakirae Head varies spatially; the highest Holocene rates (~3.5 mm/yr) occur on the NE-SW oriented part of the coastline at the western margin of Palliser Bay along the inferred axis of the Rimutaka Anticline (e.g., Wellman, 1967; Grapes & Downes, 1997), coincident with the maximum uplift (6.3 m) of BR2 calculated for the 1855 Wairarapa earthquake (e.g., Hull & McSaveney, 1996). Uplift rates diminish rapidly west of Turakirae Head such that, between the Orongorongo and Wainuiomata rivers, the rate is <1.2 mm/yr. We use the uplift rates in Table 5 (in bold) and carry them through our calculations for each profile to scale the effects of Wairarapa Fault uplift in the Hutt Valley, below.

**Table 5** Holocene uplift rates (in mm/yr) for profiles that include BR5 and/or BR4. Best rate (in **bold**) is calculated using BR5 and second best rate uses BR4 if BR5 was not identified on the profile. Rates using the beach ridge ages in Table 3 and two different sea level corrections based on values in Table 4 are presented.

| | Gibb (1986; Cal 2006) RSL | | Hayward et al. (2012) RSL | |
|---|---|---|---|---|
| | **BR5 uplift rate (best)** | **BR4 uplift rate (2nd best)** | **BR5 uplift rate (best)** | **BR4 uplift rate (2nd best)** |
| Profile 1 | **1.17** | 1.43 | **1.13** | 1.17 |
| Profile 3 | | **2.98** | | **2.64** |
| Profile 5 | | **3.00** | | **2.74** |
| Profile 6 | | **2.87** | | **2.62** |
| Profile 7 | | **3.12** | | **2.87** |
| Profile 8 | **2.74** | 3.11 | **2.70** | 2.86 |
| Profile 11 | **3.06** | 3.79 | **3.02** | 3.54 |
| Profile 12 | **3.31** | 3.97 | **3.28** | 3.72 |
| Profile 14 | **3.45** | 4.22 | **3.42** | 3.97 |
| Profile 15 | **3.42** | 4.12 | **3.38** | 3.86 |
| Profile 23 | | **2.17** | | **1.92** |

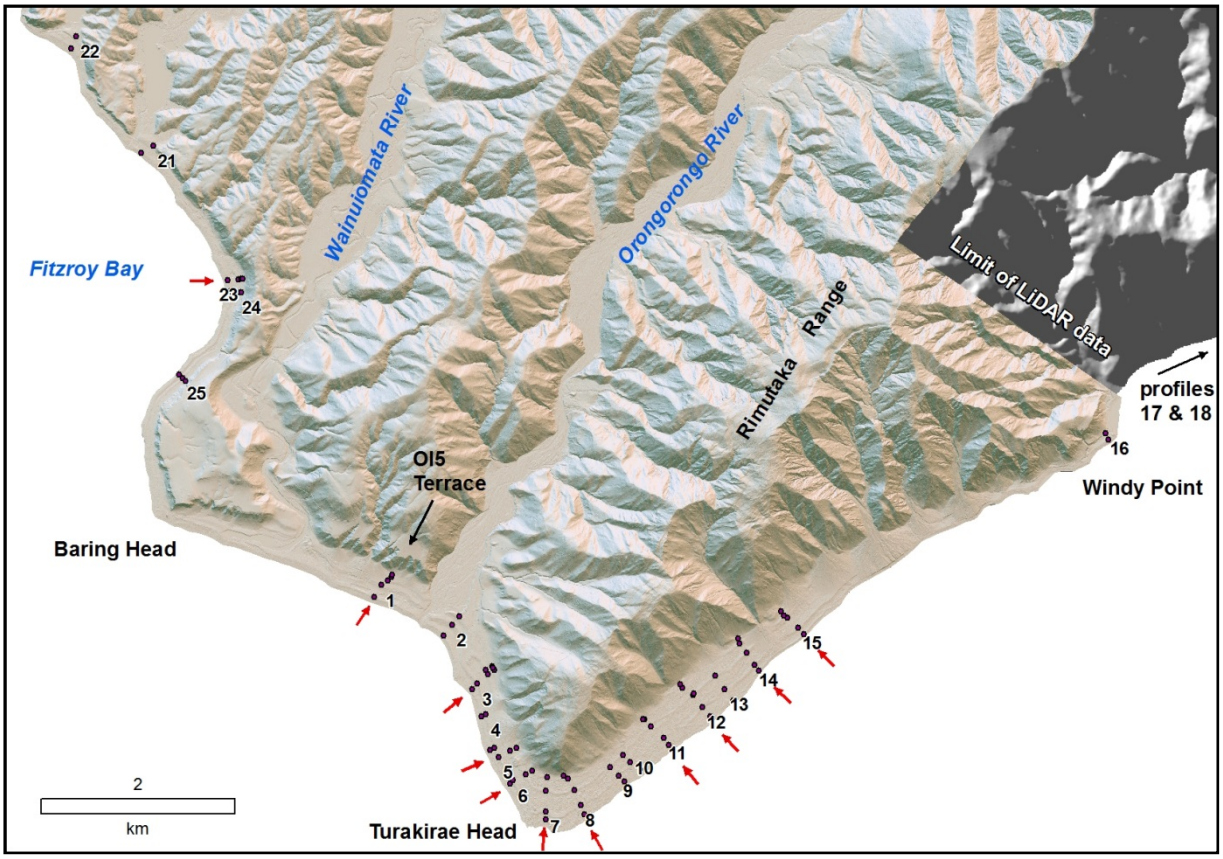


**Figure 9** Hill-shaded DEM showing location of survey profiles from Hull & McSaveney (1996) and reoccupied in this report. Only profiles for which BR5 and/or BR4 were identified (red arrows) are used in calculation of uplift rates (see Table 5). The location of the last interglacial (OI 5) marine terrace used in calculation of the Pleistocene uplift rate is also indicated.

### 5.1.3 Late Pleistocene uplift of Turakirae Head

We have also compared the Holocene uplift rate with a longer-term record calculated from raised marine terraces between the Orongorongo River and Baring Head (Figure 1) mapped by Ota et al. (1981) and Begg & Mazengarb (1996). Poor preservation of the older terraces means that we can only perform this comparison at one location (Profile 1; Figure 9). Uncertainties in the age correlations of the terraces, as well as uncertainty in the elevation of the terrace strath (i.e., the wave-cut surface beneath terrace coverbeds, which may be up to several metres thick), produce a large uncertainty in the calculated Pleistocene uplift rate. However, for Profile 1 the uplift rate calculated for the terrace, interpreted as being of Last Interglacial age (OI 5; approximately 125 ka old), is ~1 mm/yr, comparable with and corroborating the Holocene uplift rate of ~1.2 mm/yr at this location (see Table 5). Age correlations of terraces older than OI 5 are not well constrained, and therefore we do not calculate uplift rates from them.

## 5.2 Estimation of Single Event Vertical Displacement (SEVD) at Turakirae Head and scaling to the Hutt Valley

To use equation (2), we need to calculate the proportion of uplift at the Petone foreshore in the Hutt Valley during the 1855 earthquake relative to that experienced at Turakirae Head during the same earthquake. Unfortunately no raised beach is preserved in the Hutt Valley today for a direct comparison of the measurement, but uplift values of 4 feet (1.2 m) and 5 feet (1.5 m) were surveyed following the 1855 earthquake at the western and eastern ends of the foreshore, respectively (e.g., Grapes & Downes, 1997 and references therein).

The ratio of Hutt Valley uplift to Turakirae Head uplift during a Wairarapa Fault earthquake is part of equation (2), with the surveyed 1855 uplift in the Hutt Valley ($SEVD_{1855HV}$) as the numerator and the Turakirae Head single event vertical displacement (SEVD) as the denominator (see Section 5.2.1). In the equation, this ratio is then multiplied by the long-term Turakirae Head uplift rate ($Subs_{Turak}$) to yield the component of subsidence (uplift) rate attributable to Wairarapa Fault vertical deformation ($Subs_{WrF}$) at each drillhole site.

The above method is the only truly dimensionless ratio for comparing uplift between different sites. However, it uses a single measurement (in time) and assumes that the 1855 co-seismic uplift (both in the Hutt Valley and at Turakirae Head) is representative of average deformation on the Wairarapa Fault. As a test of this assumption, we calculated another estimate of the SEVD at Turakirae Head by averaging the uplift events recorded as the height differences between the beach ridges older than BR1 (Table 6; see Section 5.2.2). For each profile, the mean height difference ($SEVD_{mean}$) of 4.5 m is similar to the 1855 uplift amount ($SEVD_{1855Tk}$ in Table 6) of 4.3 m. This goes some way to corroborating the inference of typical behaviour in 1855 and gives us more confidence that the measurement of the only available Wairarapa Fault-derived uplift event in the Hutt Valley is representative of longer-term Wairarapa Fault vertical deformation there.

We also entertain the possibility that there are missing events on the Wairarapa Fault which are not recorded as discrete beach ridges at Turakirae Head. For this method we insert two extra events (between beach ridges 2 and 3, and 3 and 4, respectively), as indicated by paleoseismic investigation of the Wairarapa Fault (see Section 5.2.3, below), which reduces the mean SEVD and increases the CoV, both of which are carried through in specific branches of the logic tree (Table 3; Figure 6; Appendix 5).

For each profile we include the three different estimates of the Turakirae Head SEVD by substituting the denominator of the ratio outlined above: 1) using the 1855 uplift value at Turakirae Head ($SEVD_{1855Tk}$), which is the elevation difference between BR1 and BR2 (eqn 2a); 2) using the mean displacement ($SEVD_{mean}$), recorded as height differences between all beach ridges (eqn 2b); and 3) using a synthetic single event vertical displacement ($SEVD_{synth}$) of beach ridges allowing for possible missing events on the Wairarapa Fault (eqn 2c). We weight these three alternative methods 20%, 70% and 10%, respectively (see Appendix 3), and they are discussed in more detail in the following sub-sections.

**Table 6** Single event vertical displacement (SEVD) calculated as the height differences between adjacent beach ridges, using elevations from the LiDAR data and the Gibb 1986 sea level correction (see Section 5.1.1); we add +/- 0.3 m for elevation uncertainty to each value. See Appendix 5 for equivalent SEVD values for Hayward sea level correction, and the $SEVD_{synth}$ values for both sea level corrections.

| | BR1 to BR2 ($SEVD_{1855Tk}$) | BR2 to BR3 | BR3 to BR4 | BR4 to BR5 | MEAN ($SEVD_{mean}$) | STDEV | CoV |
|---|---|---|---|---|---|---|---|
| Profile 1 | 1.61 | 2.91 | 2.51 | 0.74 | 1.94 | 0.97 | 0.50 |
| Profile 3 | 4.25 | 5.61 | 4.82 | | 4.89 | 0.69 | 0.14 |
| Profile 5 | 4.87 | 6.76 | 3.15 | | 4.93 | 1.81 | 0.37 |
| Profile 6 | 4.72 | 6.19 | 3.25 | | 4.72 | 1.47 | 0.31 |
| Profile 7 | 4.70 | 6.02 | 4.66 | | 5.13 | 0.77 | 0.15 |
| Profile 8 | 4.77 | 6.93 | 3.63 | 2.96 | 4.57 | 1.74 | 0.38 |
| Profile 11 | 4.88 | 7.87 | 5.93 | 1.71 | 5.10 | 2.58 | 0.51 |
| Profile 12 | 5.87 | 8.42 | 5.27 | 2.54 | 5.53 | 2.42 | 0.44 |
| Profile 14 | 6.31 | 9.32 | 5.18 | 2.22 | 5.76 | 2.94 | 0.51 |
| Profile 15 | 5.03 | 9.73 | 5.53 | 2.49 | 5.70 | 3.00 | 0.53 |
| Profile 23 | 5.04 | 2.33 | 3.33 | | 3.57 | 1.37 | 0.39 |
| Mean | 4.33 | | | | 4.50 | | 0.38 |

### 5.2.1 Scaling using 1855 uplift at Turakirae Head as an estimate of SEVD

For one estimate of the SEVD at Turakirae Head, we use the amount of uplift that occurred during the most recent event: i.e., the 1855 Wairarapa earthquake. This is the elevation difference between BR2 and BR1 ($SEVD_{1855Tk}$ in Table 6; Appendix 5), which does not require sea level correction because both BR1 and BR2 are inferred to have formed under a "modern" sea level regime. This method relies heavily on Assumption 1 above, that the wave climate has not changed markedly during the late Holocene. We have recalculated the elevation difference using LiDAR data for the 11 profiles of Hull & McSaveney (1996) for which we have uplift rates (Table 5). For this branch in the logic tree we apply an uncertainty of +/-0.3 m (i.e., the beach variability estimated by Hull & McSaveney, 1996) to the elevation of each beach ridge prior to subtraction. This method uses the 1855 uplift value ($SEVD_{1855Turak}$) as the denominator and the surveyed 1855 uplift in the Hutt Valley ($SEVD_{1855HV}$) as the numerator for the ratio of Turakirae Head to Hutt Valley uplift.

$$\mathbf{Subs_{WrF}} = \mathbf{Subs_{Turak}} * \left(\frac{\mathbf{SEVD_{1855HV}}}{\mathbf{SEVD_{1855Tk}}}\right) \quad \textbf{(2a)}$$

This branch is given a 20% weighting in the logic tree.

### 5.2.2 Scaling using the mean SEVD at Turakirae Head

As another estimate of SEVD at Turakirae Head, we use the mean of the uplift values. For each profile we use the height differences between adjacent beach ridges to infer mean co-seismic single event vertical displacements for pre-historic uplift events at Turakirae Head ($SEVD_{mean}$ in Table 6; Appendix 5). The individual values at any one profile are remarkably consistent (the average coefficient of variation is about 0.38), implying that the pattern of uplift is approximately characteristic, or that a consistent amount of uplift has occurred at each profile or site for each Wairarapa Fault event in the Holocene.

We use the mean single event displacement ($SEVD_{mean}$) for each profile and scale the uplift to the Hutt Valley vertical deformation using equation (2b):

$$\mathbf{Subs_{WrF}} = \mathbf{Subs_{Turak}} * \left(\frac{\mathbf{SEVD_{1855HV}}}{\mathbf{SEVD_{mean}}}\right) \quad \textbf{(2b)}$$

This branch is given a 70% weighting in the logic tree.

### 5.2.3 Scaling using synthetic SEVD (based on trench data)

As a third estimate of SEVD, we have also entertained the possibility that there are surface rupturing earthquakes on the Wairarapa Fault which are missing from the Turakirae Head record (i.e., are not recorded as discrete beach ridges). These earthquakes are indicated by paleoseismic investigation of the Wairarapa Fault, e.g., at Cross Creek (Little et al., 2009; Van Dissen et al., 2013), and by detailed stratigraphic analysis of shallow coastal lake environments c. 10 km northwest of Turakirae Head (Cochran et al., 2007). These earthquakes are denoted in Table 3, Figure 6 and Appendix 5 by BR2A and BR3A, with respective ages of 800-920 and 3300-3690 cal. years BP (i.e., between beach ridges 2 and 3, and 3 and 4 respectively).

The addition of these “synthetic” beach ridges serves to reduce the uplift per event at Turakirae Head, but does not alter the overall uplift rate because they are inserted within the existing record and do not change the elevation of the beach ridges used to calculate the uplift rates (BR4 and BR5). We have assigned an average elevation value to each of these “synthetic” beach ridges, along each profile, as that which is half way between the older and younger beach ridges, based on the ages of the events from Van Dissen et al. (2013) (Figure 6, Figure 8, Table 4). We assign an elevation uncertainty that is normally distributed and bounded by the elevations of the enclosing beach ridges. Accordingly, BR2A is assigned an elevation half way between BR2 and BR3 that is normally distributed between the elevations of those two beach ridges; similarly BR3A has an intermediate elevation between BR3 and BR4. As above, the mean $SEVD_{synth}$ values are calculated and scaled to the Hutt Valley uplift for each profile using equation (2c):

$$\mathbf{Subs_{WrF}} = \mathbf{Subs_{Turak}} * \left(\frac{\mathbf{SEVD_{1855HV}}}{\mathbf{SEVD_{synth}}}\right) \quad \textbf{(2c)}$$

This branch is given a 10% weighting in the logic tree.

### 5.2.4 Variability of uplift at Turakirae Head

Additionally, for logic tree branches including the mean (eqn. 2b) and synthetic (eqn. 2c) scaling relationships outlined above, we incorporate published information regarding the variability of slip per event (at a point) on faults worldwide (Hecker et al., 2013). Analysis of a compilation of measured surface displacements for faults with multiple displacement measurements at a single site suggests that the coefficient of variation (CoV; standard deviation/mean) is 0.48+/-0.04; i.e., the standard deviation of displacements observed at these sites is approximately half of the mean value. For example, at a site with a mean displacement of 2 m, 68% of events would have displacements of between 1 and 3 m (Hecker et al., 2013). The style of faulting (whether strike-slip or dip-slip) makes little difference to the CoV value.

The CoV of the $SEVD_{mean}$ was calculated for the 11 profiles in Table 5. Using the Gibb (1986) sea level correction curve, the CoV varies between 0.14 and 0.52 (mean 0.38). Using the Hayward et al. (2012) sea level correction, the CoV varies between 0.45 and 0.80 (mean 0.61). For the synthetic beach ridges (with two extra events) the CoV ranges between 0.23 and 0.70 (mean 0.39) for the Gibb 1986 sea level correction, and 0.41 to 0.77 (mean 0.60) for the Hayward et al. (2012) sea level correction.

We favour the two empirically derived estimates of uplift per event from above ($SEVD_{mean}$ and $SEVD_{synth}$) and weight both of these factors at 75% in the sub-branch of the logic tree, (see Appendix 3 and section 9.3, below) but allow for the published CoV value of ~0.5 from Hecker et al. (2013) and give this a weighting of 25%.

Calculation of a CoV for the 1855 uplift ($SEVD_{1855Tk}$; the most recent event) is not possible because a CoV cannot be calculated for 1 measurement in time. However, all three estimates of SEVD ($SEVD_{mean}$, $SEVD_{synth}$ and $SEVD_{1855Tk}$, with 70%, 10% and 20% weighting, respectively) are incorporated in the logic tree (Appendix 3).

### 5.2.5 Variability of 1855 uplift measured in the Hutt Valley

Differential uplift (westward tilting) of the Hutt Valley accompanying the 1855 Wairarapa earthquake was widely reported. Grapes and Downes (1997) show contours of 1855 uplift (their Fig. 39), but the contours are very generalised and do not honour all stated data points, especially the 1.2 m at Lowry Bay, eastern Wellington Harbour (see also Figure 5, above). To account for these different estimates of 1855 uplift in the Hutt Valley ($SEVD_{1855HV}$), we employ another branch in our logic tree (Appendix 3). For one branch we use the recorded values of 1.2 m and 1.5 m at the coast (Petone wharf and Seaview) and project contours of equal uplift from the survey locations up the Hutt Valley. We infer these equal uplift contours to be parallel with the mean strike of the Wairarapa Fault (~042°) and interpolate variable uplift values for individual drillhole locations in between. This branch effectively accounts for the "tilt" factor of Begg et al. (2002). In another branch we use an average uplift value for the entire Hutt Valley of 1.4 +/- 0.3 m and apply this as a constant to the drillhole data (e.g., Begg et al., 2002). An equal weighting of 50% is given to each of these branches in the logic tree.

## 5.3 SUMMARY OF WAIRARAPA FAULT VERTICAL DEFORMATION (SUBSWRF)

At the locations of the Hutt Valley drillholes, we derive values of uplift (i.e., negative subsidence – see equation 1) rate for the component of vertical deformation attributable to the Wairarapa Fault in order to isolate the component of subsidence rate related to the Wellington Fault.

For individual profiles at Turakirae Head, we derive uplift rates and uplift per event values measured from preserved beach ridges of known or inferred age. Calculation of the uplift rates accounts for past differences in relative sea level (RSL) at the time of beach ridge formation. The majority weighting (90%) uses a RSL curve which assumes only minor variability of less than +/- 1 m from the modern sea level over the period of interest. Another sea level curve is considered (10% weighting) which has up to 2 m of fluctuation from modern sea levels.

We account for the variability of the uplift per event by incorporating three different estimates of this value in our logic tree. One uses the most recent event ($SEVD_{1855Tk}$; 1855 Wairarapa earthquake uplift value; 20% weighting), another uses the mean single event vertical displacement ($SEVD_{mean}$; average separation of all other beach ridges; 70% weighting), while the last uses the mean SEVD, but with two "extra" events inserted ($SEVD_{synth}$; based on additional information from paleoseismic trenching studies on the Wairarapa Fault; 10% weighting). For the latter two values, we also explicitly incorporate SEVD variability by employing a CoV of SEVD that is derived from internal statistics for each profile (75% weighting) and from a published value of 0.5 (25% weighting).

From these estimations of single event (uplift) displacement we derive the ratio of uplift at Turakirae Head to uplift in the Hutt Valley. We account for variation in 1855 uplift values in the Hutt Valley by factoring in a flatly-applied mean of 1.4 +/- 0.3 m ("constant") and by using values interpolated between the observed (surveyed) uplift of 1.2 m and 1.5 m in western and eastern Hutt Valley, respectively ("tilt"). These two choices in the logic tree are weighted equally (Appendix 3).

# 6.0 CONTRIBUTION OF VERTICAL DEFORMATION IN THE HUTT VALLEY FROM THE WELLINGTON FAULT

Once we know the total subsidence rate for the Hutt Valley ($Subs_{HV}$; from drillhole data) and have subtracted the contribution of uplift from the Wairarapa Fault ($Subs_{WrF}$; from the scaling relationships outlined above), the remaining vertical deformation must be a consequence of the Wellington Fault ($Subs_{WgF}$; and potentially "other" sources – see section 7). We can use the age and elevation of a paleoshoreline and divide it by the expected number of earthquakes calculated from the recurrence interval of the Wellington Fault to calculate the amount of subsidence per event (X) necessary to lower it to its current elevation. By inference, this is the expected subsidence likely to occur in a future Wellington Fault rupture event.

## 6.1 WELLINGTON FAULT RECURRENCE INTERVAL

The recurrence interval for surface rupture earthquakes (RI) for the Wellington Fault is calculated here in two ways: 1) using a measured single event displacement of geomorphic features of known age in combination with published slip rate data, and 2) using the number of events and their ages obtained from paleoseismic trench data. In the logic tree we use an equal weighting for each method. The two methods are discussed briefly, below.

### 6.1.1 RI based on single event displacement (SED) and slip rate

In our calculations using this method the RI = SED/slip rate. The SED of surface rupture of the Wellington Fault has recently been updated by Little et al. (2010). These authors measured Holocene terrace risers and paleochannels, and calculated a SED of 5 +/- 1.5 m, with a standard error of 0.75 m (Rhoades et al., 2011). The coefficient of variation is 0.3, less than the global average for point measurements on strike-slip faults (~0.5; e.g., Hecker et al., 2013).

The Late Quaternary slip rate of the Wellington Fault has also been redefined recently. Ninis et al. (2013) measured and dated displaced fluvial terraces along the Hutt River and determined a horizontal slip rate of 6.3 +1.9 / -1.2 mm/yr for the last ~100 ka. They note that this slip rate has not been constant over this time and that there have been periods of relatively fast and relatively slow activity. However, for the purposes of this study we use an average long term rate. Combining the SED and slip rate above gives a RI of ~ 800–1000 yrs.

### 6.1.2 RI based on trench data

We can also use the recurrence interval of the Wellington Fault determined from a compilation of dated events in paleoseismic trenches. This method relies on an assumption that the Wellington-Hutt Valley segment of the Wellington Fault (from offshore/Cook Strait to the southern Tararua Range) acts as a single entity that has a single rupture history (Langridge et al., 2011).

Data from trenches along the Wellington Fault indicate that there have been 9 surface rupturing earthquakes in the last c. 11.7 ka (Langridge et al., 2009, 2011; Rhoades et al., 2011). Accounting for dating uncertainties, the total time interval is 10210 to 11770 years. This gives a mean 8-inter-event RI of 1280–1470.

## 6.2 SUMMARY OF RECURRENCE INTERVAL (RI) DATA

We account for differences in the derivation of RI values for the Wellington Fault by including two methods in our calculations. One method produces a RI of ~800–1000 years while the other yields ~1300–1500 years. This is arguably the biggest uncertainty, or variability, in the calculation of subsidence per event. In our subsequent calculations, we weight each of these options equally (Appendix 3). See section 8.2 below, on sensitivity tests, for a breakdown of how the choice of weighting affects the final subsidence values.

## 7.0 OTHER FACTORS INFLUENCING VERTICAL DEFORMATION

The Wellington region has a number of surface active fault traces and is also susceptible to large earthquakes generated by slip on the subduction zone interface between the Pacific and Australia tectonic plates (e.g., Wallace et al., 2009, 2012). This section discusses whether it is conceivable that one or more of these features may contribute components of vertical deformation that may impact on our calculations.

Other known active faults in the area, including the Shepherds Gully, Ohariu, the Moonshine-Takapu, Evans Bay, Akatarawa and Whitemans Valley faults, are distant to the lower Hutt Valley. Most are known to be steeply dipping and to rupture with predominantly dextral strike-slip displacement. With the possible exception of the Ohariu Fault, which is associated with a thin Quaternary sequence at Porirua, none is intimately associated with substantial thicknesses of Quaternary deposits and hence significant vertical displacement. Further, relative long-term vertical displacements across the active faults west of the Wellington Fault can be quantified using the K surface. None shows a vertical displacement that approaches that of the Wellington Fault (e.g., Figure 1).

Vertical deformation is also recorded for the Holocene in the Wellington region (Cochran et al., 2007) with uplift dominating the western side of fault blocks and a small amount of localised subsidence on the east. Together these factors suggest that it is unlikely that any of the steeply dipping, surface rupturing active faults, other than the Wellington Fault, contribute significantly to lower Hutt Valley subsidence.

The interseismically coupled (or locked) subduction interface of the southern part of the Hikurangi margin, near Wellington, has potential to generate great (>$M_w$ 8) earthquakes (e.g., Stirling et al., 2012). Such earthquakes are associated with large fault plane slip displacements and the potential exists for significant vertical deformation at the surface. Because the Wellington region is entirely underlain by the subduction interface at a depth of ~20–30 km below the surface (Williams et al., 2013), deformation associated with these large earthquakes will impact regionally, affecting all parts of the study area similarly, rather than just locally in the lower Hutt Valley. That is, the area west of the Wellington Fault will experience vertical deformation similar to the lower Hutt Valley, and no relative displacement between them is likely.

Evidence for these large subduction zone earthquakes presently is scant and difficult to quantify (e.g., Clark et al., 2011; Wallace et al., 2014). Beneath Wellington, the subduction interface may be similar to a number of others around the world, where vertical deformation associated with rupture is partially recovered during the interseismic period (e.g., following the Mw 9.2 1964 Alaskan Earthquake; Brown et al., 1977; Prescott & Lisowski, 1977). Alternatively, if the Wellington Fault ruptures (sometimes or always) in association with subduction interface rupture, then a localised component of lower Hutt Valley subsidence may result. In this scenario, our calculations hold true, because the Wellington Fault is the principle locus of the local deformation.

If, however, the long-term regional signal (of subduction interface rupture) proves to involve subsidence, then our values calculated below are overestimates. Also, if this is the case, then there is another source of subsidence additional to the Wellington Fault affecting the Hutt Valley, and subsidence events would occur more frequently. Conversely, if the long-term regional signal is uplift, which is more likely given preservation of marine terraces along the south Wellington coast, then we have underestimated the Wellington Fault-driven subsidence per event in our calculations below.

In summary, if the long-term regional signal is significant, the pattern of vertical deformation will be different from effects of local structures such as Wellington and Wairarapa faults. Given the deformation of the K Surface and the geomorphology of the Hutt Valley, with sedimentary basins developed along the fault and westward fanning of stratigraphy beneath the Wellington Harbour, these are clearly consequences of local deformation. We therefore have to assume that the biggest player in vertical deformation in this area is local and attributable to the Wellington Fault.

In conclusion, there is little or no convincing evidence to suggest that either the other active faults in the Wellington region or the subduction interface provide significant long-term contributions to the vertical deformation of the lower Hutt Valley and we have built no contribution from such sources into our calculations.

# 8.0 MEAN SUBSIDENCE PER EVENT IN THE HUTT VALLEY DUE TO A WELLINGTON FAULT RUPTURE

## 8.1 SUBSIDENCE AT DRILLHOLE LOCATIONS (AND CONTOURS)

In this section we use our calculated values for the subsidence attributable to the Wellington Fault in the Hutt Valley ($Subs_{WgF}$ – Section 5) with published information on the RI for the Wellington Fault (Section 6) to determine the subsidence per event (single event displacement) necessary to lower the sediments in the Hutt Valley drillholes to their current positions below the valley floor. The subsidence per event, X, for the Wellington Fault at a given (drillhole) location is calculated from equation (3) and summarised to the nearest decimetre in Table 7 (see Appendix 6 for more precise values). We derive mean values for drillhole locations accommodating the weightings and uncertainties previously discussed and listed in our logic tree (see Appendix 3). Mean subsidence per event values are ~1.9 m in the west near Petone, ~1.5 m in eastern Hutt and ~1.7 m up valley at Ewen Bridge. Standard deviation (SD) values provide an indication of how well constrained the mean values are.

$$\mathbf{Subs_{WgF}} = \frac{\mathbf{X\ (m\ per\ event)}}{\mathbf{RI}} \quad \textbf{(3)}$$

**Table 7** Mean and Standard Deviation (averaging across profiles) of subsidence per event calculated for a Wellington Fault rupture at the location of each Hutt Valley drillhole. See Appendix 6 for more precise values.

| Drillhole location | Mean subsidence per event (m) | Standard deviation (m) |
|---|---|---|
| North Street | 1.7 | 0.54 |
| Gear Meat 151 | 1.8 | 0.58 |
| Gear Meat 319 | 1.9 | 0.59 |
| Gear Meat 320 | 1.9 | 0.60 |
| Wakefield Street | 1.8 | 0.55 |
| Seaview | 1.5 | 0.50 |
| Elizabeth Street | 1.5 | 0.49 |
| Marsden Street | 1.7 | 0.54 |

On Figure 10 we present contours of the values of mean Wellington Fault subsidence per event in a manner similar to Begg et al. (2002). Point data have been contoured to represent localised subsidence resulting from deformation on the Wellington Fault. We infer that subsidence is intimately associated with the Wellington Fault and therefore swing the contours to become fault-parallel to the south. We also infer that Taita Gorge, the northeastern extent of the Lower Hutt basin, where the valley is narrowest and bedrock is no deeper than 15 m below the surface across the fault (Silverstream bridges foundations drillhole data) has a subsidence value of zero. We extrapolate contours to the east of the Hutt Valley based on a constant interval equal to that between the western and eastern drillholes, while attempting to be conservative and limit (minimise) the area affected by subsidence. This pattern is also compatible with northwest (head-ward) tilting of the upper Wainuiomata Valley (Cotton, 1921; Stevens 1974; Begg et al., 1993).

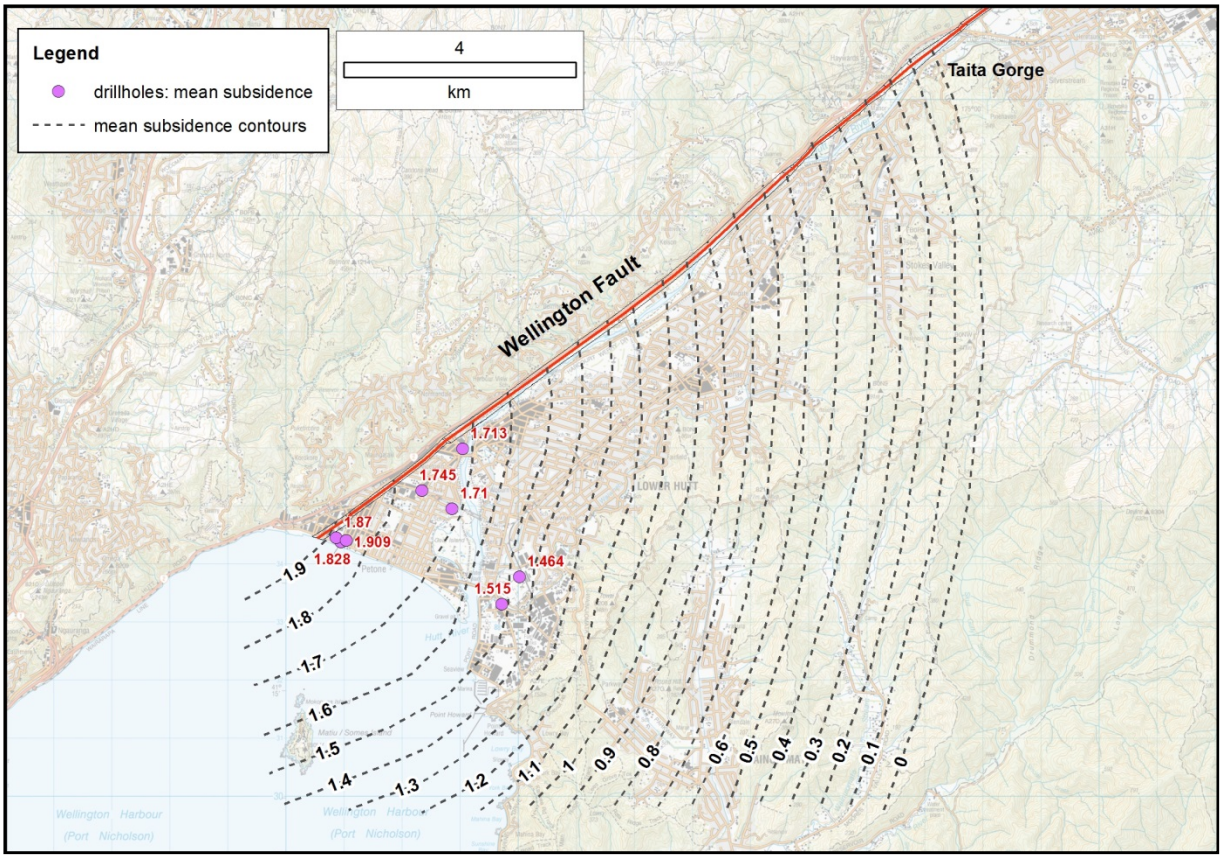


**Figure 10** Contoured values of mean subsidence per event (m) for a Wellington Fault surface rupture calculated from the methods outlined above. We assume that there is no differential vertical displacement (subsidence) across the Wellington Fault at Taita Gorge. See Section 9.3 for minimum and maximum credible subsidence values.

## 8.2 SENSITIVITY TESTS OF INPUT VARIABLES

The sensitivity of the main input variables of the logic tree was tested to determine which variable (deconsolidation factor, sea level correction, choice of SEVD value, 1855 uplift scaling factors, RI on Wellington Fault) has the most impact on the final result (Table 8). The overall average subsidence of all drillholes (-1719 mm) was used for the comparison. Where there is a branch option in the tree, each variable (or weighting choice) being tested was successively weighted at 100% while the other branch(es) at the same level were weighted at 0%; all other variables were kept constant at their original weighting value(s). The outcome of this testing is that the value of Wellington Fault-driven Hutt Valley subsidence is most sensitive to uncertainties in the recurrence interval of the Wellington Fault, with ~460 mm (about 0.5 m) deviation depending on which method of determining the RI value is chosen. Shorter Wellington Fault RIs lead to lesser amounts of estimated co-seismic subsidence in the Hutt Valley; conversely, longer Wellington Fault RIs lead to greater amounts of estimated co-seismic subsidence. The route to better constraining subsidence of the lower Hutt Valley is via better constraining the recurrence interval of Wellington Fault rupture.

The value for synthetic SEVD at Turakirae Head also has a significant impact, though it should be noted that this option in the logic tree is only assigned a 10% weight (i.e., we do not consider it a very realistic option).

**Table 8** The average subsidence value for all drillholes (1.72 m) is used to compare the sensitivity of input variables in the logic tree. The larger the values of "difference from mean" are, the more impact that that variable has on the final result. See text for full explanation. Table abbreviations: WgF: Wellington Fault; WrF: Wairarapa Fault.

| Branch or variable | Subsidence (m) | Difference from mean (m) | Logic tree weight (%) |
|---|---|---|---|
| Deconsolidation +10% | 1.72 | 0.00 | 25 |
| Deconsolidation +25% | 1.72 | 0.00 | 75 |
| | | | |
| RSL Gibb | 1.72 | 0.00 | 90 |
| RSL Hayward | 1.75 | -0.03 | 10 |
| | | | |
| WgF RI from SED & SR | 1.26 | 0.46 | 50 |
| WgF RI from trench data | 2.18 | -0.46 | 50 |
| | | | |
| WrF CoV calculated | 1.72 | 0.00 | 75 |
| WrF CoV 50% | 1.72 | 0.00 | 25 |
| | | | |
| Turakirae $SEVD_{1855Tk}$ | 1.64 | 0.08 | 20 |
| Turakirae $SEVD_{mean}$ | 1.68 | 0.04 | 70 |
| Turakirae $SEVD_{synth}$ | 2.16 | -0.44 | 10 |

This page is intentionally left blank.

# 9.0 MAPPING THE SINGLE EVENT DISPLACEMENT SUBSIDENCE IN THE LOWER HUTT VALLEY

## 9.1 GRIDDING AND PRODUCTION OF POST EVENT SEA LEVEL CONTOURS

We use the contoured subsidence per event values for the mean Wellington Fault rupture (Figure 10) to create GIS grid files and subtract the estimated subsidence from the LiDAR elevation data in a forward-modelling approach to generate a picture of the future ground surface following an average, or mean, Wellington Fault subsidence event in the Hutt Valley. A post-event sea level (zero m contour) is extracted from the model to show areas at or below sea level following such an event.

### 9.1.1 Description of grids and methodology

Contours of mean subsidence were made into GIS grid files with a 1 m cell size using the "create tin" and "tin to raster" functions in ArcMap 10.1. The resulting grids were added (so that negative topography is subtracted) to the LiDAR DEM to give a "digital future model" (DFM) incorporating one "average" subsidence event (Figure 11). The model was clipped to include the zone surrounding the Wellington Fault (Beetham et al., 2013).

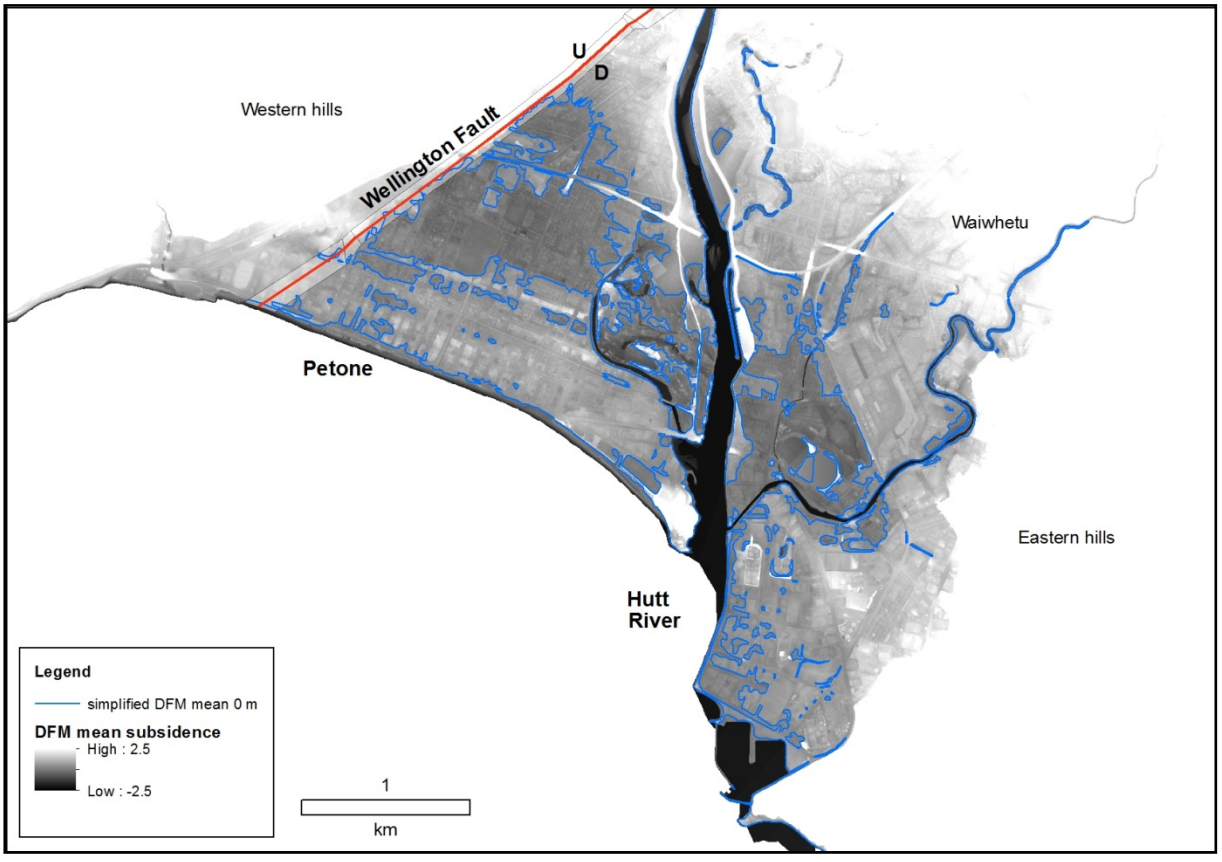


**Figure 11** A digital "future" elevation model with contoured, gridded mean subsidence subtracted from the LiDAR DEM, for SE of the Wellington Fault (northwest of the fault the original LiDAR DEM is shown). The symbology has been stretched from -2.5 m = black to +2.5 m = white to accentuate the relatively flat valley floor. The blue outline is a simplified version of the modelled zero metre contour, which separates areas that would subside below sea level (darker greys) from those that would remain above (paler greys).

The zero metre elevation contour line (blue) on Figure 11 (effectively a post-event sea level) was then extracted from the DFM using the "contour" function (see Figure 12). Black and darker greys on Figure 11, such as northern Petone to Alicetown and Moera to Seaview, represent areas modelled to subside below sea level, whereas the paler grey to white areas remain above sea level.

## 9.2 MEAN SUBSIDENCE PER EVENT

The mean post-event sea level reveals that large parts of Petone that are currently only between 1 and 2 m ASL (i.e., the "Petone area of low relief") and the area between Moera and Seaview would potentially become below sea level following an "average" Wellington Fault rupture (Figure 12). This "new" sea level does not take into account the effects of any potential land level changes resulting from earthquake shaking induced liquefaction or lateral spreading.

As another comparison, we made a pre-1855 earthquake DEM by subtracting a grid made from the uplift contours shown on Figure 5 from the LiDAR DEM using the same methods as outlined above (green line on Figure 13 and Figure 14).

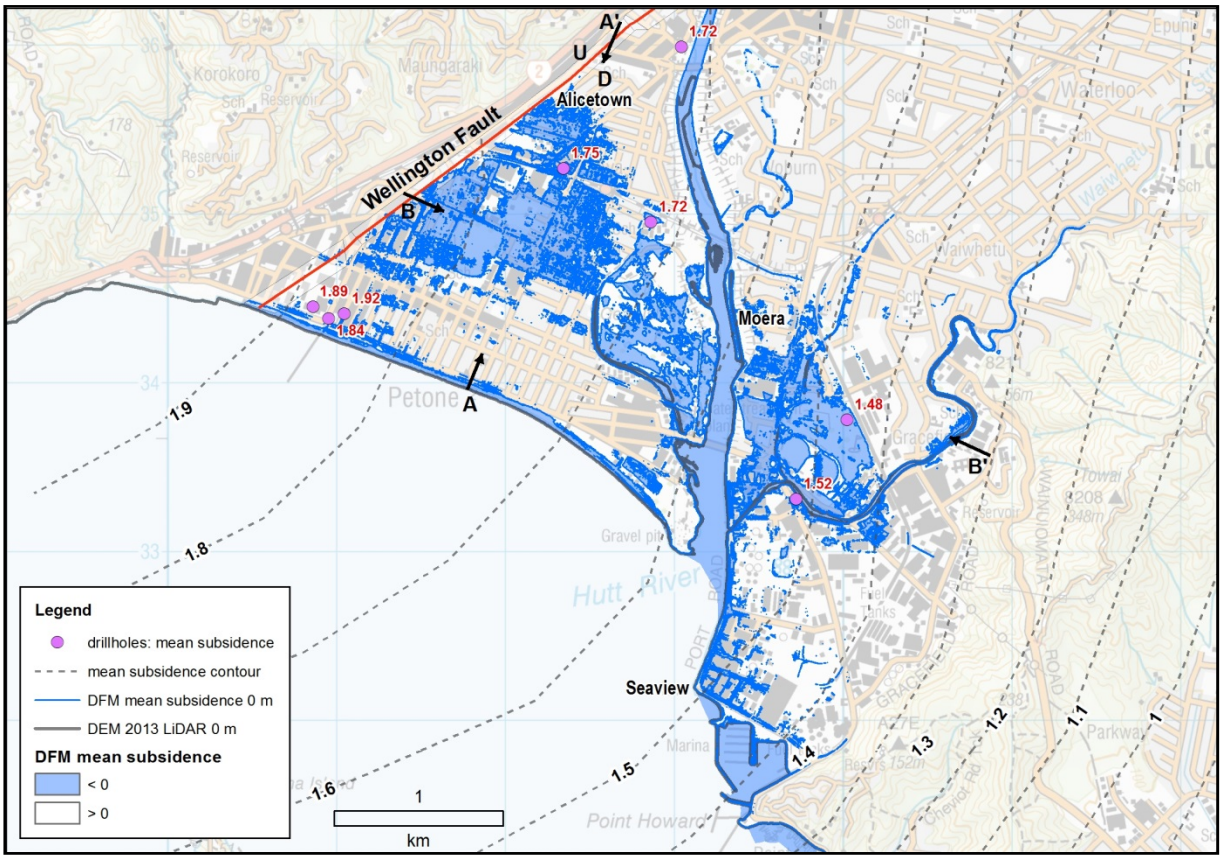


**Figure 12** Following a Wellington Fault rupture with mean subsidence values, the area coloured blue in this figure will be at or below sea level. Large parts of Petone, Alicetown, Gear Island and Moera-Seaview will be heavily affected. Contours (dotted lines) are subsidence values in metres calculated for a mean Wellington Fault surface rupture. The annotations A-A' and B-B' mark the locations of the cross section illustrated in Figure 13. Background map is LINZ Topo50.

Figure 13 shows topographic profiles from Petone to Alicetown (A-A' on Figure 12) and Petone to Gracefield (B-B') based on the current LiDAR DEM (black) and the post-mean subsidence event (blue). The mean Wellington Fault subsidence produces topography similar to pre-1855 elevations (green) for the eastern Hutt Valley (about 1.5 m lower than today). This similarity may be useful in establishing mitigation measures (see Discussion below) and for helping people to understand the magnitude of potential land level changes.

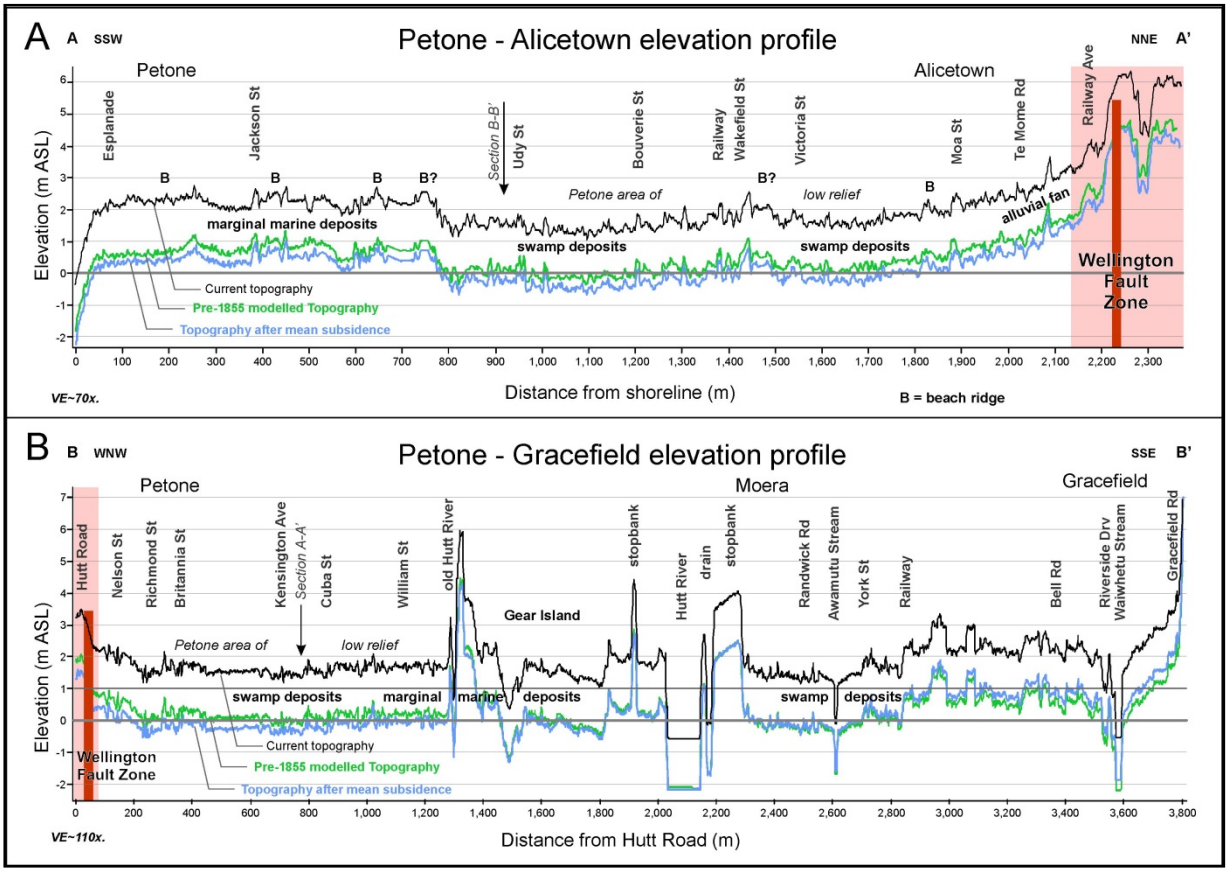


**Figure 13** Topographic profiles based on current LiDAR DEM (black), the modelled mean subsidence event (blue) and the modelled pre-1855 topography (green); see Figure 12 for profile locations. A: section A-A' runs parallel to Cuba Street from the Esplanade and projects NNE to the Wellington Fault (red) north of Alicetown. The three superimposed profiles are parallel because line of section runs along the subsidence contours. B: section B-B' runs across the valley, parallel to Udy Street and approximately perpendicular to section A-A'. For an "average" Wellington Fault rupture, there is about 0.3 m more modelled subsidence in the west near Petone and about 0.2 m less in the east compared with pre-1855 (modelled) topography. For this reason, the green (1855 uplift) surface lies above the blue (post-Wellington Fault rupture line in the west, but reverses this configuration by the eastern end of the profile.

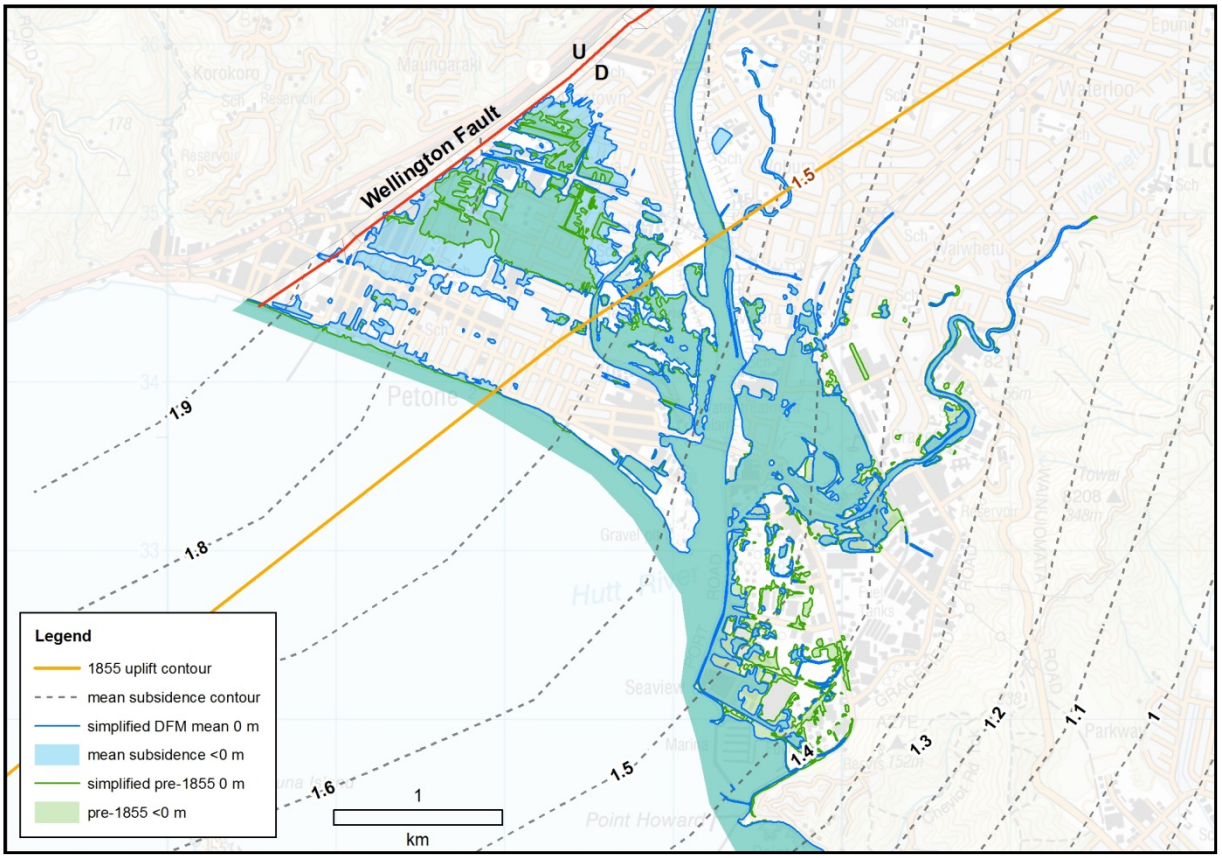


**Figure 14** Comparison of simplified modelled sea levels prior to the 1855 Wairarapa earthquake (green) with a post Wellington Fault rupture event (blue). The more regional signal from the Wairarapa Fault produces broader uplift in the valley (orange contour line, in metres) than comparatively localised effects from the Wellington Fault (grey dotted lines, also in metres). Single event uplift and subsidence for these modelled events are approximately equal (~1.6 m) near Moera, while the western Petone area will suffer greater subsidence (about 0.3 m more) in a Wellington Fault rupture than was uplifted in 1855.

In detail however, there is about 0.3 m greater subsidence in the western Hutt Valley close to the Wellington Fault than there was uplift in 1855 (compare blue and green outlines on Figure 13 and Figure 14). This is due to the local effects of increased subsidence (tilting) immediately adjacent to the fault as opposed to the “regional” or distal signal received from the Wairarapa Fault in this part of the Wellington Peninsula. This reiterates that low-lying parts of Petone to Alicetown would subside below sea level with a Wellington Fault rupture and potentially be inundated.

Figure 15 shows a reconstructed historical map of the Petone – Lower Hutt area for the early 1840s, prior to the 1.2 to 1.5 m of uplift that affected the area during the 1855 Wairarapa earthquake (Stevens, 1991). This map illustrates the generally low-lying, swampy nature of this part of the valley, and also the course of the Hutt (Heretaunga) River to the west of Gear Island. Note also that the scarp of the Wellington Fault forms an abrupt transition from Te Momi swamp in the east to higher ground at the foot of the Western Hills, implying that it has a major influence on the local geomorphology.

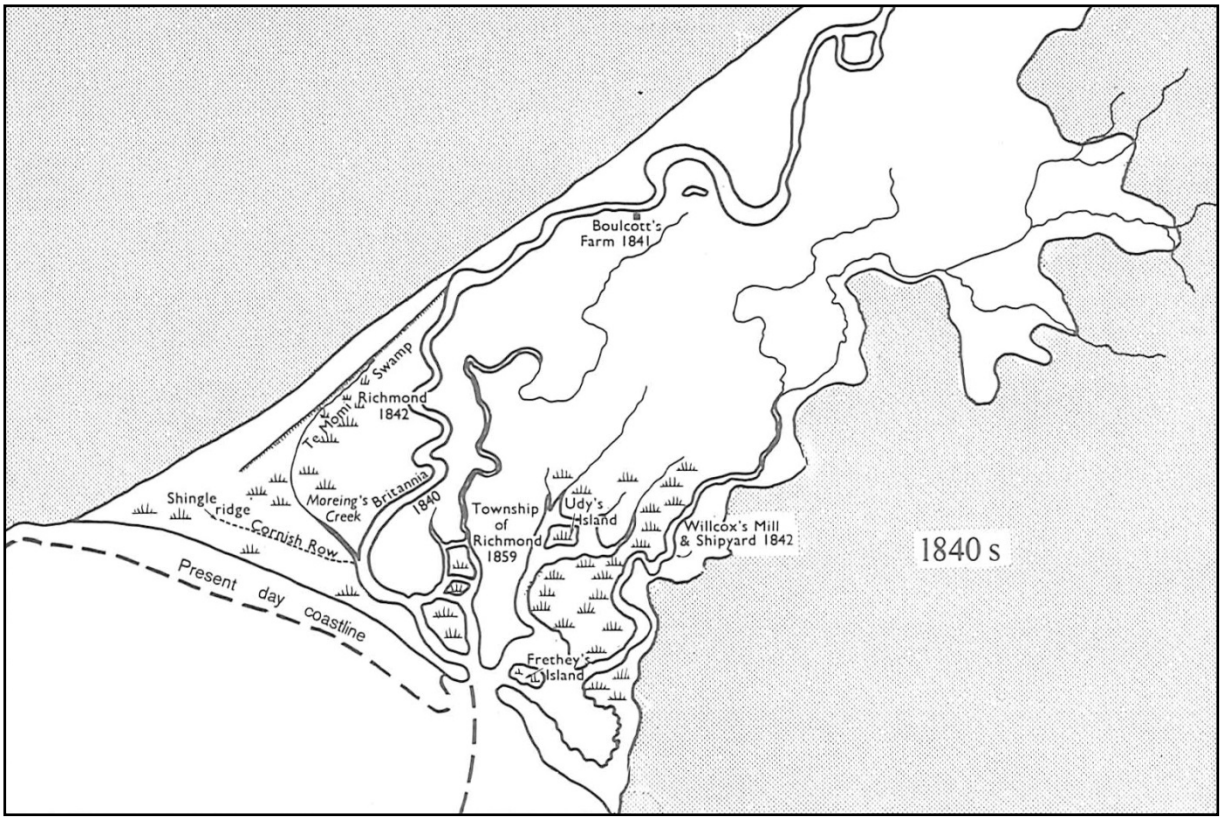


**Figure 15** Sketch of the lower Hutt Valley in the 1840's (after Stevens 1991) illustrating the generally low-lying and swampy nature of the valley before the ~1.5 m uplift that occurred during 1855 Wairarapa earthquake. Modelling suggests that the post-Wellington Fault rupture landscape would share many of the features shown on this map, although western Petone and Alicetown may be more severely impacted.

## 9.3 EVENT TO EVENT VARIABILITY OF DISPLACEMENT ON THE WELLINGTON FAULT

The above results of mean subsidence, including standard deviation (Table 7) give us an indication of how well constrained the mean values of past (Holocene) subsidence are, but do not take into account the natural variability of how large or small the next event could be. Looking towards the next event, this variability (either side of our mean values) can be estimated using a coefficient of variation (CoV; = SD / mean) to yield a *standard deviation of displacement events* (**$SD_E$**; technically the 68% confidence limits).

We entertain a range of options for our CoV value (Table 9). We use a combination of the published CoV for SED on the Wellington Fault, derived from offset terraces at Te Marua, Upper Hutt (CoV1 = 0.3; Little et al., 2010) and give this a weighting of 50%. We also factor in our SEVD for uplifted beach ridges at Turakirae Head, which is a measure of the CoV for single event vertical displacement on the Wairarapa Fault (CoV2 = 0.406; for combined Gibb/Hayward RSL 90%/10%) and weight this 40%. We also use the published value of CoV for SED on faults worldwide (CoV3 = 0.5; Hecker et al., 2012) and weight this value 10%.

**Table 9** Options, weighting and final value for the coefficient of variation used to estimate the range of future displacement sizes per event in the Hutt Valley for a Wellington Fault rupture.

| CoV options | Value | Weight | Prod. | Source |
|---|---|---|---|---|
| CoV1 | 0.3 | 50% | 0.15 | Wellington Fault at Te Marua (Little et al., 2010) |
| CoV2 | 0.406 | 40% | 0.163 | CoV from SEVD at Turakirae Head (RSL combined) |
| CoV3 | 0.5 | 10% | 0.05 | CoV from Hecker et al. (2013) |
| **Final CoV** | | | **0.363** | |

The final weighted CoV is therefore 0.363, which we can then apply to our mean subsidence per event and standard deviation (SD) from Table 7 using equation (4), below, to yield an estimate of standard deviation for displacement events ($SD_E$) and finally calculate a range of magnitudes (+/- 1 $SD_E$) of future events (Table 10).

$$\mathrm{SD_E} = \sqrt{(\mathrm{SD})^2 + (\mathrm{mean\ subs.} \times \mathrm{CoV})^2} \quad \textbf{(4)}$$

**Table 10** Final drillhole subsidence per event, event variability ($SD_E$) using a CoV of 0.363 from above, and maximum and minimum credible subsidence values (at +/- 1 $SD_E$). See text for derivation of values.

| Drillhole | Mean Subs (m) | $SD_E$ (m) | Mean + $SD_E$ "maximum credible" (m) | Mean - $SD_E$ "minimum credible" (m) |
|---|---|---|---|---|
| North Street | 1.72 | ±0.83 | 2.55 | 0.89 |
| Gear Meat 151 | 1.84 | ±0.88 | 2.72 | 0.96 |
| Gear Meat 319 | 1.89 | ±0.90 | 2.79 | 0.99 |
| Gear Meat 320 | 1.92 | ±0.92 | 2.84 | 1.00 |
| Wakefield Street | 1.75 | ±0.84 | 2.59 | 0.91 |
| Seaview | 1.52 | ±0.74 | 2.26 | 0.78 |
| Elizabeth Street | 1.48 | ±0.72 | 2.20 | 0.76 |
| Marsden Street | 1.72 | ±0.83 | 2.55 | 0.89 |

### 9.3.1 Minimum credible subsidence

"Minimum credible" subsidence (mean -1 $SD_E$) is around 1 m near Petone, ranging to 0.75 m in the east near Parkside Road and nearly 0.9 m up the valley near Ewen Bridge (Table 10). These "minimum credible" values are similar to the range of average values calculated by Begg et al. (2002).

The resulting future sea level for the "minimum credible" subsidence is presented in Figure 16, which shows relatively little change compared with the modern sea level. Some parts of Petone (e.g., near North Park/Udy St) are modelled to become below sea level, similarly for low-lying channels of the old Hutt River at Gear Island/Memorial Park. The Hutt River would be tidal up valley as far as Lower Hutt Central, and side streams and drains would not drain as well as today. Some of the area between Moera and Seaview, in particular Hutt Park Raceway, would also lie below sea level and be poorly drained. The effects of liquefaction and/or lateral spreading are not modelled.

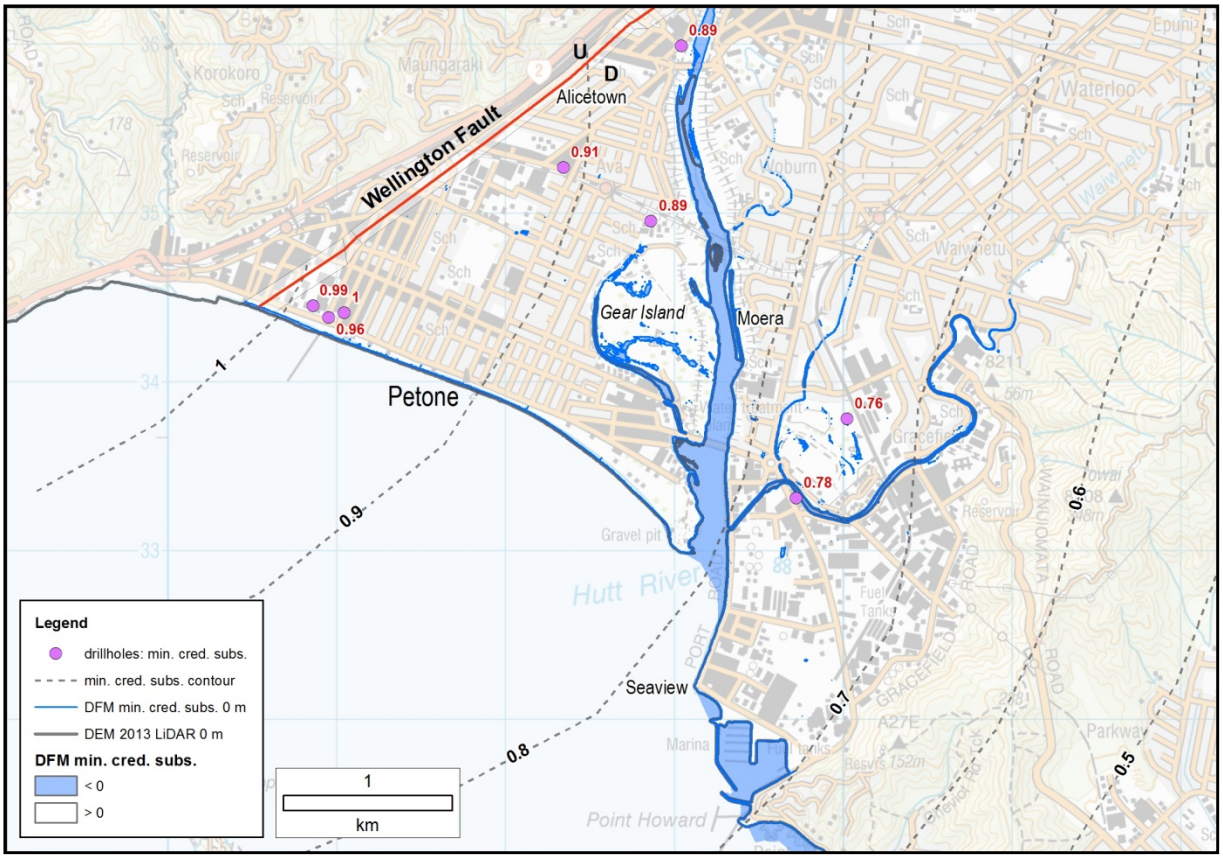


**Figure 16** Contours of "minimum credible" subsidence (dotted lines) in metres calculated for a Wellington Fault surface rupture. The resulting zero metre elevation contour (blue) shows small parts of Petone, Gear Island and Moera would lie below sea level. Background map is LINZ Topo50.

### 9.3.2 Maximum credible subsidence

"Maximum credible" subsidence (mean +1 $SD_E$) is much larger than the "minimum credible" subsidence, reflecting the large uncertainties carried through in the calculations. However, in a "maximum credible" scenario, subsidence is about 2.8 m near Petone, ranging to 2.2 m in the east near Parkside Road and about 2.5 m up valley near Ewen Bridge.

Under this "maximum credible" scenario, Figure 17 shows large parts of the lower Hutt Valley as far up valley as Alicetown, Woburn, Waiwhetu and Gracefield would be inundated by the sea. Petone, Moera and Seaview would all lie below sea level. This would severely affect habitability across all of these suburbs; multiple infrastructural elements would be adversely affected as well. The effects of liquefaction and/or lateral spreading are not modelled.

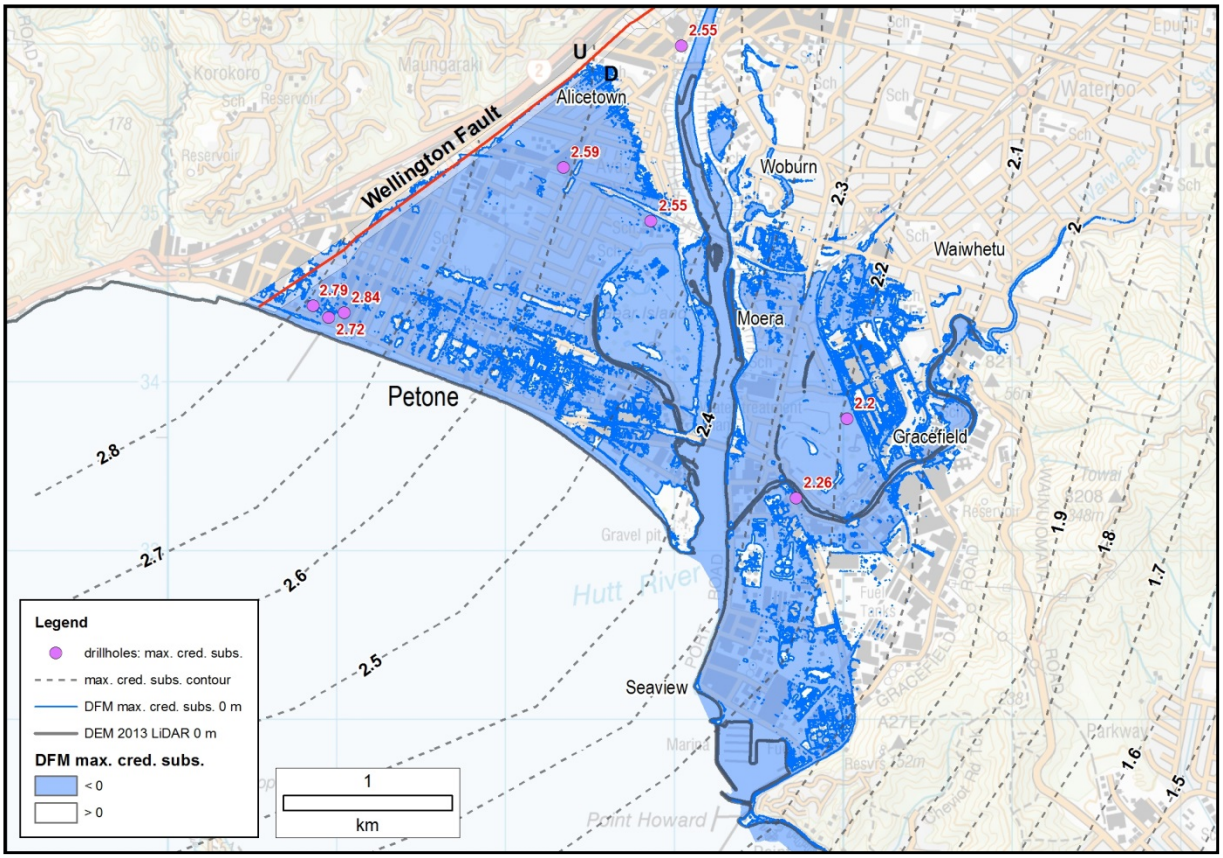


**Figure 17** Contours of "maximum credible" subsidence (dotted lines) in metres calculated for a Wellington Fault surface rupture. The resulting zero metre elevation contour (blue) shows large parts of the lower Hutt Valley would subside below sea level. Background map is LINZ Topo50.

# 10.0 DISCUSSION

## 10.1 SOCIAL AND PLANNING IMPACTS OF THE ANALYSIS

This report reiterates the potential for significant parts of the lower Hutt Valley, including Petone, to be severely affected by permanent ground deformation (subsidence) by as much as 1.9 m in an "average" Wellington Fault rupture. Areas between Alicetown and Petone, Moera and Seaview, currently at elevations of only 1–2 m above sea level, would subside below mean sea level in a future Wellington Fault rupture event. This subsidence will be additional to, and exacerbated by, other hazards mentioned below.

One of the central focuses of the Royal Commission Inquiry into the Christchurch earthquakes was to identify other areas around the country that may be at risk from the effects of severe liquefaction and would need to become "red zoned". Major recommendations (i.e., 186–187) from that report (Canterbury Earthquakes Royal Commission, 2012) included:

- Sections 6 and 7 of the Resource Management Act 1991 should be amended to ensure that regional and district plans (including the zoning of new areas for urban development) are prepared on a basis that acknowledges the potential effects of earthquakes and liquefaction, and to ensure that those risks are considered in the processing of resource and subdivision consents under the Act.
- Regional councils and territorial authorities should ensure that they are adequately informed about the seismicity of their regions and districts. Since seismicity should be considered and understood at a regional level, regional councils should take a lead role in this respect, and provide policy guidance as to where and how liquefaction risk ought to be avoided or mitigated.
- Applicants for resource and subdivision consents should be required to undertake such geotechnical investigations as may be appropriate to identify the potential for liquefaction risk, lateral spreading or other soil conditions that may contribute to building failure in a significant earthquake. Where appropriate, resource and subdivision consents should be subject to conditions requiring land improvement to mitigate these risks.

While, as might be expected under the circumstances, the Canterbury Earthquakes Royal Commission was focused particularly on damage from liquefaction, their comments apply equally to permanent ground deformation that may exacerbate the risks to Lower Hutt, and which need to be considered within a land use planning and emergency management context.

## 10.2 OTHER HAZARDS OF THE HUTT VALLEY

As well as subsidence and surface fault rupture from a large Wellington Fault event, the southern part of Lower Hutt is susceptible to a range of natural hazards. It is beyond scope of this report to include detail here, but these hazards are listed below, with references for further reading.

- ground shaking (Standards Australia/New Zealand, 2004; Boon et al., 2010; 2011);
- surface fault rupture (Van Dissen et al., 2010);
- liquefaction, including lateral spreading (Saunders & Berryman, 2012; Beetham et al., 2012; see also Tonkin & Taylor, 2013 where tectonic subsidence and subsidence attributed to liquefaction in Christchurch is assessed);
- tsunami (MCDEM, 2008; Leonard et al., 2008; Power, 2013; Wellington Region Emergency Management Office, 2013);
- flooding; (Wellington Regional Council, 2001); and also the addition of debris due to landsliding in the catchment;
- landslides (Brabhaharan et al., 1994; Grapes & Downes, 1997);
- climate change (Bell & Hannah, 2012), including sea level rise.

There are major implications for land use planning from these hazards, all of which (excepting climate change) may result from a Wellington Fault rupture event. Flooding is included because fault rupture and/or subsidence will severely alter drainage networks and potentially lead to loss of stop-bank elevation and integrity. The longer-term effects from alteration of drainage networks in Christchurch City (e.g., Flockton area) are only now being addressed, three years later.

## 10.3 IMPLICATIONS

The current best estimate for the likelihood of Wellington Fault rupture in the next 100 years is c. 10% (Rhoades et al., 2011). This value sits comfortably within the range of hazards probabilities that society routinely expects to plan for and mitigate. Without mitigation, a Wellington Fault rupture event that results in the subsidence outlined in this report will have catastrophic consequences for the Hutt Valley.

Subsidence similar to that expected from a Wellington Fault event has occurred elsewhere, resulting in the flooding of urban areas. Figure 18 shows the results from Golcuk, Turkey, where this low-lying coastal area on the margin of Izmit Bay subsided by 1–2 m during the Izmit (Marmara Sea) earthquake in 1999 (Sharpe et al., 2000). As a consequence, there was a loss of habitable land area, and the area was subsequently re-zoned into parks and a marina. Similar consequences are expected from a Wellington Fault event (as shown in Figure 11 and Figure 16). In the scenarios outlined above, flooding could extend close to the Lower Hutt CBD. The current land use of the area within the possible floodable zone is a mix of residential, business, industrial and commercial.

**Figure 18** Permanent ground deformation resulted in flooding of an urban area, Golcuk, Turkey, following the Izmit earthquake in 2000. Photo: R Van Dissen.

As well as the possible loss of life, damage to buildings and impact to the local economy, there are numerous implications associated with subsidence of the Hutt Valley, including (but not limited to):

- Preparing evacuation procedures for getting people out of an area that is under water, likely with damaged roading;
- Insurance – from EQC and private insurers;
- Loss of services, including power, road, water and sewerage, Sea View port;
- Greater susceptibility to other hazards, such as landslides, floods, storm surge, tsunami, sea level rise; and
- Impeded drainage, which will be exacerbated by rising sea levels.

However, with this knowledge there is also an opportunity to plan for an event of this magnitude – for example, focusing future development in other areas of the Hutt Valley, such as the CBD.

## 10.4 MITIGATION OPTIONS

There are a number of options for Hutt City Council and Greater Wellington Regional Council to consider for increasing resilience, and limiting future losses. Prior to deciding what measures should be taken, we suggest a risk assessment of the area should be undertaken to assess what the consequences could be. For example, the number of people living in the area, location and number of schools, critical facilities, aged-care facilities, important commercial and industrial activities, etc.

It seems clear that given the information presented in this report and the recommendations of the Canterbury Earthquake Royal Commission, doing nothing is not an option. Discussion from this point on focuses on the variety of mitigation options available. Further, it is acknowledged that the hazard cannot be eliminated or significantly reduced in the short term without wildly unrealistic expenditure. While the following medium- and long-term options are not mutually exclusive, careful selection of a range of options could be used to develop a manageable strategy to mitigate future risks.

### 10.4.1 Review the Hutt City Plan

Currently the Hutt City Plan does not include rules for liquefaction, climate change, or tsunami. Recently, through the Plan Change 29 submission process (as outlined in Saunders & Beban, 2014), additional planning provisions were included for the Petone West plan change area. These included:

- A natural hazard specific objective: To mitigate the risks to people and development from natural hazards to an acceptable level. Avoidance might be necessary in some cases.
- All new buildings require a case-by-case assessment of the natural hazard risks and consequences. These are specific references to the ground rupture, subsidence, liquefaction and tsunami risks as well as the requirement for sea level rise to be considered.
- Emergency facilities were made a Non-Complying Activity for the entire Petone Mixed Use Area, in response to the risk from natural hazards.
- In response to the natural hazard risk, Places of Assembly, Childcare Facilities, Education and Training Facilities, Commercial Activities (accommodating more than 300 people), Community Activities/Facilities, Housing for the Elderly and Residential Facility were made a Discretionary Activity. Any development that includes these activities must consider the natural hazard risk and measures to avoid or reduce this risk.

However, these additional planning provisions only relate to the Petone Plan Change 29 area, *not* for the rest of Hutt City. As part of the Plan Change 29 process, it was recommended that a review of the natural hazards chapter (i.e. section 14H) of the Hutt City Plan be undertaken to incorporate other hazards. With the possibility of metre-scale subsidence, the consequences of a range of hazards (e.g., liquefaction, tsunami, flooding and sea level rise) are increased – thus social, economic, cultural, infrastructural and health and safety risks are similarly increased. We recommend that this should become a priority

for Hutt City Council, as required under the Resource Management Act, Local Government Act, and Civil Defence Emergency Management Act (Saunders & Beban, 2012). The Wellington Regional Natural Hazards Strategy, currently being devised, will have a significant impact on how Hutt City Council plans for natural hazards and associated risks in the future.

### 10.4.2 Managed retreat

As the hazard area has been defined, there is an opportunity for a retreat plan to be developed for the relocation of critical facilities. This would need to be incorporated into the long term and annual plan process, and will require engagement with other agencies for non-council facilities.

### 10.4.3 Limit development

Within the defined hazard area, further development could be limited. This limitation could apply to critical infrastructure and facilities (e.g., electricity sub stations, fire stations, police stations, main pipelines for water and sewage). At the same time, or at a signalled later stage, consideration could be given to restricting infill housing or changes of land use likely to increase risks to life safety (e.g., retirement homes, schools).

### 10.4.4 Pre-event recovery planning for land use

Develop a recovery plan for the area, pre-event, detailing options for how the land will be managed. While this plan may change post-event, the value of these plans is thinking about the issues ahead of time and detailing them. Further guidance is available from Becker et al. (2008).

### 10.4.5 Emergency management

This option relies on developing emergency management plans to cope with the disaster once it occurs; for example, response and recovery issues including rescue, evacuation, and transportation challenges. This option should accompany the other options, as it is a response action only, and does not reduce future risks.

### 10.4.6 Education, awareness, and information availability

Raising awareness and educating decision makers, developers and the public is crucial so that:

- Decision makers can assist in reducing future risks;
- Developers can assess the actual risks; and
- The public can make informed decisions about their personal risk (i.e., economic, property, social, cultural).

Key to this is information availability. The information needs to be accessible and in ‘plain English’, to allow for further understanding and dissemination of information. Information could refer back to the pre-1855 ground levels, to show that what we are likely to experience is what the ground was like prior to the 1855 Wairarapa earthquake.

This page is intentionally left blank.

## 11.0 RECOMMENDATIONS FOR FUTURE WORK

Although the recent It's Our Fault studies have increased our knowledge and understanding of local and regional seismic hazard, one of the least well-constrained parameters that we use in our calculations is the recurrence interval of the Wellington Fault. Future paleoseismology studies (e.g., trenching, surveying of displaced features) may help to improve our knowledge of fault recurrence interval, and it may then be appropriate to revisit the calculations outlined above with better-constrained data. The breadth of the range from "minimum credible" to "maximum credible" subsidence is largely attributable to the uncertainty in recurrence interval of the Wellington Fault.

Work on identifying the evidence for large subduction-related earthquakes in the geological record, and their effects on land surface levels, is on-going. Once these studies are completed it may be appropriate to revisit the calculations outlined in this report armed with new data.

It may be possible to directly test the subsidence per event for the Wellington Fault by trenching the scarp and assessing faulted or displaced stratigraphy. Trenching at a site like the Hutt Central School could also add to our knowledge of the timing of individual events, recurrence interval and/or slip rate for the fault as a whole. It may also clarify fault single event vertical displacement.

Assuming that the modelled values of subsidence in this report are correct, are there practicable and economically viable engineering solutions that may allow habitation of areas below sea level (e.g., by a system of dikes and pumps)? We recommend an assessment of such engineering solutions so that they may be considered in the range of mitigation options.

Before deciding on mitigation options, a risk assessment should be undertaken to determine who and what is at risk within the area. This could include (but should not be limited to) an assessment of critical facilities, educational facilities, aged-care facilities, residential dwellings, key infrastructure, commercial and industrial businesses. Once this has been completed, mitigation options can be prioritised in areas of greatest risk.

## 12.0 CONCLUSIONS

In this report we use a database of subsurface drillhole information within a carefully considered regional geological context to calculate subsidence associated with Wellington Fault rupture for the lower Hutt Valley. The derived values incorporate corrections for past variations in sea level and also for post-depositional consolidation. We have utilised all available data in our calculations and factored in all plausible contributors to lower Hutt Valley subsidence.

Uncertainty in data and/or variation derived from alternative interpretations is carried through our calculations using weighting factors within a structured logic tree. Uncertainty in the recurrence interval on the Wellington Fault is the major contributor to the variation in subsidence between the “minimum credible” and “maximum credible” values.

Mean subsidence per event values are about 1.9 m in the west near Petone, 1.5 m in eastern Hutt, and 1.7 m up valley at Ewen Bridge. “Minimum credible” and “maximum credible” scenarios are also calculated and presented. By subtracting an elevation grid of these calculated mean, “minimum credible” and “maximum credible” subsidence events on the current Hutt Valley topography we can model the likely landscapes following such Wellington Fault-rupturing earthquakes.

The landscape in the lower Hutt Valley following a mean Wellington Fault rupture would be similar to that prior to the c. 1.4 m uplift associated with the 1855 Wairarapa earthquake. This similarity is potentially useful for communicating the likely impact of such an “average” Wellington Fault surface rupturing earthquake. Without mitigation, a Wellington Fault event accompanied by the subsidence outlined in this report will have catastrophic consequences for the Hutt Valley. We believe that the data presented in this report, along with recommendations of the Canterbury Earthquakes Royal Commission, provide a powerful case for developing a comprehensive mitigation strategy for such events. Prior to deciding on specific techniques to build into this mitigation strategy, we recommend a risk assessment of the area be undertaken to assess what the consequences (i.e., losses) could be. A number of options for mitigating this hazard, improving resilience and limiting future losses are suggested for consideration. Hutt City Council and Greater Wellington Regional Council could include a range of these options in a suitable strategy.

## 13.0 ACKNOWLEDGEMENTS

This study was part funded by GWRC and HCC. Part funding was also from GNS funded job 44000905-00. Thanks to Ursula Cochran and Kate Clark for supplying sea level data. Thanks also to Sigrun Hreinsdottir for discussions regarding GPS velocities and to Christine Prior for discussion about recalibrating carbon dates.

We thank Drs Nicola Litchfield and Jim Cousins for their thorough reviews, which greatly improved this report.

## 14.0 REFERENCES

Antonioli, F.; Bard, E.; Potter, E.-K.; Silenzi, S.; Improta, S. 2004: 215-ka History of sea-level oscillations from marine and continental layers in Argentarola Cave speleothems (Italy). *Global and Planetary Change 43* (2004) 57–78. doi:10.1016/j.gloplacha.2004.02.004.

Bassinot, F.; Labeyrie, L.; Vincent, E.; Quidelleur, X.; Lancelot, N.J.; Lancelot, Y. 1994: The astronomical theory of climate and the age of the Brunhes-Matuyama magnetic reversal. *Earth and Planetary Science Letters 126* (1994) 91–108.

Becker, J.; Saunders, W.S.A.; Hopkins, L.; Wright, K.; & Kerr, J. 2008: *Pre-event recovery planning for land use in New Zealand: an updated methodology*. Lower Hutt: GNS Science.

Beetham, R.D.; Cousins, W.J.; Craig, M.; Dellow, G.D.; van Dissen, R.J. 2012: Hutt Valley trunk wastewater earthquake vulnerability study. *GNS Science Consultancy Report 2012/234.* 51 p.

Begg, J.G.; Mildenhall, D.C.; Lyon, G.L.; Stephenson, W.R.; Funnell, R.H.; Van Dissen, R.J.; Bannister, S.C.; Brown, L.J.; Pillans, B.; Harper, M.A.; Whitten, J. 1993: A paleoenvironmental study of subsurface Quaternary sediments at Wainuiomata, Wellington, New Zealand, and tectonic implications. *New Zealand Journal of Geology and Geophysics, 36(4):* 461–473.

Begg, J.G.; Mazengarb, C. 1996: Geology of the Wellington area: sheets R27, R28, and part Q27, scale 1:50,000. Lower Hutt: Institute of Geological & Nuclear Sciences. *Institute of Geological & Nuclear Sciences geological map 22.* 128 p. + 1 fold. Map.

Begg, J.G.; Van Dissen, R.J.; Rhoades, D.A.; Lukovic, B.; Heron, D.W.; Darby, D.J.; Brown, L.J. 2002: Coseismic subsidence in the Lower Hutt Valley resulting from rupture of the Wellington Fault. *Institute of Geological & Nuclear Sciences Client Report 2002/140.* 70p.

Bell, R.G.; Hannah, J. 2012: *Sea-level variability and trends: Wellington Region*. Hamilton: NIWA.

Boon, D.P.; Perrin, N.D.; Dellow, G.D.; Lukovic, B. 2010: *It's Our Fault – geological and geotechnical characterisation and site subsoil class revision of the Lower Hutt Valley*. Lower Hutt: GNS Science.

Boon, D.P.; Perrin, N.D.; Dellow, G.D.; Van Dissen, R.; Lukovic, B. 2011: *NZS1170.5:2004 site subsoil classification of Lower Hutt*. Paper presented at the 9th Pacific Conference on Earthquake Engineering.

Brabhaharan, P.; Hancox, G.T.; Perrin, N.D.; Dellow; G.D. 1994: Earthquake-induced slope failure hazard study, Wellington Region, *Works Consultancy Services Ltd. and GNS Report prepared for Wellington Regional Council.*

Brown, L.D.; Reilinger, R.E.; Holdahl, S.R.; Balazs, E.I. 1977: Postseismic crustal uplift near Anchorage, Alaska. *Journal of Geophysical Research 82*: 3369–3378.

Canterbury earthquakes Royal Commission 2012: Volume 7, Section 5: Canterbury Regional Council and Christchurch City Council – management of earthquake risk.

Carne, R.C.; Little, T.A.; Rieser, U. 2011: Using displaced river terraces to determine Late Quaternary slip rate for the central Wairarapa Fault at Waiohine River, New Zealand, *New Zealand Journal of Geology and* Geophysics 54(2): 217–236.

Clark, K.J.; Hayward, B.W.; Cochran, U.A.; Grenfell, H.R.; Hemphill-Haley, E.; Mildenhall, D.C.; Hemphill-Haley, M.A.; Wallace, L.M. 2011: Investigating subduction earthquake geology along the southern Hikurangi margin using paleoenvironmental histories of intertidal inlets. *New Zealand Journal of Geology and Geophysics 54:* 255–271.

Clement, A.J.; Sloss, C.R.; Fuller, I.C. 2012: Late Quaternary geomorphology of the Manawatu coastal plain, North Island, New Zealand. *Quaternary International 221 (2010)*: 36–45; doi:10.1016/j.quaint.2009.07.005.

Cochran, U.A.; Berryman, K.R.; Zachariasen, J.; Mildenhall, D.C.; Hayward, B.W.; Southall, K.; Hollis, C.J.; Barker, P.; Wallace, L.M.; Alloway, B.V.; Wilson, K.J. 2006: Paleoecological insights into subduction zone earthquake occurrence, eastern North Island, New Zealand. *Geological Society of America Bulletin, 118(9/10):* 1051–1074.

Cochran, U.A.; Hannah, M.; Harper, M.; Van Dissen, R.J.; Berryman, K.R.; Begg, J.G. 2007: Detection of large, Holocene earthquakes using diatom analysis of coastal sedimentary sequences, Wellington, New Zealand. *Quaternary Science Reviews, 26(7/8):* 1129–1147; doi:10.1016/j.quascirev.2007.01.008.

Cochran, U.A.; Reid, C.M.; Clark, K.J.; Litchfield, N.J.; Marsden, I.; Ries, W. 2014: The Avon-Heathcote Estuary as a recorder of coseismic vertical deformation. *GNS Science Consultancy Report 2014/128.* 50 p. + 1 CD.

Cotton, C.A. 1921: The warped land-surface on the south-eastern side of the Port Nicholson depression, Wellington, N.Z. *Transactions and proceedings of the New Zealand Institute, 53:* 131–143.

Cotton, C.A. 1957: Tectonic features in a coastal setting at Wellington. *Transactions of the Royal Society of New Zealand 84:* 761–790.

EQ Spectra 2014, Special Issue: 2010–2011 Canterbury earthquake sequence. *Earthquake Spectra*, 30: 1–605.

Gibb, J.G. 1986: A New Zealand regional Holocene eustatic sea-level curve and its application to determination of vertical tectonic movements: a contribution to IGCP-Project 200. p. 377–395 IN: *Recent crustal movements of the Pacific region.* Wellington: Royal Society of New Zealand. *Bulletin / Royal Society of New Zealand 24.*

GNS Active Fault Database: http://data.gns.cri.nz/af/

Grapes, R.H.; Downes, G. 1997: The 1855 Wairarapa, New Zealand, earthquake: analysis of historical data. *Bulletin of the New Zealand National Society for Earthquake Engineering, 30(4):* 271–368.

Hayward, B.W.; Grenfell, H.R.; Sabaa, A.T.; Clark, K.J. 2012: Foraminiferal evidence for Holocene synclinal folding at Porangahau, southern Hawkes Bay, New Zealand. *New Zealand Journal of Geology and Geophysics, 55(1):* 21–35; doi: 10.1080/00288306.2011.615845.

Hecker, S.; Abrahamson, N. A.; Wooddell K. E. 2013: Variability of Displacement at a Point: Implications for Earthquake-Size Distribution and Rupture Hazard on Faults. *Bulletin of the Seismological Society of America, 103 (2A):* 651–674.

Hull, A.G.; McSaveney, M.J. 1996: A 7000-year record of great earthquakes at Turakirae Head, Wellington, New Zealand. *Institute of Geological & Nuclear Sciences client report 33493B.10.* 14 p. figs.

Hutt City Council (LiDAR).

Imbrie, J.; Hays, J.D.; Martinson, D.G.; McIntyre, A.; Mix, A.C.; Morley, J.J.; Pisias, N.G.; Prell, W.L.; Shackleton, N.J. 1984: The orbital theory of Pleistocene climate: Support from a revised chronology of the marine d18O record. *in* Milankovitch and Climate, Part 1, edited by A. Berger, pp. 269–305, Springer, New York.

IPCC, 2013: Climate Change 2013: The Physical Science Basis. Working Group I to the Fifth Assessment Report of the Intergovernmental Panel on Climate Change. *Eds. Stocker, Qin, Plattner, Tignor, Allen, Boschung, Nauels, Xia, Bex and Midgley*. Cambridge University Press.

Kulkarni, R.B.; Youngs, R.R.; Coppersmith, K.J. 1984: Assessment of confidence intervals for results of seismic hazard analysis, in *Proceedings of the Eighth World Conference on Earthquake Engineering, San Francisco, Vol. 1*, 263–270.

Langridge, R.M.; Van Dissen, R.J.; Villamor, P.; Little, T.A. 2009: It's our fault: Wellington Fault paleo-earthquake investigations: final report. *GNS Science consultancy report 2008/344.* 45 p.

Langridge, R.M.; Van Dissen, R.J.; Rhoades, D.A.; Villamor, P.; Little, T.; Litchfield, N.J.; Clark, K.J.; Clark, D. 2011: Five thousand years of surface ruptures on the Wellington Fault, New Zealand : implications for recurrence and fault segmentation. *Bulletin of the Seismological Society of America, 101(5):* 2088–2107; doi: 10.1785/0120100340.

Leonard, G.S.; Power, W.; Lukovic, B.; Smith, W.; Johnston, D.; Downes, G. 2008: *Tsunami evacuation zones for Wellington and Horizons regions defined by a GNS-calculated attenuation rule*. Lower Hutt: GNS Science.

Lisiecki, L.E.; Raymo, M.E. 2005: A Pliocene-Pleistocene stack of 57 globally distributed benthic D18O records. *Paleoceanography, (20),* PA1003, doi:10.1029/2004PA001071.

Little, T.A.; Van Dissen, R.J.; Schermer, E.; Carne, R. 2009: Late Holocene surface ruptures on the southern Wairarapa fault, New Zealand: link between earthquakes and the uplifting of beach ridges on a rocky coast. *Lithosphere, 1(1):* 4–28; doi:10.1130/L7.1.

Little, T.A.; Van Dissen, R.J.; Rieser, U.; Smith, E.G.C.; Langridge, R.M. 2010: Coseismic strike slip at a point during the last four earthquakes on the Wellington Fault near Wellington, New Zealand. *Journal of Geophysical Research. Solid Earth, 115:* B05403, doi:10.1029/2009JB006589.

Martinson, D.G.; Pisias, N.G.; Hays, J.D.; Imbrie, J.; Moore Jr., T.C.; Shackleton, N.J. 1987: Age dating and the orbital theory of the ice ages: development of a high-resolution 0 to 300,000-year chronostratigraphy. *Quaternary Research 27* (1987): 1–29.

MCDEM 2008: *Tsunami evacuation zones: Director's guideline for Civil Defence Emergency Management Groups [DGL08/08]*. Wellington: Ministry of Civil Defence and Emergency Management.

McSaveney, M.J.; Graham, I.J.; Begg, J.G.; Beu, A.G.; Hull, A.G.; Kim, K.; Zondervan, A. 2006: Late Holocene uplift of beach ridges at Turakirae Head, south Wellington coast, New Zealand. *New Zealand Journal of Geology and Geophysics, 49(3):* 337–358.

Moore, P.R. 1987: Age of the raised beach ridges at Turakirae Head, Wellington: a reassessment based on new radiocarbon dates. *Journal of the Royal Society of New Zealand, 17(3):* 313–324.

Ninis, D.; Little, T.A.; Van Dissen, R.J.; Litchfield, N.J.; Smith, E.G.C.; Wang, N.; Rieser, U.; Henderson, C.M. 2013: Slip rate on the Wellington fault, New Zealand, during the Late Quaternary: evidence for variable slip during the Holocene. *Bulletin of the Seismological Society of America, 103(1):* 559–579; doi: 10.1785/0120120162.

NZSEE 2010, Special Issue: Preliminary observations of the September 2010 Darfield (Canterbury) earthquake sequence. *Bulletin of the New Zealand Society for Earthquake Engineering,* 43: 215–439.

NZSEE 2011, Special Issue: Effects of the 22 February 2011 Christchurch earthquake and its aftershocks. *Bulletin of the New Zealand Society for Earthquake Engineering*, 44: 181–430.

Ota, Y.; Williams, D.N.; Berryman, K.R. 1981: Wellington 1:50 000, parts Q27, R27, R28. Late Quaternary Tectonic map.

Parliamentary Commissioner for the Environment 2014: Changing climate and rising seas: understanding the environment. http://www.pce.parliament.nz/assets/Uploads/Changing-Climate-and-Rising-Seas-Web.pdf.

Pillans, B.; Chappell, J.; Naish, T.R. 1998: A review of the Milankovitch climatic beat: template for Plio-Pleistocene sea-level changes and sequence stratigraphy. *Sedimentary Geology, 122(1/4):* 5–21.

Power, W.L. 2013: Review of tsunami hazard in New Zealand (2013 update). *GNS Science Consultancy Report 2013/131.* 222 p.

Prescott, W.H.; Lisowski, M. 1977: Deformation at Middleton Island, Alaska, during the decade after the Alaska earthquake of 1964. *Bulletin of the Seismological Society of America 67*: 579–586.

Rabineau, M.; Berne, S.; Olivet, J.-L.; Aslanian, D.; Guillocheau, F.; Joseph, P. 2006: Paleo sea levels reconsidered from direct observation of paleoshoreline position during Glacial Maxima (for the last 500,000 yr). *Earth and Planetary Science Letters 252* (2006) 119–137; doi:10.1016/j.epsl.2006.09.033.

Rafter Radiocarbon Laboratory, GNS.

Read, S.A.L.; Begg, J.G.; Van Dissen, R.J.; Perrin, N.D.; Dellow, G.D. 1991: Regional natural disaster reduction plan – seismic hazard. Geological setting of the Lower Hutt Valley and Wainuiomata, including distribution of materials and geotechnical properties (Part 7 of 1990 study). *DSIR Geology and Geophysics contract report 1991/45.* 23 p.

Reyners, M. 1998: Plate coupling and the hazard of large subduction thrust earthquakes at the Hikurangi subduction zone, New Zealand. *New Zealand Journal of Geology and Geophysics 41*: 343–354.

Rhoades, D.A.; Van Dissen, R.J.; Langridge, R.M.; Little, T.A.; Ninis, D.; Smith, E.G.C.; Robinson, R. 2011: Re-evaluation of conditional probability of rupture of the Wellington-Hutt Valley segment of the Wellington Fault. *Bulletin of the New Zealand Society for Earthquake Engineering, 44(2):* 77–86.

Saunders, W.S.A.; Beban, J.G. 2012: *Putting R(isk) in the RMA: Technical Advisory Group recommendations on the Resource Management Act 1991 and implications for natural hazards planning*. Lower Hutt: GNS Science.

Saunders, W.S.A.; Beban, J.G. 2014: *Petone Plan Change 29: An example of science influencing land use planning policy*. Lower Hutt: GNS Science.

Saunders, W.S.A.; Berryman, K.R. 2012: *Just add water: when should liquefaction be considered in land use planning?* (Vol. 47). Lower Hutt: GNS Science.

Sharpe, R.D.; Bradshaw, D.; Brown, N.; Van Dissen, R.; Kirkcaldie, D.; McManus, K.J.; Pham, T.; Stevenson, C. 2000: Marmara Sea Earthquake reconnaissance report: Report of the NZSEE reconnaissance team on the 17 August 1999 Marmara Sea, Turkey Earthquake. *Bulletin of the New Zealand Society for Earthquake Engineering* 33 (2): 65–104.

Siddall, M.; Rohling, E.J.; Almogi-Labin, A.; Hemleben, Ch.; Meischner, D.; Schmelzer, I.; Smeed, D.A. 2005: Sea-level fluctuations during the last glacial cycle. *Letters to Nature; Nature, 423*: 853.

Standards Australia/New Zealand 2004: *NZS 1170.5 Structural design actions – Part 5: Earthquake actions*: Standards New Zealand.

Stevens, G.R. 1974: Rugged landscape: the geology of central New Zealand, including Wellington, Wairarapa, Manawatu and Marlborough Sounds. DSIR Publishing. Wellington.

Stevens, G.R. 1991: *On Shaky Ground. A geological guide to the Wellington metropolitan area*. Geological Society of New Zealand Guidebook No 10.

Stirling, M.W.; McVerry, G.H.; Berryman, K.R. 2002: A new seismic hazard model for New Zealand. *Bulletin of the Seismological Society of America 92(5):* 1878–1903.

Stirling, M.; McVerry, G.; Gerstenberger, M.; Litchfield, N.; Van Dissen, R.; Berryman, K.; Barnes, P.; Wallace, L.; Villamor, P.; Langridge, R.; Lamarche, G.; Nodder, S.; Reyners, M.; Bradley, B.; Rhoades, D.; Smith, W.; Nicol, A.; Pettinga, J.; Clark, K.; Jacobs, K. 2012: National seismic hazard model for New Zealand: 2010 update. *Bulletin* of the Seismological Society of America 102 (4): 1514–1542. doi: 10.1785/0120110170.

Tonkin & Taylor 2013: Liquefaction vulnerability study. Consultancy report 52020.0200/v.1.0. Prepared for EQC.

Van Dissen, R.; Barnes, P.; Beavan, J.; Cousins, J.; Dellow, G.; Francois-Holden; C.; Fry, B.; Langridge, R.; Litchfield, N.; Little, T.; McVerry, G.; Ninis, D.; Rhoades, D.; Robinson, R.; Saunders, W.; Villamor, P.; Wilson, K.; Barker, P.; Berryman, K.; Benites, R.; Brackley, H.; Bradley, B.; Carne, R.; Cochran, U.; Hemphill-Haley, M.; King, A.; Lamarche, G.; Palmer, N.; Perrin, N.; Pondard, N.; Rattenbury, M.; Read, S.; Semmens, S.; Smith, E.; Stephenson, W.; Wallace, L.; Webb, T.; Zhao, J. 2010: It's Our Fault: better defining earthquake risk in Wellington. *in proceedings,* 11th IAEG Congress, Auckland, New Zealand, 5–10 September, 2010: 737–746.

Van Dissen, R.J.; Rhoades, D.A.; Little, T.; Litchfield, N.J.; Carne, R.; Villamor, P. 2013: Conditional probability of rupture of the Wairarapa and Ohariu faults, New Zealand. *New Zealand Journal of Geology and Geophysics, 56(2):* 53–67; doi: 10.1080/00288306.2012.756042.

Wallace, L.M.; Reyners, M.E.; Cochran, U.A.; Bannister, S.C.; Barnes, P.M.; Berryman, K.R.; Downes, G.L.; Eberhart-Phillips, D.; Fagereng, A.; Ellis, S.M.; Nicol, A.; McCaffrey, R.; Beavan, R.J.; Henrys, S.A.; Sutherland, R.; Barker, D.H.N.; Litchfield, N.J.; Townend, J.; Robinson, R.; Bell, R.E.; Wilson, K.J.; Power, W.L. 2009: Characterizing the seismogenic zone of a major plate boundary subduction thrust : Hikurangi Margin, New Zealand. *Geochemistry Geophysics Geosystems, 10(10):* Q10006, doi:10.1029/2009GC002610.

Wallace, L.M.; Barnes, P.; Beavan, J.; Van Dissen, R.J.; Litchfield, N.J.; Mountjoy, J.; Langridge, R.M.; Lamarche, G.; Pondard, N. 2012: The kinematics of a transition from subduction to strike-slip: an example from the central New Zealand plate boundary. *Journal of Geophysical* Research 117: B02405. doi:10.1029/2011JB008640.

Wallace, L.M.; Cochran, U.A.; Power, W.L.; Clark, K.J. 2014: Earthquake and tsunami potential of the Hikurangi subduction thrust, New Zealand. *Oceanography 27:* 104–117.

Wellington Region Emergency Management Office 2013: Wellington region tsunami evacuation zones: Lower Hutt. 2013, from http://www.getprepared.org.nz/sites/default/files/uploads/lower-hutt-petone.pdf.

Wellington Regional Council 2001: *Hutt River Floodplain Management Plan – for the Hutt River and its environment*. Wellington: Wellington Regional Council.

Wellman, H.W. 1967: Tilted marine beach ridges at Cape Turakirae, New Zealand. *Journal of geosciences Osaka City University 10*: 123–129.

Williams, C.A.; Eberhart-Phillips, D.; Bannister, S.; Barker, D.H.N.; Henrys, S.; Reyners, M.; Sutherland, R. 2013: Revised interface geometry for the Hikurangi Subduction Zone, New Zealand. *Seismological Research Letters 84:* 1066–1073.

Wood, R.A.; Davy, B.W. 1992: Interpretation of geophysical data collected in Wellington Harbour. *Institute of Geological & Nuclear Sciences client report 1992/78*. 18 p. + figs.

# APPENDICES

This page is intentionally left blank.

# A1.0 APPENDIX 1: DRILLHOLE DATA

**Table A1.1** Drillhole physical information, including name, depth/end of hole (EOH), height above sea level and location. Coordinates are in New Zealand Transverse Mercator (NZTM).

| Locality | Depth/ EOH (m) | Collar Height (m) | NZTM Easting | NZTM Northing |
|---|---|---|---|---|
| North Street (Wilford) | 128 | 1.5 | 1758860 | 5434955 |
| Elizabeth Street | 73.6 | 1.9 | 1760020 | 5433785 |
| Petone (Gear Meat 319) | 115.5 | 2.7 | 1756860 | 5434455 |
| Petone (Gear Meat 320) | 114.6 | 2.6 | 1757040 | 5434415 |
| Petone (Gear Meat 151) | 311.2 | 2.4 | 1756950 | 5434385 |
| Wakefield Street | 134.1 | 1.4 | 1758340 | 5435275 |
| Seaview (Parkside Road) | 181.4 | 1.8 | 1759720 | 5433315 |
| Marsden Street (Ewen Bridge) | 151.3 | 4.9 | 1759040 | 5435995 |

**Table A1.2** Depths (m) of paleoshorelines identified from drillhole data (observed and "decompacted" values from Begg et al. (2002), then after adding decompaction uncertainties of +/- 10% and +/- 25%, and finally allowing for relative sea levels from Table 1). The final columns show the calculated subsidence rates (mm/yr, with uncertainties) for each paleoshoreline.

| **North Street (Wilford)** | | depth from drillhole log | | | decompacted | | | uncertainty +/- 10% | | uncertainty +/- 25% | | depth accounting for relative sea level (RSL) | | | rate accounting for RSL (2014) | | |
|---|---|---|---|---|---|---|---|---|---|---|---|---|---|---|---|---|---|
| Elevations of shoreline horizons | age (ka) | mean | min | max | mean | min | max | min | max | min | max | mean | min | max | mean | min | max |
| Base of Holocene marine | 9 | -13.7 | -15.2 | -12.2 | -13.46 | -14.96 | -11.96 | -14.98 | -11.93 | -15.02 | -11.89 | 4.55 | 8.11 | 0.98 | 0.51 | 0.90 | 0.11 |
| Top of OI 5e | 114 | -79.6 | -81.1 | -78.1 | -79.6 | -81.1 | -78.1 | -81.1 | -78.1 | -81.1 | -78.1 | -74.60 | -68.10 | -81.10 | -0.65 | -0.60 | -0.71 |
| Base of last interglacial | 128 | -80.8 | -82.3 | -79.3 | -80.8 | -82.3 | -79.3 | -82.3 | -79.3 | -82.3 | -79.3 | -83.80 | -81.30 | -86.30 | -0.65 | -0.64 | -0.67 |

| **Elizabeth Street** | | depth from drillhole log | | | decompacted | | | uncertainty +/- 10% | | uncertainty +/- 25% | | depth accounting for relative sea level (RSL) | | | rate accounting for RSL (2014) | | |
|---|---|---|---|---|---|---|---|---|---|---|---|---|---|---|---|---|---|
| Elevations of shoreline horizons | age (ka) | mean | min | max | mean | min | max | min | max | min | max | mean | min | max | mean | min | max |
| Base of Holocene marine | 9 | -13.0 | -14.5 | -11.5 | -13.00 | -14.50 | -11.50 | -14.50 | -11.50 | -14.50 | -11.50 | 5.00 | 8.50 | 1.50 | 0.56 | 0.94 | 0.17 |
| Top of last interglacial | 78 | -49.6 | -51.1 | -48.1 | -44.80 | -46.30 | -43.30 | -46.78 | -42.82 | -47.50 | -42.10 | -29.80 | -22.10 | -37.50 | -0.38 | -0.28 | -0.48 |
| Base of OI 5a | 83 | -51.4 | -52.9 | -49.9 | -46.60 | -48.10 | -45.10 | -48.58 | -44.62 | -49.30 | -43.90 | -30.60 | -22.90 | -38.30 | -0.37 | -0.28 | -0.46 |

| **Petone (Gear Meat 319)** | | depth from drillhole log | | | decompacted | | | uncertainty +/- 10% | | uncertainty +/- 25% | | depth accounting for relative sea level (RSL) | | | rate accounting for RSL (2014) | | |
|---|---|---|---|---|---|---|---|---|---|---|---|---|---|---|---|---|---|
| Elevations of shoreline horizons | age (ka) | mean | min | max | mean | min | max | min | max | min | max | mean | min | max | mean | min | max |
| Base of Holocene marine | 9 | -19.9 | -21.4 | -18.4 | -17.24 | -18.74 | -15.74 | -19.01 | -15.47 | -19.41 | -15.08 | 0.76 | 4.93 | -3.41 | 0.08 | 0.55 | -0.38 |
| Top of last interglacial | 78 | -81.4 | -82.9 | -79.9 | -81.31 | -82.81 | -79.81 | -82.82 | -79.80 | -82.83 | -79.79 | -66.31 | -59.79 | -72.83 | -0.85 | -0.77 | -0.93 |
| Base of last interglacial | 128 | -102.2 | -103.7 | -100.7 | -102.11 | -103.61 | -100.61 | -103.62 | -100.60 | -103.63 | -100.59 | -105.11 | -102.59 | -107.63 | -0.82 | -0.80 | -0.84 |

| **Petone (Gear Meat 320)** | | depth from drillhole log | | | decompacted | | | uncertainty +/- 10% | | uncertainty +/- 25% | | depth accounting for relative sea level (RSL) | | | rate accounting for RSL (2014) | | |
|---|---|---|---|---|---|---|---|---|---|---|---|---|---|---|---|---|---|
| Elevations of shoreline horizons | age (ka) | mean | min | max | mean | min | max | min | max | min | max | mean | min | max | mean | min | max |
| Base of Holocene marine | 9 | -23.0 | -24.5 | -21.5 | -17.09 | -18.59 | -15.59 | -19.18 | -15.00 | -20.07 | -14.11 | 0.91 | 5.89 | -4.07 | 0.10 | 0.65 | -0.45 |
| Top of last interglacial | 78 | -87.0 | -88.5 | -85.5 | -86.97 | -88.47 | -85.47 | -88.47 | -85.47 | -88.48 | -85.46 | -71.97 | -65.46 | -78.48 | -0.92 | -0.84 | -1.01 |
| Base of last interglacial | 128 | -101.3 | -102.8 | -99.8 | -101.30 | -102.80 | -99.80 | -102.80 | -99.80 | -102.80 | -99.80 | -104.30 | -101.80 | -106.80 | -0.81 | -0.80 | -0.83 |

| **Petone (Gear Meat 151)** | | depth from drillhole log | | | decompacted | | | uncertainty +/- 10% | | uncertainty +/- 25% | | depth accounting for relative sea level (RSL) | | | rate accounting for RSL (2014) | | |
|---|---|---|---|---|---|---|---|---|---|---|---|---|---|---|---|---|---|
| Elevations of shoreline horizons | age (ka) | mean | min | max | mean | min | max | min | max | min | max | mean | min | max | mean | min | max |
| Base of Holocene marine | 9 | -24.3 | -25.8 | -22.8 | -23.29 | -24.79 | -21.79 | -24.89 | -21.68 | -25.04 | -21.53 | -5.29 | -1.53 | -9.04 | -0.59 | -0.17 | -1.00 |
| Top of last interglacial | 78 | -79.5 | -81.0 | -78.0 | -79.05 | -80.55 | -77.55 | -80.60 | -77.51 | -80.66 | -77.44 | -64.05 | -57.44 | -70.66 | -0.82 | -0.74 | -0.91 |
| Top of OI 5e | 114 | -98.6 | -100.1 | -97.1 | -98.23 | -99.73 | -96.73 | -99.76 | -96.69 | -99.82 | -96.63 | -93.23 | -86.63 | -99.82 | -0.82 | -0.76 | -0.88 |
| Base of last interglacial | 128 | -103.4 | -104.9 | -101.9 | -103.28 | -104.78 | -101.78 | -104.79 | -101.76 | -104.81 | -101.74 | -106.28 | -103.74 | -108.81 | -0.83 | -0.81 | -0.85 |
| Top of Karoro interglacial | 190 | -133.2 | -134.7 | -131.7 | -127.61 | -129.11 | -126.11 | -129.67 | -125.55 | -130.51 | -124.71 | -109.61 | -101.71 | -117.51 | -0.58 | -0.54 | -0.62 |
| Base of Karoro interglacial | 222 | -152.7 | -154.2 | -151.2 | -136.88 | -138.38 | -135.38 | -139.96 | -133.80 | -142.34 | -131.43 | -126.88 | -116.43 | -137.34 | -0.57 | -0.52 | -0.62 |

| **Wakefield Street** | | depth from drillhole log | | | decompacted | | | uncertainty +/- 10% | | uncertainty +/- 25% | | depth accounting for relative sea level (RSL) | | | rate accounting for RSL (2014) | | |
|---|---|---|---|---|---|---|---|---|---|---|---|---|---|---|---|---|---|
| Elevations of shoreline horizons | age (ka) | mean | min | max | mean | min | max | min | max | min | max | mean | min | max | mean | min | max |
| Base of Holocene marine | 9 | -18.4 | -19.9 | -16.9 | -17.90 | -19.40 | -16.40 | -19.45 | -16.34 | -19.52 | -16.27 | 0.11 | 3.73 | -3.52 | 0.01 | 0.41 | -0.39 |
| Top of last interglacial | 78 | -73.5 | -75.0 | -72.0 | -72.89 | -75.61 | -71.39 | -74.45 | -71.33 | -74.54 | -71.24 | -57.89 | -51.24 | -64.54 | -0.74 | -0.66 | -0.83 |
| Base of OI 5c | 106 | -87.9 | -89.4 | -86.4 | -86.58 | -88.08 | -85.08 | -88.21 | -84.95 | -88.41 | -84.75 | -70.58 | -63.75 | -77.41 | -0.67 | -0.60 | -0.73 |

| **Seaview (Parkside Road)** | | depth from drillhole log | | | decompacted | | | uncertainty +/- 10% | | uncertainty +/- 25% | | depth accounting for relative sea level (RSL) | | | rate accounting for RSL (2014) | | |
|---|---|---|---|---|---|---|---|---|---|---|---|---|---|---|---|---|---|
| Elevations of shoreline horizons | age (ka) | mean | min | max | mean | min | max | min | max | min | max | mean | min | max | mean | min | max |
| Base of Holocene marine | 9 | -19.2 | -20.7 | -17.7 | -19.15 | -20.65 | -17.65 | -20.66 | -17.65 | -20.66 | -17.64 | -1.15 | 2.36 | -4.66 | -0.13 | 0.26 | -0.52 |
| Top of last interglacial | 78 | -47.0 | -48.5 | -45.5 | -41.12 | -42.62 | -39.62 | -43.21 | -39.03 | -44.09 | -38.15 | -26.12 | -18.15 | -34.09 | -0.33 | -0.23 | -0.44 |
| Base of last interglacial | 128 | -63.4 | -64.9 | -61.9 | -61.60 | -63.10 | -60.10 | -63.28 | -59.92 | -63.55 | -59.65 | -64.60 | -61.65 | -67.55 | -0.50 | -0.48 | -0.53 |

| **Marsden Street (Ewen Bridge)** | | depth from drillhole log | | | decompacted | | | uncertainty +/- 10% | | uncertainty +/- 25% | | depth accounting for relative sea level (RSL) | | | rate accounting for RSL (2014) | | |
|---|---|---|---|---|---|---|---|---|---|---|---|---|---|---|---|---|---|
| Elevations of shoreline horizons | age (ka) | mean | min | max | mean | min | max | min | max | min | max | mean | min | max | mean | min | max |
| Base of Holocene marine | 9 | -13.9 | -15.4 | -12.4 | -13.90 | -15.40 | -12.40 | -15.40 | -12.40 | -15.40 | -12.40 | 4.10 | 7.60 | 0.60 | 0.46 | 0.84 | 0.07 |
| Top of last interglacial | 78 | -70.6 | -72.1 | -69.1 | -69.10 | -70.60 | -67.60 | -70.81 | -67.53 | -71.03 | -67.31 | -54.10 | -47.31 | -61.03 | -0.69 | -0.61 | -0.78 |
| Base of last interglacial | 128 | -88.9 | -90.4 | -87.4 | -88.90 | -90.40 | -87.40 | -90.40 | -87.40 | -90.40 | -87.40 | -91.90 | -89.40 | -94.40 | -0.72 | -0.70 | -0.74 |
| Top of Karoro interglacial | 190 | -122.9 | -124.4 | -121.4 | -122.81 | -124.31 | -121.31 | -124.32 | -121.30 | -124.33 | -121.29 | -104.81 | -98.29 | -111.33 | -0.55 | -0.52 | -0.59 |

# A2.0 APPENDIX 2: SUMMARY OF DECONSOLIDATION AND SUBSIDENCE RATES FOR HUTT VALLEY DRILLHOLES

**Table A2.1** Summary of mean subsidence rates for each deconsolidation option.

| Drillhole | number of shorelines | subsidence rate (deconsolidated +/- 10%) | | | subsidence rate (deconsolidated +/- 25%) | | | median rate accounting for sea level RSL (2014) using +/- 10% values | | | median rate accounting for sea level RSL (2014) using +/- 25% values | | |
|---|---|---|---|---|---|---|---|---|---|---|---|---|---|
| | | mean | min | max | mean | min | max | mean | min | max | mean | min | max |
| North Street (Wilford) | 2 | -0.967 | -1.006 | -0.877 | -0.967 | -1.008 | -0.875 | -0.655 | -0.616 | -0.693 | -0.655 | -0.616 | -0.693 |
| Hutt Rd-Wakefield 455* | 9 ka uplift | -0.979 | -1.148 | -0.810 | -0.979 | -1.151 | -0.807 | 1.021 | 1.412 | 0.630 | 1.021 | 1.415 | 0.627 |
| Hutt Rd-Wakefield 456* | 9 ka uplift | -1.649 | -1.818 | -1.479 | -1.649 | -1.823 | -1.475 | 0.351 | 0.743 | -0.041 | 0.351 | 0.747 | -0.045 |
| Gear Meat 151 | 5 | -1.093 | -1.134 | -1.052 | -1.093 | -1.140 | -1.046 | -0.818 | -0.737 | -0.850 | -0.818 | -0.736 | -0.850 |
| Gear Meat 319 | 2 | -1.252 | -1.328 | -1.176 | -1.252 | -1.343 | -1.161 | -0.836 | -0.784 | -0.887 | -0.836 | -0.784 | -0.887 |
| Gear Meat 320 | 2 | -1.268 | -1.356 | -1.181 | -1.268 | -1.389 | -1.148 | -0.869 | -0.817 | -0.920 | -0.869 | -0.817 | -0.920 |
| Wakefield Street | 2 | -1.247 | -1.316 | -1.177 | -1.247 | -1.320 | -1.173 | -0.704 | -0.631 | -0.777 | -0.704 | -0.629 | -0.779 |
| Seaview (Parkside Road) | 2 | -1.045 | -1.114 | -0.976 | -1.045 | -1.119 | -0.972 | -0.420 | -0.364 | -0.476 | -0.420 | -0.357 | -0.482 |
| Elizabeth Street | 2 | -0.860 | -0.932 | -0.788 | -0.860 | -0.938 | -0.782 | -0.375 | -0.289 | -0.462 | -0.375 | -0.280 | -0.471 |
| Marsden St (Ewen Bridge) | 3 | -0.943 | -0.995 | -0.891 | -0.943 | -0.996 | -0.890 | -0.694 | -0.609 | -0.738 | -0.694 | -0.607 | -0.738 |

*not used in calculations.

# A3.0 APPENDIX 3: LOGIC TREE PARAMETERS AND STRUCTURE OUTLINE

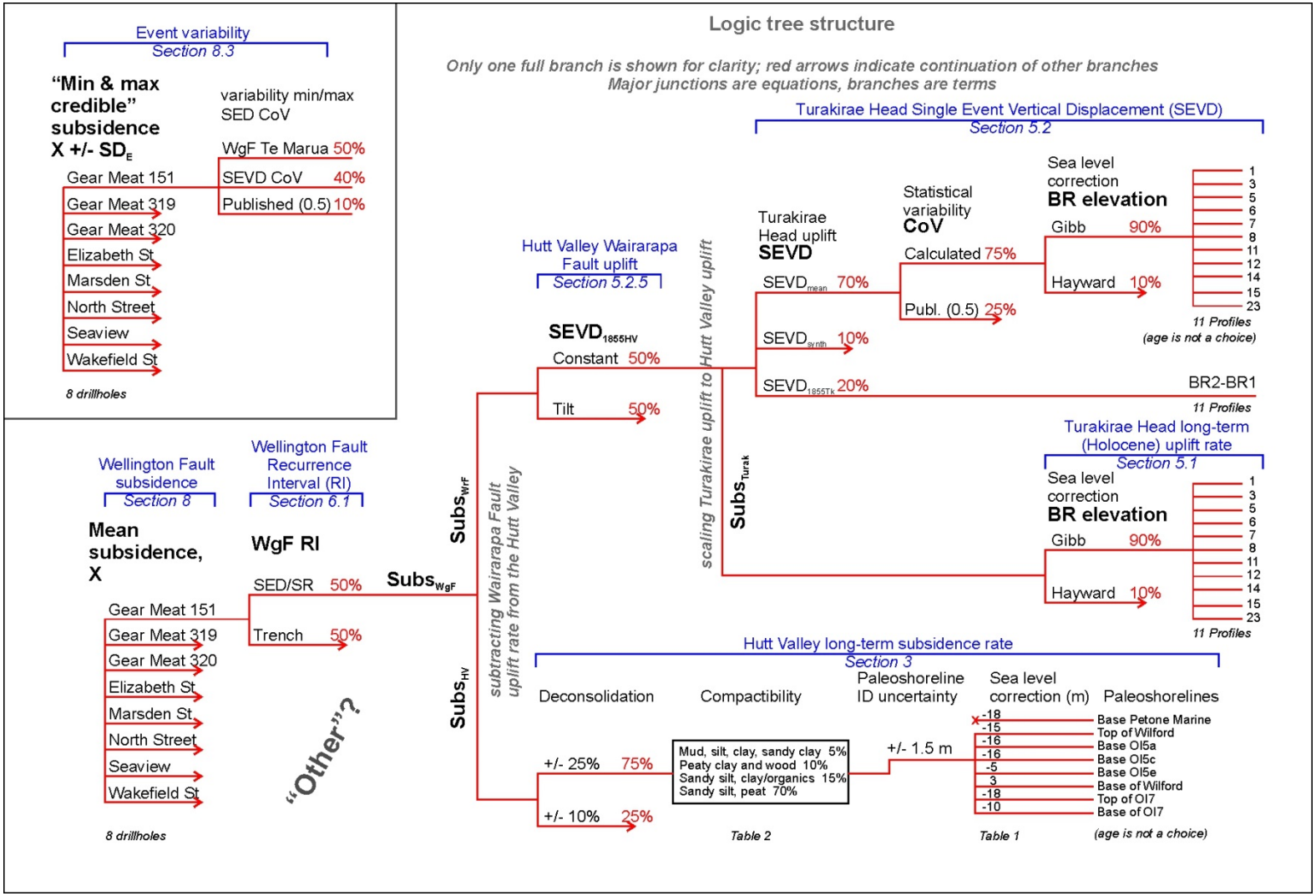

# A4.0 APPENDIX 4: BEACH RIDGE PROFILE ELEVATION DATA

**Table A4.1** Survey locations from Hull & McSaveney (1996) re-occupied remotely using GIS and compared with corresponding LiDAR data. * data and values from Hull & McSaveney (1996); all values are in metres; RASTERVALUE is elevation from bi-linear interpolation of LiDAR data at corresponding survey point; Difference is difference between Hull & McSaveney (1996) survey and LiDAR elevations.

| NZMG_N* | NZMG_E* | Notes* | Profile No* | Ridge* | Elevation* | RASTERVALUE | Difference |
|---|---|---|---|---|---|---|---|
| 5974966 | 2668421 | Top storm beach | 1 | br1/01 | 5.2 | 5.202 | -0.002 |
| 5975092 | 2668493 | Crest storm beach | 1 | br2/01 | 7 | 6.813 | 0.187 |
| 5975136 | 2668559 | Crest of ridge | 1 | br3/01 | 10.1 | 9.726 | 0.374 |
| 5975174 | 2668599 | | 1 | br4/01? | 12.6 | 12.241 | 0.359 |
| 5975199 | 2668605 | Crest of ridge | 1 | br5/01? | 13.8 | 13.479 | 0.321 |
| | | | | | | | |
| 5974569 | 2669137 | Top of ridge | 2 | br1/02 | 4.2 | 4.300 | -0.100 |
| 5974682 | 2669224 | Modified ridge top | 2 | br2/02 | 8 | 7.781 | 0.219 |
| 5974769 | 2669296 | Top of ridge | 2 | br3/02 | 13.1 | 12.878 | 0.222 |
| | | | | | | | |
| 5974015 | 2669430 | | 3 | br1/03 | 3.3 | 3.059 | 0.241 |
| 5974071 | 2669488 | | 3 | br2/03 | 7.4 | 7.305 | 0.095 |
| 5974172 | 2669595 | Top of modified ridge | 3 | br3/03 | 13 | 12.916 | 0.084 |
| 5974214 | 2669573 | Back edge road | 3 | br3/03 | 13.2 | 12.919 | 0.281 |
| 5974212 | 2669658 | Top of ridge | 3 | br4/03 | 18.2 | 18.074 | 0.126 |
| 5974233 | 2669650 | Top of ridge | 3 | br4/03 | 17.9 | 17.751 | 0.149 |
| 5974254 | 2669642 | | 3 | br4/03 | 17.6 | 17.371 | 0.229 |
| 5974233 | 2669650 | | 3 | br4/03? | 17.9 | 17.751 | 0.149 |
| | | | | | | | |
| 5973737 | 2669532 | Crest of ridge | 4 | br1/04 | 3.4 | 3.185 | 0.215 |
| 5973753 | 2669576 | Top of beach | 4 | br2/04 | 7.8 | 7.477 | 0.323 |
| | | | | | | | |
| 5973386 | 2669619 | Top of ridge | 5 | br1/05 | 3.2 | 2.898 | 0.302 |
| 5973315 | 2669707 | | 5 | br2/05 | 8.1 | 7.914 | 0.186 |
| 5973411 | 2669663 | Top of ridge; edge of road | 5 | br2/05 | 7.9 | 7.622 | 0.278 |
| 5973379 | 2669824 | Top of ridge | 5 | br3/05 | 14.7 | 14.529 | 0.171 |
| 5973410 | 2669892 | | 5 | br4/05? | 18.1 | 17.679 | 0.421 |
| | | | | | | | |
| 5973035 | 2669822 | | 6 | br1/06 | 3.7 | 3.442 | 0.258 |
| 5973072 | 2669857 | | 6 | br2/06 | 8.5 | 8.159 | 0.341 |
| 5973132 | 2669984 | | 6 | br3/06 | 14.7 | 14.347 | 0.353 |
| 5973172 | 2670051 | | 6 | br4/06 | 17.8 | 17.597 | 0.203 |
| | | | | | | | |
| 5972665 | 2670194 | Storm beach | 7 | br1/07 | 3.1 | 2.908 | 0.192 |

| NZMG_N* | NZMG_E* | Notes* | Profile No* | Ridge* | Elevation* | RASTERVALUE | Difference |
|---|---|---|---|---|---|---|---|
| 5972748 | 2670197 | Top of ridge | 7 | br2/07 | 7.9 | 7.611 | 0.289 |
| 5972964 | 2670194 | | 7 | br3/07 | 13.9 | 13.632 | 0.268 |
| 5973107 | 2670208 | Top of beach | 7 | br4/07 | 18.5 | 18.291 | 0.209 |
| 5972724 | 2670598 | Top of modern storm beach | 8 | br1/08 | 3.1 | 3.046 | 0.054 |
| 5972814 | 2670556 | Crest of ridge | 8 | br2/08 | 7.8 | 7.817 | -0.017 |
| 5972973 | 2670490 | | 8 | br3/08 | 14.9 | 14.748 | 0.152 |
| 5973088 | 2670427 | | 8 | br4/08 | 18.6 | 18.376 | 0.224 |
| 5973120 | 2670381 | Top of ridge 5 | 8 | br5/08 | 22 | 21.834 | 0.166 |
| | | | | | | | |
| 5973058 | 2671005 | Top of modern storm ridge | 9 | br1/09 | 3.2 | 3.040 | 0.160 |
| 5973123 | 2670951 | Top of 1855 ridge | 9 | br2/09 | 8 | 7.736 | 0.264 |
| 5973205 | 2670864 | | 9 | br3/09 | 14.7 | 14.437 | 0.263 |
| | | | | | | | |
| 5973189 | 2671175 | Top of storm beach | 10 | br1/10 | 3.2 | 2.941 | 0.259 |
| 5973259 | 2671070 | | 10 | br2/10? | 8.3 | 8.996 | -0.696 |
| 5973335 | 2670990 | Top of storm beach | 10 | br3/10 | 16.3 | 16.067 | 0.233 |
| | | | | | | | |
| 5973438 | 2671468 | Top of modern storm ridge | 11 | br1/11 | 3.2 | 2.996 | 0.204 |
| 5973512 | 2671415 | Top of 1855 ridge | 11 | br2/11 | 8 | 7.878 | 0.122 |
| 5973630 | 2671286 | Top of ridge | 11 | br3/11 | 15.9 | 15.752 | 0.148 |
| 5973703 | 2671214 | | 11 | br4/11? | 21.9 | 21.686 | 0.214 |
| 5973705 | 2671199 | | 11 | br5/11? | 24.2 | 23.896 | 0.304 |
| | | | | | | | |
| 5973735 | 2671898 | Top of modern ridge | 12 | br1/12 | 2.8 | 2.635 | 0.165 |
| 5973833 | 2671813 | Top of ridge | 12 | br2/12 | 8.9 | 8.507 | 0.393 |
| 5973953 | 2671715 | Crest of ridge | 12 | br3/12 | 17.1 | 16.969 | 0.131 |
| 5973968 | 2671727 | Crest of ridge | 12 | br3/12 | 17.1 | 16.890 | 0.210 |
| 5974030 | 2671610 | Crest of ridge | 12 | br4/12 | 22.4 | 22.203 | 0.197 |
| 5974063 | 2671583 | Crest of ridge | 12 | br5/12 | 25.6 | 25.239 | 0.361 |
| | | | | | | | |
| 5973894 | 2672135 | Modern storm beach | 13 | br1/13 | 2.1 | 1.788 | 0.312 |
| 5974015 | 2672047 | Crest of ridge | 13 | br2/13 | 8.4 | 8.026 | 0.374 |
| 5974154 | 2671947 | Top of ridge | 13 | br3/13 | 17.5 | 17.327 | 0.173 |
| | | | | | | | |
| 5974205 | 2672401 | Crest of modern storm beach | 14 | br1/14 | 3.3 | 3.022 | 0.278 |

| NZMG_N* | NZMG_E* | Notes* | Profile No* | Ridge* | Elevation* | RASTERVALUE | Difference |
|---|---|---|---|---|---|---|---|
| 5974269 | 2672357 | Top of 1855 ridge | 14 | br2/14 | 9.7 | 9.337 | 0.363 |
| 5974390 | 2672270 | Crest of ridge | 14 | br3/14 | 18.9 | 18.657 | 0.243 |
| 5974491 | 2672202 | Crest of ridge | 14 | br4/14 | 24.1 | 23.833 | 0.267 |
| 5974540 | 2672186 | Crest of ridge | 14 | br5/14 | 26.8 | 26.551 | 0.249 |
| | | | | | | | |
| 5974584 | 2672867 | Top of modern ridge | 15 | br1/15 | 3.5 | 3.468 | 0.032 |
| 5974655 | 2672803 | End of ridge | 15 | br2/15 | 8.6 | 8.496 | 0.104 |
| 5974753 | 2672696 | Crest of ridge | 15 | br3/15 | 18.6 | 18.231 | 0.369 |
| 5974780 | 2672657 | | 15 | br4/15 | 24.1 | 23.761 | 0.339 |
| 5974824 | 2672629 | | 15 | br5/15 | 27.2 | 26.753 | 0.447 |
| | | | | | | | |
| 5976598 | 2676020 | Crest modern beach | 16 | br1/16 | 4.1 | 3.279 | 0.821 |
| 5976664 | 2675989 | Crest of ridge | 16 | br2/16 | 6.8 | 6.454 | 0.346 |
| | | | | | | | |
| 5977748 | 2678401 | Crest of ridge | 17 | br1/17 | 5.5 | n/a | |
| 5977807 | 2678414 | Crest of ridge | 17 | br2/17 | 8.6 | n/a | |
| | | | | | | | |
| 5977781 | 2678143 | Crest modern ridge | 18 | br1/18 | 5.3 | n/a | |
| 5977837 | 2678151 | Crest 1855 ridge | 18 | br2/18 | 8.3 | n/a | |
| | | | | | | | |
| 5979558 | 2666009 | Top of beach | 21 | br1/21 | 4.9 | 2.728 | 2.172 |
| 5979635 | 2666133 | Crest of ridge | 21 | br2/21 | 8.4 | 7.999 | 0.401 |
| | | | | | | | |
| 5980643 | 2665281 | Top modern ridge | 22 | br1/22 | 6.4 | 5.265 | 1.135 |
| 5980766 | 2665334 | | 22 | br2/22 | 9.2 | 8.800 | 0.400 |
| | | | | | | | |
| 5978245 | 2666905 | Top dune | 23 | br1/23 | 5.3 | 3.288 | 2.012 |
| 5978251 | 2667013 | Top dune | 23 | br2/23 | 8.7 | 8.332 | 0.368 |
| 5978258 | 2667043 | ridge | 23 | br3/23 | 10.8 | 10.660 | 0.140 |
| 5978260 | 2667061 | ridge | 23 | br4/23 | 14.3 | 13.986 | 0.314 |
| | | | | | | | |
| 5978126 | 2666928 | Crest of dune | 24 | br1/24 | 5.8 | 3.777 | 2.023 |
| 5978120 | 2667004 | Crest of ridge | 24 | br2/24 | 6.9 | 6.645 | 0.255 |
| 5978118 | 2667041 | ridge | 24 | br3/24 | 10.3 | 10.093 | 0.207 |
| | | | | | | | |
| 5977270 | 2666397 | Crest of beach | 25 | br1/25 | 3.2 | 3.096 | 0.104 |
| 5977235 | 2666436 | 1855 crest, road centreline | 25 | br2/25 | 5.2 | 4.971 | 0.229 |
| 5977205 | 2666469 | | 25 | br3/25 | 6.8 | 6.538 | 0.262 |

# A5.0 APPENDIX 5: SINGLE EVENT DISPLACEMENT MEASUREMENTS AT TURAKIRAE HEAD

**Table A5.1** Height differences (m) between beach ridges along profiles where BR5 and/or BR4 were identified. The difference is inferred to represent single event vertical displacements (SEVD) on the Wairarapa Fault, Values are corrected for paleo-sea levels using the Hayward et al. (2012) sea level curves; we assign +/- 0.3 m for elevation uncertainty (e.g., Hull & McSaveney, 1996). See text Section 5.2 for the same data corrected using Gibb (1986) sea level curves.

| | BR1 to BR2 ($SEVD_{1855Tk}$) | BR2 to BR3 | BR3 to BR4 | BR4 to BR5 | MEAN ($SEVD_{mean}$) | STDEV | CoV |
|---|---|---|---|---|---|---|---|
| Profile 1 | 1.61 | 3.91 | 0.26 | 1.74 | 1.88 | 1.51 | 0.80 |
| Profile 3 | 4.25 | 6.61 | 2.57 | | 4.48 | 2.03 | 0.45 |
| Profile 5 | 4.87 | 7.76 | 0.90 | | 4.51 | 3.45 | 0.76 |
| Profile 6 | 4.72 | 7.19 | 1.00 | | 4.30 | 3.12 | 0.72 |
| Profile 7 | 4.70 | 7.02 | 2.41 | | 4.71 | 2.31 | 0.49 |
| Profile 8 | 4.77 | 7.93 | 1.38 | 3.96 | 4.51 | 2.70 | 0.60 |
| Profile 11 | 4.88 | 8.87 | 3.68 | 2.71 | 5.04 | 2.71 | 0.54 |
| Profile 12 | 5.87 | 9.42 | 3.02 | 3.54 | 5.46 | 2.92 | 0.53 |
| Profile 14 | 6.31 | 10.32 | 2.93 | 3.22 | 5.69 | 3.44 | 0.60 |
| Profile 15 | 5.03 | 10.73 | 3.28 | 3.49 | 5.63 | 3.49 | 0.62 |
| Profile 23 | 5.04 | 3.33 | 1.08 | | 3.15 | 1.99 | 0.63 |
| Mean | 4.33 | | | | 4.52 | | 0.61 |

**Table A5.2** Height differences (m) between beach ridges along profiles where BR5 and/or BR4 were identified, with the addition of extra surface rupturing earthquake events as identified by trenching studies on the Wairarapa Fault (e.g., Van Dissen et al., 2013). Heights are corrected for paleo-sea levels using the Gibb (1986) sea level curves; we assign +/- 0.3 m for elevation uncertainty (e.g., Hull & McSaveney, 1996).

| | BR1 to BR2 ($SEVD_{1855Tk}$) | BR2 to BR2A | BR2A to BR3 | BR3 to BR3A | BR3A to BR4 | BR4 to BR5 | MEAN ($SEVD_{synth}$) | STDEV | CoV |
|---|---|---|---|---|---|---|---|---|---|
| Profile 1 | 1.61 | 1.46 | 1.46 | 1.26 | 1.26 | 0.74 | 1.30 | 0.31 | 0.24 |
| Profile 3 | 4.25 | 2.81 | 2.81 | 2.41 | 2.41 | | 2.94 | 0.76 | 0.26 |
| Profile 5 | 4.87 | 3.38 | 3.38 | 1.57 | 1.57 | | 2.96 | 1.40 | 0.47 |
| Profile 6 | 4.72 | 3.09 | 3.09 | 1.62 | 1.62 | | 2.83 | 1.29 | 0.45 |
| Profile 7 | 4.70 | 3.01 | 3.01 | 2.33 | 2.33 | | 3.08 | 0.97 | 0.32 |
| Profile 8 | 4.77 | 3.47 | 3.47 | 1.81 | 1.81 | 2.96 | 3.05 | 1.13 | 0.37 |
| Profile 11 | 4.88 | 3.94 | 3.94 | 2.97 | 2.97 | 1.71 | 3.40 | 1.10 | 0.32 |
| Profile 12 | 5.87 | 4.21 | 4.21 | 2.64 | 2.64 | 2.54 | 3.68 | 1.33 | 0.36 |
| Profile 14 | 6.31 | 4.66 | 4.66 | 2.59 | 2.59 | 2.22 | 3.84 | 1.63 | 0.42 |
| Profile 15 | 5.03 | 4.87 | 4.87 | 2.77 | 2.77 | 2.49 | 3.80 | 1.24 | 0.33 |
| Profile 23 | 5.04 | 1.16 | 1.16 | 3.33 | | | 2.67 | 1.88 | 0.70 |
| Mean | 4.33 | | | | | | 3.28 | | 0.39 |

**Table A5.3** Height differences (m) between beach ridges along profiles where BR5 and/or BR4 were identified, with the addition of extra surface rupturing earthquake events as identified by trenching studies on the Wairarapa Fault (e.g., Van Dissen et al., 2013). Heights are corrected for paleo-sea levels using the Hayward et al. (2012) sea level correction; we assign +/- 0.3 m for elevation uncertainty (e.g., Hull & McSaveney, 1996).

| | BR1 to BR2 ($SEVD_{1855Tk}$) | BR2 to BR2A | BR2A to BR3 | BR3 to BR3A | BR3A to BR4 | BR4 to BR5 | MEAN ($SEVD_{synth}$) | STDEV | CoV |
|---|---|---|---|---|---|---|---|---|---|
| Profile 1 | 1.61 | 1.96 | 1.96 | 0.13 | 0.13 | 1.74 | 1.25 | 0.88 | 0.70 |
| Profile 3 | 4.25 | 3.31 | 3.31 | 1.28 | 1.28 | | 2.69 | 1.34 | 0.50 |
| Profile 5 | 4.87 | 3.88 | 3.88 | 0.45 | 0.45 | | 2.71 | 2.10 | 0.78 |
| Profile 6 | 4.72 | 3.59 | 3.59 | 0.50 | 0.50 | | 2.58 | 1.95 | 0.76 |
| Profile 7 | 4.70 | 3.51 | 3.51 | 1.20 | 1.20 | | 2.83 | 1.56 | 0.55 |
| Profile 8 | 4.77 | 3.97 | 3.97 | 0.69 | 0.69 | 3.96 | 3.01 | 1.82 | 0.61 |
| Profile 11 | 4.88 | 4.44 | 4.44 | 1.84 | 1.84 | 2.71 | 3.36 | 1.39 | 0.41 |
| Profile 12 | 5.87 | 4.71 | 4.71 | 1.51 | 1.51 | 3.54 | 3.64 | 1.81 | 0.50 |
| Profile 14 | 6.31 | 5.16 | 5.16 | 1.46 | 1.46 | 3.22 | 3.80 | 2.06 | 0.54 |
| Profile 15 | 5.03 | 5.37 | 5.37 | 1.64 | 1.64 | 3.49 | 3.76 | 1.78 | 0.47 |
| Profile 23 | 5.04 | 1.66 | 1.66 | 1.08 | | | 2.36 | 1.81 | 0.77 |
| Mean | 4.33 | | | | | | 3.30 | | 0.60 |

# A6.0 APPENDIX 6: SUBSIDENCE PER EVENT CALCULATED FOR A WELLINGTON FAULT SURFACE RUPTURE

**Table A6.1** Mean and Standard Deviation (averaging across profiles) of subsidence per event calculated for a Wellington Fault rupture at the location of each Hutt Valley drillhole. See Section 8 of the text for derivation and discussion of the values.

| Drillhole location | Mean subsidence per event (m) | Standard deviation (m) |
|---|---|---|
| North Street | 1.722 | 0.544 |
| Gear Meat 151 | 1.838 | 0.577 |
| Gear Meat 319 | 1.885 | 0.588 |
| Gear Meat 320 | 1.919 | 0.597 |
| Wakefield Street | 1.751 | 0.552 |
| Seaview | 1.524 | 0.498 |
| Elizabeth Street | 1.475 | 0.486 |
| Marsden Street | 1.718 | 0.543 |


www.gns.cri.nz

**Principal Location**

1 Fairway Drive
Avalon
PO Box 30368
Lower Hutt
New Zealand
T +64-4-570 1444
F +64-4-570 4600

**Other Locations**

Dunedin Research Centre
764 Cumberland Street
Private Bag 1930
Dunedin
New Zealand
T +64-3-477 4050
F +64-3-477 5232

Wairakei Research Centre
114 Karetoto Road
Wairakei
Private Bag 2000, Taupo
New Zealand
T +64-7-374 8211
F +64-7-374 8199

National Isotope Centre
30 Gracefield Road
PO Box 31312
Lower Hutt
New Zealand
T +64-4-570 1444
F +64-4-570 4657